Reports from

Arctic Biology Field Course
Qeqertarsuaq 2014

[5 - 31 July]

Arctic Station
University of Copenhagen

Title: Arctic Biology Field Course, Qeqertarsuaq 2014

Published by: Arctic Station
University of Copenhagen
3953 Qeqertarsuaq
Greenland

Section for Marin Biology
University of Copenhagen
Universitetsparken 4, 1st floor
2100 Copenhagen Ø
Denmark

Publishing eyar: 2015

Edited by: Niels Daugbjerg, Section for Marin Biology

ISBN: 978-87-89143-20-0

Front page photos: Niels Daugbjerg

Citation: The report can be cited in full:

Arctic Biology Field Course, Qeqertarsuaq 2014. N. Daugbjerg (Ed.), 2015. Arctic Station, University of Copenhagen, p. 1-99.

or in parts:

Authors(s), 2015. Title of paper, In: Arctic Biology Field Course, Qeqertarsuaq 2014. N. Daugbjerg (Ed.), 2015. Arctic Station, University of Copenhagen, pp. x-x.

For further information about Arctic Station: www.arktiskstation.ku.

List of content

Preface and acknowledgements

Niels Daugbjerg and John Fleng Steffensen (Marine Biological Section, Dept. of Biology, University of Copenhagen)

The Arctic Biology Field course held in 2014 marked the last of the 3-4 week long summer courses held regularly since 1973 at the Arctic Station, Qeqertarsuaq. Having multiple weeks for conducting research projects students were given the opportunity to obtain a significant amount of practical experience working in the arctic environment. The course in 2014 was organized by Dept. of Biology, University of Copenhagen and lasted 27 days. Though all four student projects conducted were marine and included phytoplankton biology (coordinated by Niels Daugbjerg) and fish physiology (coordinated by John Fleng Steffensen), a number of terrestrial excursions were made. On our way to Qeqertarsuaq we made a picnic to the incredibly Ilulissat Icefjord and during our stay at Arctic Station we made small hikes to e.g. Engelskmandens Havn and Kuannit. All good courses also include a football match against the local team. A game was planned for Sunday 20th July and despite not having the prober gear for playing on a clay pitch it was a fun game (and we only lost by a single goal). Two non-marine talks were given during the course. One addressed arctic land plants and a presentation of the CENPERM project by Anders Michelsen and the other was on the geology of the area by Ole Stecher, the scientific leader at the Arctic Station.

The selected projects and students were:

1) Effects of low pH on summer phytoplankton (Sofie Bjørnholt Mogensen, Nadia Brogård Nord and Jesper Sonne)
2) Phytoplankton focussing on diatom diversity and abundance (Liv Louise Victoria Backhaus, Nicolai Fassel and Ditte Bjerregaard Jensen)
3) Physiology and optimal temperature in four fish living in the Arctic (Emilie Maria Falk Kallenbach, Eva Marie Nive Kleist Johansen and Jeppe Nedergaard Pedersen)
4) Optimum temperature for aerobic scope in Arctic charr (Aslak Kappel Hansen, Mads Kristian Reinholdt Jensen and David Bille Byriel)

Project 1 and 2 (as chapter 1-2 in this report) were supervised by Niels Daugbjerg. Project 3 and 4 (as chapter 3-4) were supervised by John Fleng Steffensen and co-supervised by Morten Bo Søndergaard Svendsen, PhD student.

On behalf of all participants we thank the staff at the Arctic Station for given us all the logistic support needed to perform the projects. Particularly we thank the crew on board “Porsild”, Frederik Grønvold, Søren Fisker and Erik Wille and the scientific leader Ole Stecher and the station manager Kjeld (Akaaraq) Mølgaard. The Dept of Biology at the Faculty of Science and the Board for the Arctic Station covered all expenses and we are grateful for this support.

Photo in front of the main building of the Arctic Station showing the participants of the Arctic Biology Field Course 2014 together with the technical staff. (**1**) Ditte Bjerregaard Jensen, (**2**) Jesper Sonne, (**3**) Eva Marie Nive Kleist Johansen, (**4**) Sofie Bjørnholt Mogensen, (**5**) Søren Fisker, (**6**) Morten Bo Søndergaard Svendsen, (**7**) Liv Louise Victoria Backhaus, (**8**) Jeppe Nedergaard Pedersen, (**9**) Emilie Maria Falk Kallenbach, (**10**) Mads Kristian Reinholdt Jensen, (**11**) Nadia Brogård Nord, (**12**) David Bille Byriel, (**13**) Nicolai Andreas Munk Fassel, (**14**) John Fleng Steffensen, (**15**) Aslak Kappel Hansen, (**16**) Niels Daugbjerg, (**17**) Erik Wille, (**18**) Frederik Grønvold, (**19**) Kjeld Mølgaard

The effect of low pH on an Arctic phytoplankton summer community in Disko Bay, West Greenland

Sofie Bjørnholt Mogensen, Nadia Brogård Nord and Jesper Sonne

Arctic field course, July 2014

Supervisors: Niels Daugbjerg and Per Juel Hansen

Submitted: 17.03.2015

Abstract

Oceans of the world take up nearly a quarter of the atmospheric carbon dioxide emitted from anthropogenic sources and biological respiration processes. In relation to the strong recent increase in the atmospheric concentration of this greenhouse gas; the future world has to consider the consequences of ocean acidification. Possible impacts of acidification on marine microorganisms have been investigated by several previous studies but these have so far presented inconsistant results and mainly been conducted for species in monoculture. Here, we present the first study of the effects of acidification on a coastal plankton community during summer, south of Disko Island, Greenland. The variation in chlorophyll *a* concentration and abundance of key phytoplankton species were followed at four different pH values for 16 days. One pH corresponding to *in situ* measurements of 8.1 and three other treatments with pH lowered to 7.7, 7.4 and 7.1 by bubbling with gaseous carbon dioxide. Overall, we observed a decrease in biomass and cell concentration of the phytoplankton communities. In addition, we found no statistical support for poorer growth in acidified treatments. By conducting follow-up analyses, we assess that this unexpected result is most likely caused by limitation of nutrients in the collected bottom seawater used for experimental dilution. In addition to the nutrient depleted bottom water, we found an *in situ* plankton community in their declining state with low biomass. During the experiment (8-26 July, 2014), we also measured pH down the costal water column at two stations south of Disko Island. Throughout the period we observed negligible temporal fluctuations. Vertically, we observed a tendency of decrease in pH from approx. 8.3 at the depth of chlorophyll *a* maximum to approx. 8.0, below the pycnocline. This study has contributed with important knowledge of how the impact of acidification seems to be insignificant for nutrient limited plankton communities and additionally of how pH naturally fluctuates down through the water column across the Arctic summer.

Introduction

Ocean acidification, induced by recent climate change may cause radical changes in structure and composition of the marine plankton communities and is therefore receiving increased attention by marine ecologists (Berge et *al.* 2010; Caron & Hutchins 2012). Carbon emissions from anthropogenic sources have massively increased the atmospheric CO_2 concentration by 30 % since the pre-industrial era, which by the end of this century is expected to reach 140 % if the emissions continue unabated (Houghton et *al.* 2001). The world's oceans take up nearly a quarter of the emitted CO_2, which in equilibrium with carbonic acid (H_2CO_3) and bicarbonate (HCO_3^-) result in a reduction of ocean pH (Raven et *al.* 2005; Sabine et *al.* 2004). The solubility of inorganic carbon increases with decreasing temperature and salinity, thus the magnitude of acidification tend to increase towards the Polar Regions. For future perspectives, this tendency is expected to further increase with higher exposure of ocean surface from the accelerating loss of ice cover (Stroeve et *al.* 2007).

Acidification may have a strong negative effect on especially unicellular organisms as their intracellular environment is, in comparison to multicellular organisms, stronger affected by the extracellular environment. Changes in pH may therefore affect various physiological parameters related to membrane potential and enzyme activity (Houghton et *al.* 2001; Langer et *al.* 2006). Conversely, carbon induced acidification may potentially be beneficial to phototrophic organisms in cases of carbon limitation. The literature reflects contradicting views of the possibility of carbon limitations of phytoplankton in natural seawater. The prime enzyme for photosynthetic CO_2 fixation (RUBISCO) has been suggested not to be substrate saturated under the present-day concentration of CO_2. Hence, the concentration of dissolved inorganic carbon (DIC) may set the limit of algal growth (Beardall & Raven 2004). However, carbon-concentrating mechanisms (CCM's) are widespread among photosynthetic organisms to ensure RUBISCO not to be carbon limited (Badger et *al.* 1998). Also, the availability of nutrients in the oceans in respect to the C:N:P ratio (or Redfield ratio) in phototrophic unicellular organisms, suggests that nutrients are the limiting component for algal growth (Moore *et* al. 2013).

$$CO_2 + H_2O \leftrightarrow HCO_3^- + H^+ \leftrightarrow CO_3^{2-} + 2H^+$$

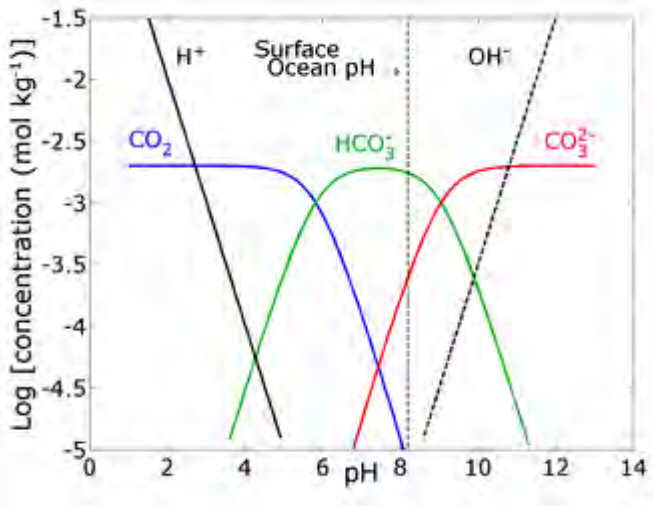

Figure 1: Bjerrum plot of the carbonate system of seawater, indicating typical concentrations of the dissolved carbonate species (copied from http://www.eoearth.org/view/article/154468/). Above; the carbon-water equilibrium equation.

Phytoplankton is able to utilize HCO_3^- and/or CO_2 for photosynthesis. In seawater with pH of 8-8.2, HCO_3^- constitutes about 90 percent of the total DIC, where CO_2 only represent about 1 percent (Key et *al.* 2004). During acidification, the equilibrium will alter the carbon speciation towards increased CO_2 concentrations (Figure 1) (Thoisen et *al.* 2014; Rost et *al.* 2008). The buffering capability of HCO_3^- and CO_3^{2-} results in overall low pH fluctuations in the water column and less changes in pH than otherwise expected from acidification (Raven et *al.* 2005; Riebesell 2004). This especially accounts for open ocean systems where the biological activity usually is low. In contrast, coastal systems experience much larger fluctuations on annual and even diurnal time scales. Leaching of nutrients from the terrestrial upland increase productivity with associated photosynthesis and respiration processes constantly altering the concentration of free CO_2 (Duarte et *al.* 2013). In addition, physical processes as upwelling, where acidified bottom water is transported to the upper water column, has been shown to cause fluctuations in pH (Feely *et al.* 2008). In one shallow coastal marine system, pH has been observed; following diurnal variations of 1.8 pH-units (Middelboe & Hansen 2007). As a result, coastal phytoplankton communities are expected to be better adapted to fluctuations in pH and therefore less sensitive to changes in pH in comparison to oceanic communities.

Although a comprehensive effort have been allocated to quantify effects of climate change on the chemical marine environment, relatively few studies have focused on how climate induced acidification influences plankton communities in the Arctic. Previous experimental studies on the subject have so far produced inconsistent results. Some studies found a high resilience to acidification (Kim 2006; Nielsen et *al.* 2010), while others have described various negative effects (Riebesell et *al.* 2007; Rose et *al.* 2009; Thoisen et *al.* 2014; Tortell et *al.* 2002). These studies have

mainly been carried out with species in monoculture excluding indirect effects from competition and grazing (Berge et *al.* 2010). On the other hand, species do not evolve in isolation, but are rather entangled in complex networks of interspecific interactions. Hence, when quantifying impacts of future climate change on biological systems, we argue that it is essential to account for these factors. Using the same study site and experimental design as Thoisen et *al.* (2014), we here investigate the effect of acidification on a coastal plankton community during summer south of Disko Island, Greenland. Our experiment is the first to be conducted for an Arctic summer community where productivity likely has started to decrease after having reached its maximum during spring (Nielsen 2005). The effect on concentration of chlorophyll *a* and key plankton species were followed at four different pH values. Four pH treatments were carried out. One treatment had a pH corresponding to *in situ* measurements, while pH in the three other treatments were lowered by bubbling with gaseous CO_2, to reach pH of 7.7, 7.4 and 7.1, respectively. Thereby, our treatments should directly reflect climate change scenarios. Simultaneously with these experiments, we measured vertical pH profiles at the sampling stations in order to assess variations in pH profiles for an Arctic marine system during summer. Specifically we raise the following hypothesis: (1) In supplementation to Thoisen et *al.* (2014), we expect a negative effect of acidification on concentration of chlorophyll *a* and cells of key phytoplankton species; (2) we expect the phytoplankton community to become dominated by few competitive species when exposed to acidification; (3) we expect that pH *in situ* will have less fluctuations compared to the observed in Thoisen et *al.* (2014) during spring due to the absence of ice cover during summer.

Materials and methods

Study site and sample processing

pH profiles were constructed at four times during the experimental period (i.e. the 8th, 13th, 18th, and 26th of July). Water samples were collected from the surface down to 250 meters at Torkels station (N 69^{o} 14.66; W 53^{o} 20.28) on the 8th July and down to 85 meters depth at Laksebugt (N 69^{o} 16.66; W 53^{o} 57.01) the three other times (Figure 2). Both locations are south of Disko Island. Water was collected in 0.5 L polycarbonate bottles which were carefully sealed with parafilm to avoid air bubbles and gas exchange. The bottles were kept in a cooling box and transported to the laboratory were pH was measured as quickly as possible with a pH meter (Jenway 3510 pH meter). CTD profiles were computed with a CTD (Sea-Bird SBE19plus) every day of water collection. Water samples for experimental use were collected in triplicates of 20 L from the Laksebugt location at chlorophyll *a* maximum (i.e. 35 meters depth). The water was reverse filtrated through 250 µm mesh to remove grazing meso-zooplankton and stored cool at 4 °C until added to experimental bottles. Extra 20 L of water from chl. *a* maximum (i.e. 24 m) were collected the 19th of July (day 8 of the experiment) at Oles Station, N 69^{o} 11.12; W 53^{o} 31.05 (Figure 2) to replace pH treatment 7.7 which died out very early in the experiment. The 8th of July, 150 L of water were collected from Torkels Station underneath the pycnocline (i.e. 80 meters) using a 30 L Niskin bottle. This deep seawater was used for sample dilution throughout the experiment (see description below). The deep water samples were additionally filtered through 0.6 µm and stored in darkness at 4 °C for respectively avoiding presence and activity of photosynthetic organisms.

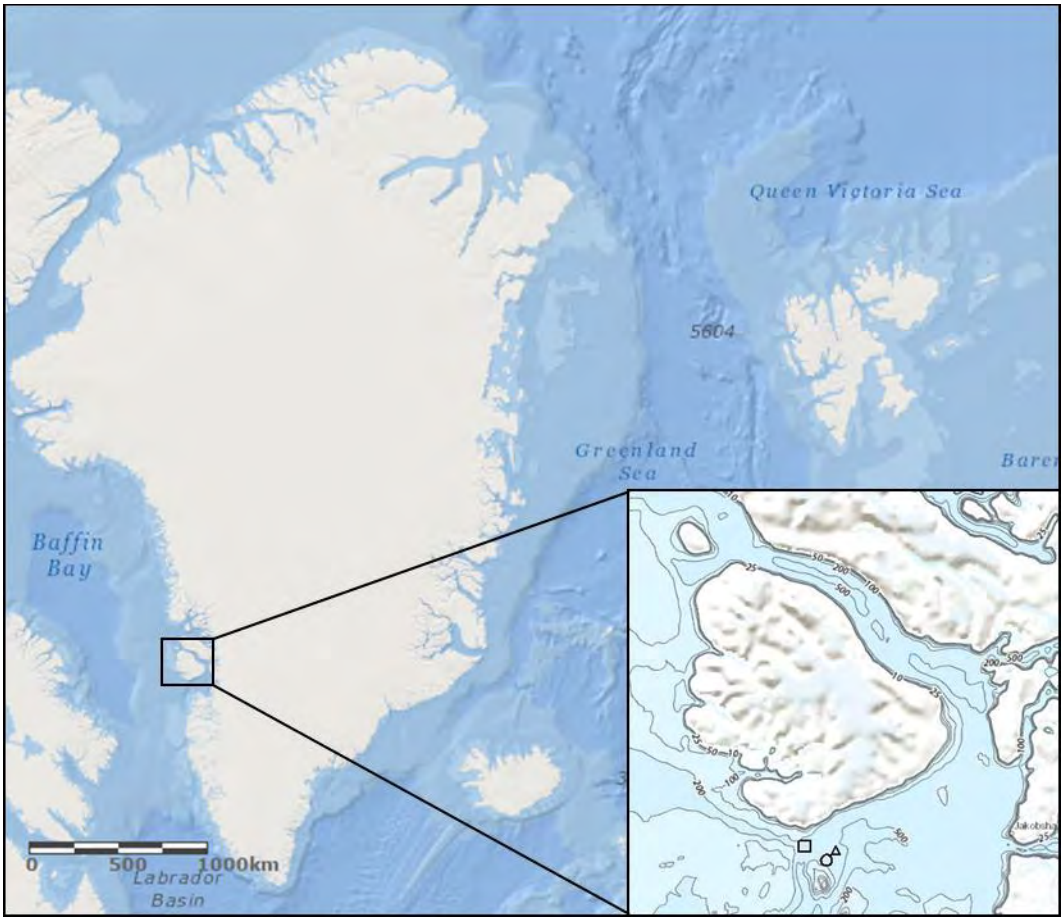

Figure 2: Map showing the sampling stations south of Disko Island, West Greenland (from web 1) along with a contour illustration of the bathymetric depth profile. The square shows the position of Laksebugt, the circle shows the position of Oles station and the triangle shows the position of Torkels station.

Experimental conditions and setup

The experiment were conducted in 12 1 L and 3 0.5 L polycarbonate bottles placed on a plankton wheel at 4 °C under constant exposure of light (~ 80 µE m^{-2} s^{-1}).

From the chlorophyll maximum samples, we set up 1 L triplicates of four pH treatments: one with *in situ* pH at 8.1 and three treatments with pH lowered in steps of 0.5 units per 12 hour to 7.7, 7.4 and 7.1, respectively. Hence, after 12 hours incubation, all bottles had reached their pH set points. To reflect natural climate conditions, pH was lowered using gaseous CO_2, which together with H_2O is in equilibrium with bicarbonate (HCO_3^-) and carbonic acid (H_2CO_3). The filtered deep seawater was acidified to a pH of 4.96 and subsequently added slowly to the incubations bottles for obtaining a pH corresponding to the respective treatments with an accuracy of 0.04. All incubation bottles were filled to capacity and sealed with parafilm, allowing no headspace, to avoid gas exchange and possible negative effects of trapped air bubbles on the phytoplankton community. Throughout the rest of the experiment, pH were lowered to the respective pH treatments in four separate 2 L bottles with filtered deep seawater and subsequently used for dilution at each time of sampling, in case the filtered deep seawater had pH below 8.1 the pH were elevated by adding 0.1 M NaOH.

Sample collection and measurements

Samples were taken for measurements of chlorophyll *a*, phaeophytin and enumeration of key plankton species. Chl. *a* concentrations were measured by filtrating 250 or 140 ml of water samples through either 0.3 µm, 0.4 µm or 0.2 µm filter (0.2 µm membrane filter, Poretics® Products; 0.3 µm glass fibre filter, Advantec®; 0.4 µm nuclepore Track-Etch membrane, Whatman®). The chlorophyll *a* was extracted from the filters by adding 3 or 5 ml of ethanol to a glass tube, and leaving it cold for at least 24 hours. Afterwards, the glass tubes were centrifuged for minimum three minutes, and 1.3 ml of the supernatant was transferred to round glass cuvettes. The measurements were conducted on a fluorometer (Triology, Turner designs®, module: CHL A ACID), in two steps; with and without addition of one drop of HCl, resulting in chlorophyll *a* and phaeophytin concentrations, respectively. Additionally, we collected samples for analysing dissolved inorganic carbon (DIC) concentrations at day 8 and 16 and nutrient concentration at day 0, 3 (All, except 7.7A), 12 (7.7 and 8.1) and 14 (7.4 and 7.1). Samples were analyzed for 7.7A on day 8 (day 0 for 7.7A). DIC samples were collected in 12 ml glass vials, and fixed with 100 µL saturated solution of Hg_2Cl_2. The vials were filled so no air was trapped insight, and stored dark and cold until analyses were conducted at the Marine Biological Section, Helsingør, Copenhagen University. Nutrient samples was collected in 15 ml falcon tubes and immediately frozen to -18°C. The nutrient analyses were performed at the Freshwater Biology Section at Copenhagen University. Both nutrient and DIC analyses were performed two month after return (see description below).

The volumes of water removed for sampling were replaced by filtered seawater of the desired pH. If the dilution with adjusted pH was insufficient to obtain a pH respective to the treatments, we subsequently added stronger acidified seawater. The frequency of sampling was typically every second or third day according to the putative increase in chl. *a* concentration. pH and temperature were measured directly before and after dilution.

Enumeration and identification

For plankton enumeration, we selected; *Thalassiosira* spp*., Phaeocystis* spp., *Pseudo-nitzschia* spp**.**, *Chaetoceros* spp. and a cryptophyte species. These species were all easily recognizable and well represented in the initial samples. Importantly, they were all autotrophic organisms as their growths are not additionally limited by organic food resources. At the last day in the experiment, we also enumerated small ciliates and *Gyrodinium* spp. Samples were processed by transferring 120 ml from the incubation bottles (60 ml from 7.7A) to brown glass bottles containing acidic Lugol's iodine (1 % final concentration) and stored dark and cold (5 °C). Due to time constraints only replicate 1 was continuously followed. Chosen species were identified and enumerated using an inverted microscope (Olympus CK2 or Labovert FS) with 50 ml sedimentation chambers (Hydro-Bios Kiel) and a settling time of at least 24 hours. Throughout the experiment, we noticed an increase in heterotrophic ciliates and dinoflagellates; we therefore quantified these in the last counted samples. A minimum of 20 cells l^{-1} was assumed if species were undetected in one sample, and later rediscovered. All cell counts were finally log-transformed to improve visualization.

DIC

DIC (dissolved inorganic carbon) were analysed by an IRGA (infrared gas analyzer) on Marine Biological Section in Helsingør, Denmark. All DIC samples were compared to a standard of 2 mM HCO_3^- (bicarbonate), thus prior to all sample analyses, a standard was continuously measured. Each sample ran in triplicates by the same method. 80 µl of fluid were drawn from the samples with a syringe and readily injected into an acid containing chamber where DIC was converted into CO_2. The systems carrier gas was nitrogen (N_2) and the absorption of the CO_2 was detected by the gas analyser coupled to a computer. The program Prologger® was used to calculate an integral of the data output.

Nutrients

The total N and P (inorganic and organic) were analysed at Freshwater Biology Section in Copenhagen, Denmark.

The frozen samples were thawed in a refrigerator overnight and directly analysed the following day. 8.4 ml of each sample were transferred to glass vials and 1.6 ml persulfate solution (50 g potassium persulfate ($K_2S_2O_8$) and 3 g sodium hydroxide (NaOH) in 1000 ml MilliQ-water) were added. A standard series were conducted with 50, 100, 200, 400 and 800 µg nitrate (NO_3^-) or phosphate (PO_4^{3-}) L^{-1}. Two samples of each concentration and three blank (demineralized water) were transferred to vials and persulfate solution were added as described for the experimental samples.

All the samples were autoclaved for 30 min at 120 °C. The samples were then cooled to room temperature and 2.5 ml borate buffer (30.9 g boric acid (H_3BO_3) and 4 g NaOH (in 250 ml MilliQ-water) were added and the samples were well mixed.

The total nitrogen content of the samples was analysed on an auto analyser (Alpkem RFA300).

To determine the total phosphorus content in the samples; 2 ml of each sample were transferred to cuvettes and 200 µl mixed reagent containing ascorbic acid were added. After 1 hour the absorbance were measured on a UV-Visible Recording Spectrophotometer (UV-160A Shimadzu) at 882 nm with demineralised water as reference.

The total phosphorus and nitrogen content was calculated by using the standard curve ($r^2 = 0.99$).

Calculations

DIC

DIC, dissolved inorganic carbon, was measured on an IRGA (infrared gas analyzer), and Equation 1 were used for calculations. [DIC] is the concentration in mM, [standard] is the concentration of the HCO^{3-} standard (2.0 mM), ∫standard and ∫sample are the computed integrals, respectively. Since the same volume of standard and sample were injected (80 µL), there is no need for a volume correction.

Eq.1 $$DIC[mM] = \frac{[standard]}{\int standard} * \int sample$$

The [DIC] was further calculated into three different carbon species (HCO_3^-, CO_3^{2-} and CO_2*), relative to the measured pH, temperature and salinity. This was carried out in the program CO2Sys EXCEL Makro using the following available inputs;

Set of constants: K1, K2 (from Mehrbach et *al.* 1973 refit by Dickson & Millero 1987) $KHSO_4$: Dickson
pH scale: Seawater scale (mol/kg-SW)
Further information about the program CO2Sys EXCEL Makro can be found in Lewis &Wallace (1998).

Nutrients
Total phosphorous was analysed on a spectrophotometer at 882 nm, and the following Equation 2 was used for calculations. Abs(882nm) is the absorbance at 882 nm, Abs(blind) is absorbance from the blind sample, 0.0007, and 0.0005 are derived from the standard curve ($y = ax + b$), and $M(PO_4^{3-})$ is the molar mass of phosphate.

Eq.2 $$TP\ [\mu M] = \frac{\frac{((abs(882nm) - abs(blind)) + 0.0007}{0.0005}}{M(PO_4{}^{3-})}$$

Nitrate was analysed on an auto-analyzer, and equation 3 was used for calculating final values.

Eq.3 $$TN\ [\mu M] = \frac{\frac{\left(\frac{\int N-1 + \int N-2}{2} - \int blind\right) - 42.4}{37.8}}{M(NO_3{}^{-})}$$

∫N-1 and ∫N-2 are integrals, ∫blind is the integral of the blind, 42.4, and 34.8 are values from the standard curve ($y = ax + b$), and $M(NO_3^-)$ is the molar mass of nitrate.

Standard curves, and the following calculations were all performed in Excel.

Statistics

Differences in chlorophyll *a* concentration across treatment 8.1, 7.7, 7,4 and 7,1 and time was tested by fitting linear models using generalized and ordinary least squares (GLS and OLS, respectively). Relative model quality was evaluated through Akaike information criterion (AIC), which is a maximum likelihood approach to account for the trade-off between model fit and model complexity. Here, higher-quality modes have lower AIC values and models with ΔAIC are generally considered to be equally fit (Diniz *et al.* 2008). By including a correlation structure, which assumes decreasing relatedness among units with increased difference in time of sampling, our model considerably improved (ΔAIC = 28.67), suggesting the presence of temporal autocorrelation among samples (Zuur *et al.* 2009). To account for residual heteroscedasticity, we additionally included a VarIdent variance structure, which allow each treatment to have different variance. By doing so, we additionally improved AIC by 13.269. The chlorophyll *a* concentration was square root transformed to obtain residual normality.
The total phosphorus and nitrogen concentrations were analysed by one-way ANOVA, for evaluation of difference between days. All statistics were carried out using R version 3.1.1 (R Core Team 2014).

Results

Physical and chemical conditions at study site

Figure 3 A-F shows the 6 CTD- and 4 pH-profiles measured during the experimental period. Measured parameters for the CTD were salinity, temperature, fluorescence (RFU) and irradiance. We found temperatures between 0 and 10 ˚C with warmest degrees in the upper water layer and temperatures of 1-4 ˚C at chl. *a* maximum. The 11th of July differs from the others; on this date the temperature at chl. *a* maximum were 8.5 ˚C. When looking at salinity we generally found values from 31.5 to 34 while we found almost freshwater at the surface the 11th July. The four pH profiles revealed pH values between 8.0-8.4; we observed the highest values in the surface layers and a decrease down through the water column.

The irradiance decreases from around 2000 (highest measured value) to 0 µE m^{-2} s^{-1} within the first 40 meters, consistent for all the profiles. The fluorescence (RFU) peaks appeared between 20 and 40 meters, and all at very low irradiance.

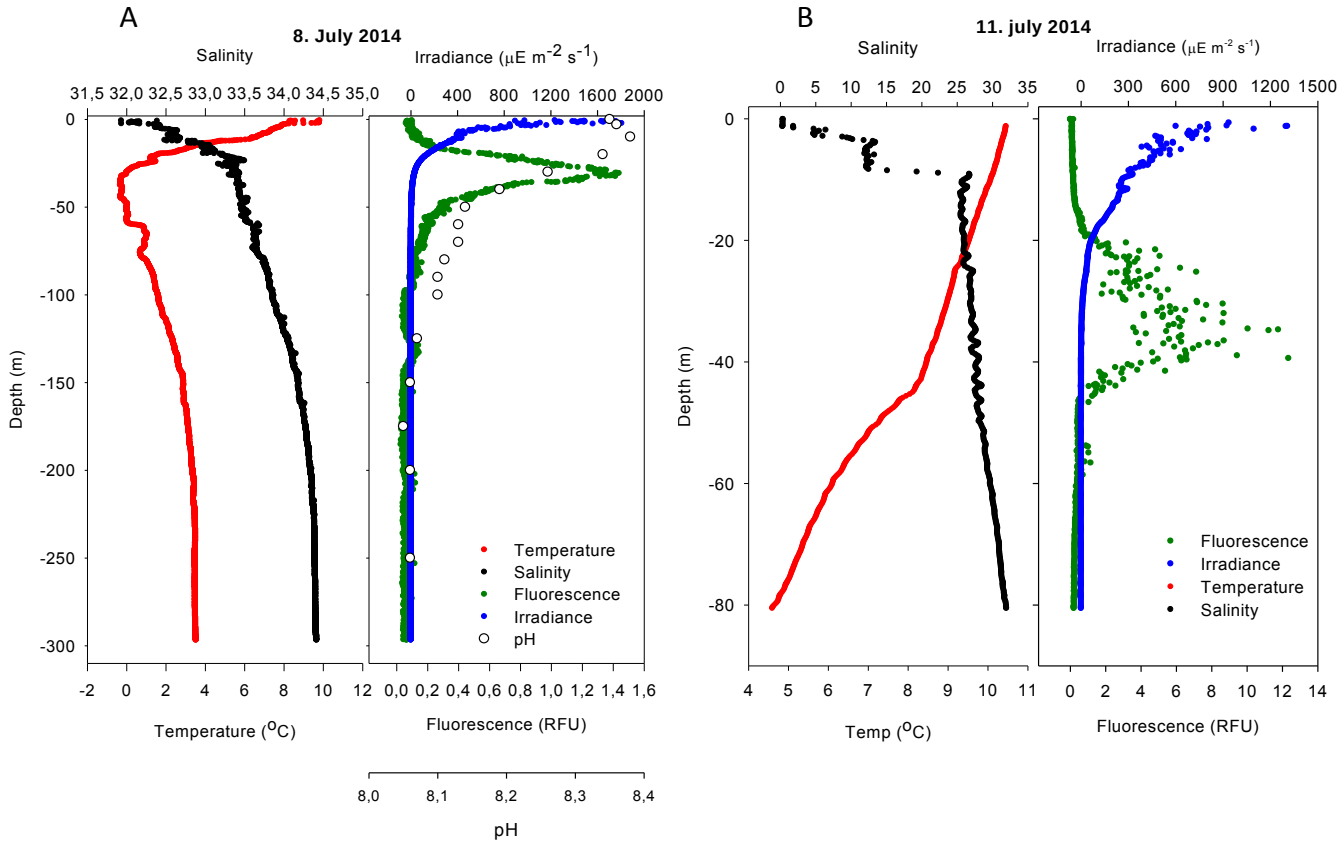

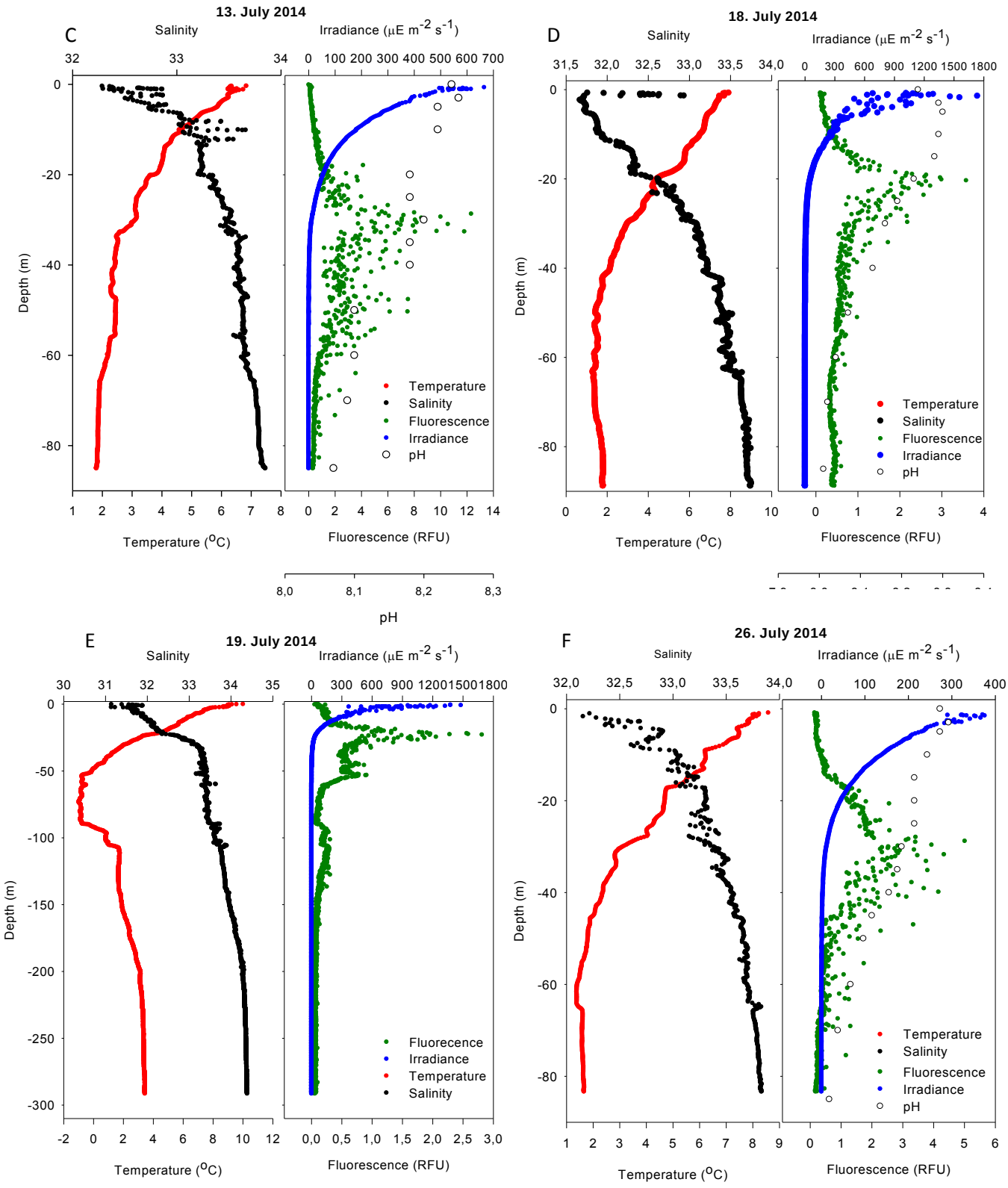

Figure 3: CTD profiles describing the Temperature (red), Salinity (black), Irradiance (blue), pH (black rings), and Fluorescence (green) down through the water column. A: The 8th of July (collection of deep water at 80 m), B: The 11th of July (collection of experimental water from chl. a maximum), C: 13th of July, D: 18th of July, E: 19th of July (collection of experimental water from chl. a maximum for treatment 7.7A), F: 26th of July.

Experimental pH, temperature and light conditions

Figure 4 shows the pH measured throughout the experiment. The four pH treatments (8.1, 7.7, 7.7A 7.4, 7.1) were kept at 8.08±0.01, 7.67±0.02, 7.66±0.01, 7.44±0.01, and 7.18±0.02 (means ±SE n= 30, 30, 18, 39 and 39), respectively. The acidic seawater for dilution had a pH of 4.96 ±0.04 Temperature measured continuously for all experimental bottles were 5.33 ± 0.87 ˚C (mean ±SD, n=153) and light 81.6 ± 13.7 µmol photons m^2 s^{-1}(mean ± SD n=5).

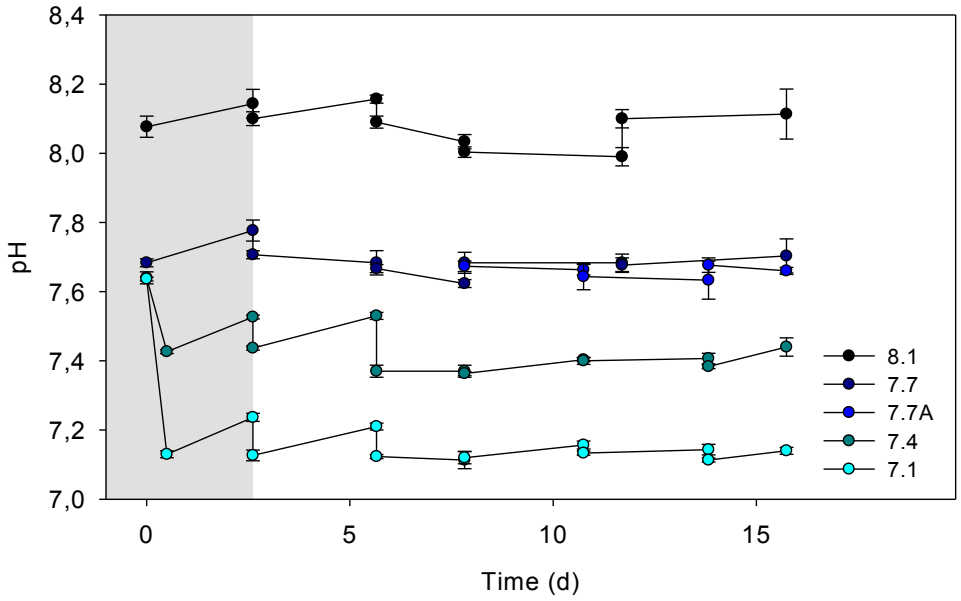

Figure 4: Experimental measurements of pH for the four treatments. Data points are mean ±SD, n=3.

DIC

The dissolved inorganic carbon (DIC) samples were collected on day 8 and 16, mimicking midway and end concentrations of DIC. Figure 5 provides a barplot of the total inorganic carbon measured in our samples. Only one replicate have been analysed for deep seawater (80 m) and for 7.7A on day 8 and 16. DIC increased with decreasing pH, from approximately 2.2 at 8.1 to 2.7 at pH 7.1. DIC fluxes between 2-3 mM applying to all the samples. Standard deviation were approximately ±0.06, for n=3.

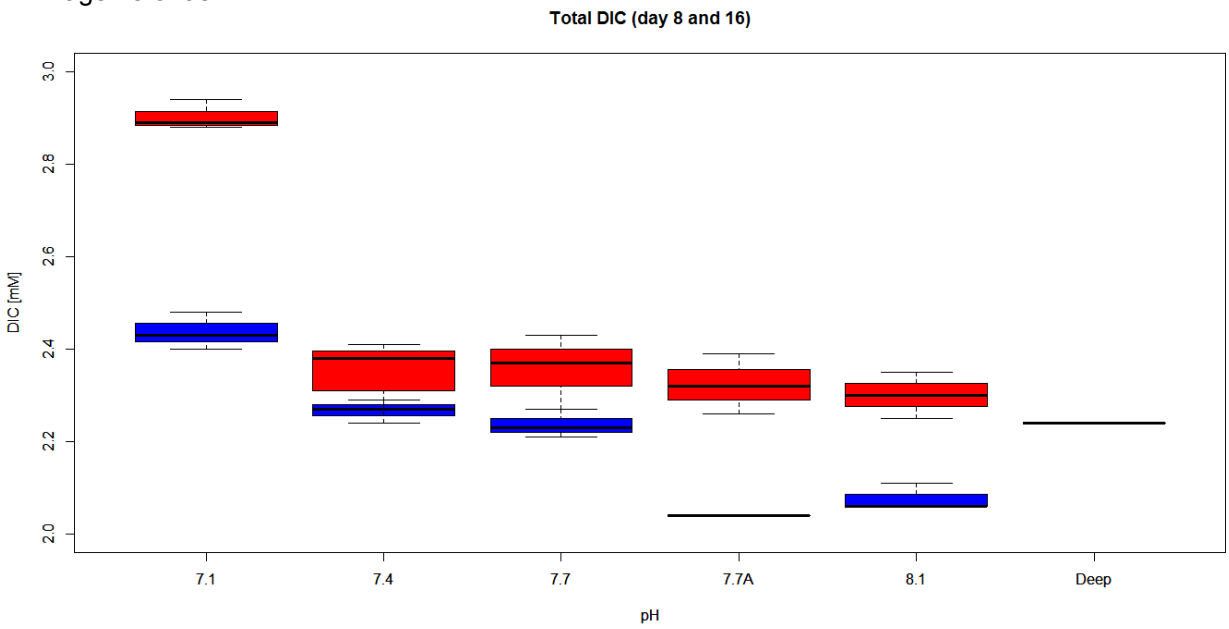

Figure 5: Boxplot of total dissolved inorganic carbon (DIC) concentrations [mM] from day 8 (blue) and 16 (red). All data points are mean ±SD, n = 3; except for 7.7A and Deep on day 8, and 16, respectively as n = 1.

The DIC concentrations were further analysed into relative distributions of chemical species, and Figure 6 shows the percentage of the different species for the two days, mean concentrations of the triplicates has been used. HCO_3^- was the dominating species, with values above 90 % at all pH treatments, whereas CO_2 and CO_3^{2-} reached maximum values at pH 7.1 and 8.1, respectively.

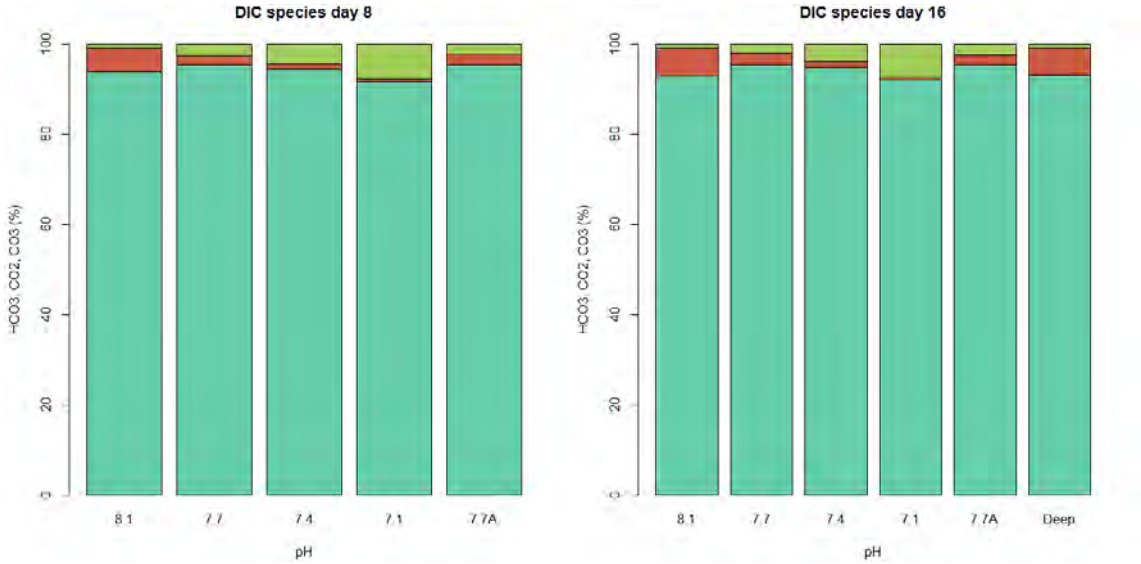

Figure 6: Barplot of three different carbon species (HCO_3^-, CO_2, and CO_3^{2-}) in percent (%), divided into pH. Blue=HCO_3^-, green = CO_2*, red = CO_3^{2-}.*

Nutrients

Figure 7 and 8 illustrates boxplots of the concentrations of total N and P. No significant differences were found between the concentrations (one-way ANOVA, $p > 0.05$). The total P concentrations varied between 0.1 and 0.25 µM, with relatively similar values between treatments. The total N concentrations were between 1.5-8 µM. The calculated nutrient ratio for our study was about 16250:20:1, for C, N, and P, respectively.

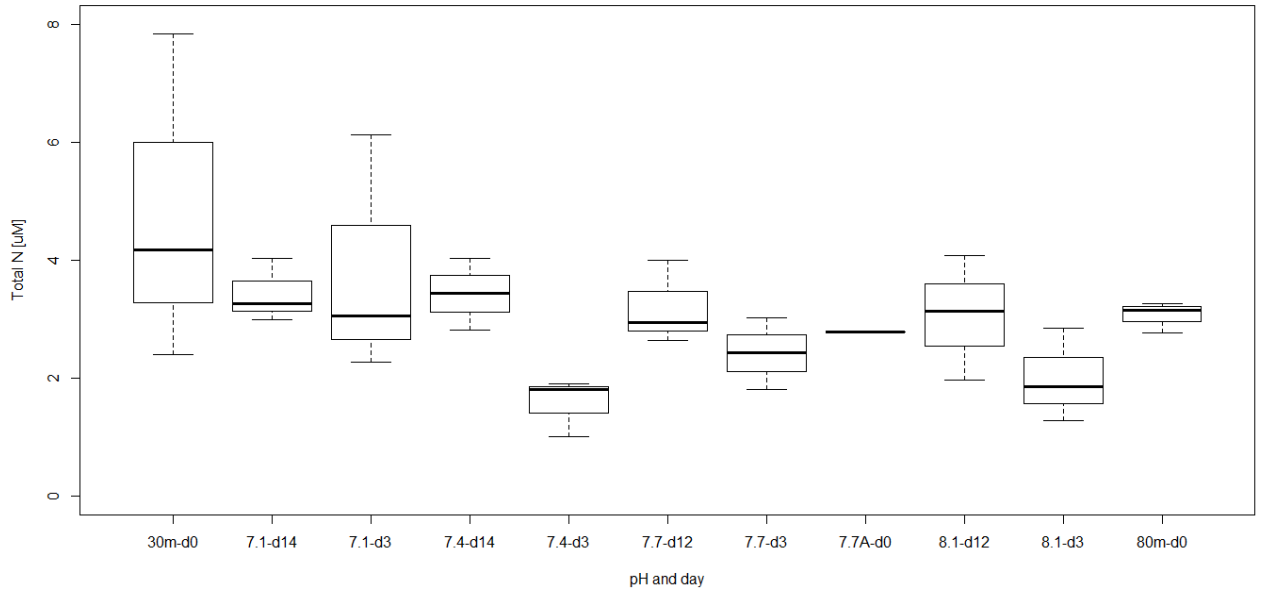

Figure 7: Boxplot of total nitrogen concentrations at different pH treatments and time points e.g. d0 corresponds to day 0. All data points represents mean ±SD, n=3, except for 7.7A-d0, which has n=1.

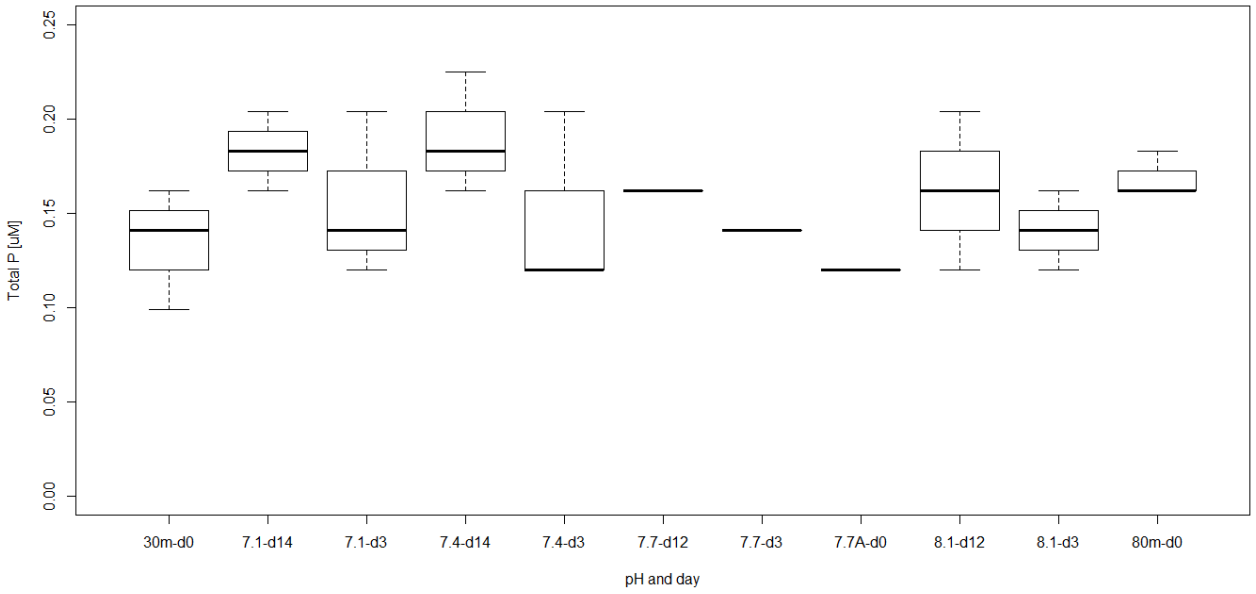

Figure 8: Boxplot of total phosphorous concentrations at pH treatments at different time points e.g. d0 corresponds to day 0. All data points represents mean ±SD, n=3, except for 7.7A-d0, which has n=1.

Concentration of chl. a and phaeophytin

The phytoplankton community in the four pH treatments generally had a low or no growth throughout the experimental period. The chl. *a* concentration were ~1 µg l^{-1} at the beginning of the experiment for all treatments, and the bottles with pH 8.1, 7.7A, 7.4 and 7.1 experience initial growth. At day 6, 8.1 decreases while 7.4 and 7.1 stays at constant concentrations. Treatment 7.7 reaches ~0 µg l^{-1} early in the experiment, and 7.7A had growth until the end of the experiment. For this reason, we regard treatment 7.7 as an outlier for which we minimize the interpretation of the

data henceforth. Figure 9 A-E shows the development of chl. *a* and phaeophytin concentrations as well as the chl. *a*/phaeophytin ratio for all experimental bottles throughout the experiment. Overall we observe high concentration of phaeophytin, which exceeded the concentration of chl. *a* in all but measurement from treatment pH 8.1 and 7.4 at day six. We identified measurement outliers at day 16 where the measured chl. *a* concentrations were 0 or close to 0 µg l^{-1} and had correspondingly high phaeophytin concentrations irrespective of the prior measurements at day 12 or 14. We suspected the cuvettes, used for the measurements, to have contained residues of acid and these were therefore excluded (Graphs containing data for day 16 is to be found in Appendix 1).

A

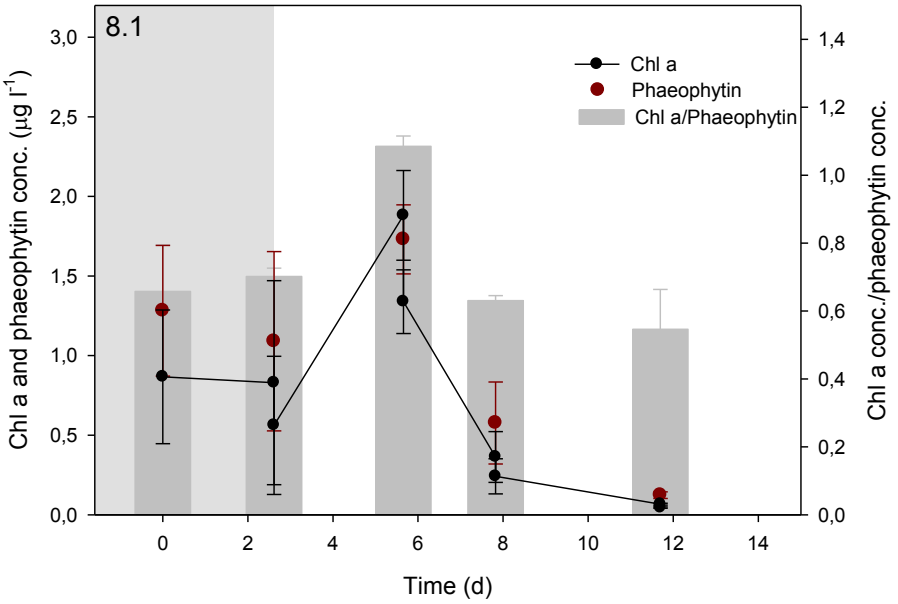

B

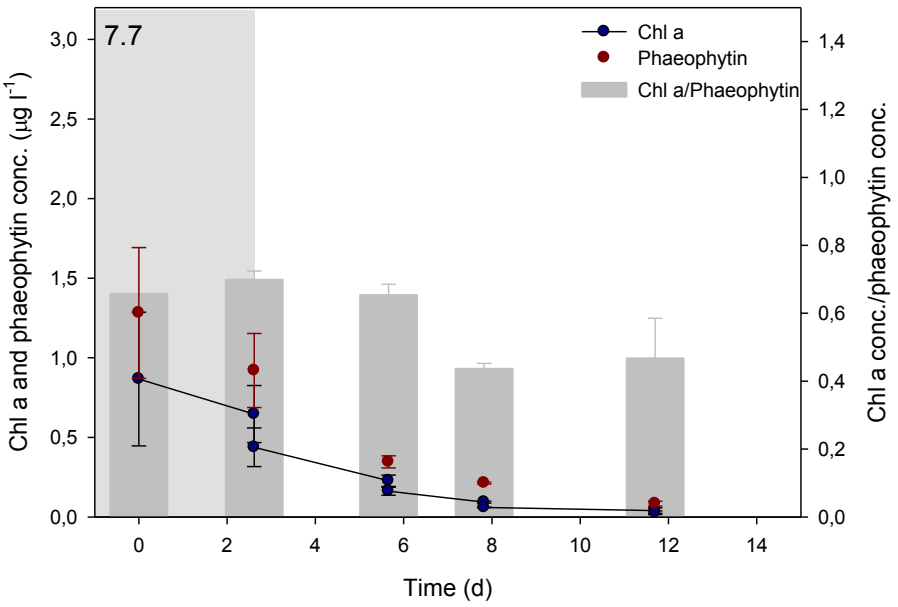

C

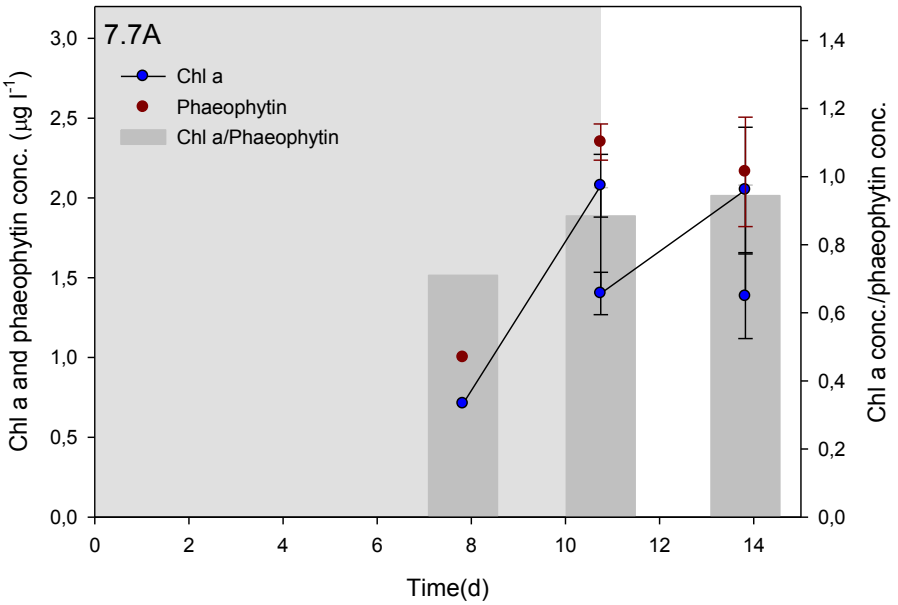
7.7A
Chl a
Phaeophytin
Chl a/Phaeophytin
Chl a and phaeophytin conc. (µg l-1)
Chl a conc./phaeophytin conc.
Time(d)
0,0
0,5
1,0
1,5
2,0
2,5
3,0
0,2
0,4
0,6
0,8
1,0
1,2
1,4
0
2
4
6
8
10
12
14

D

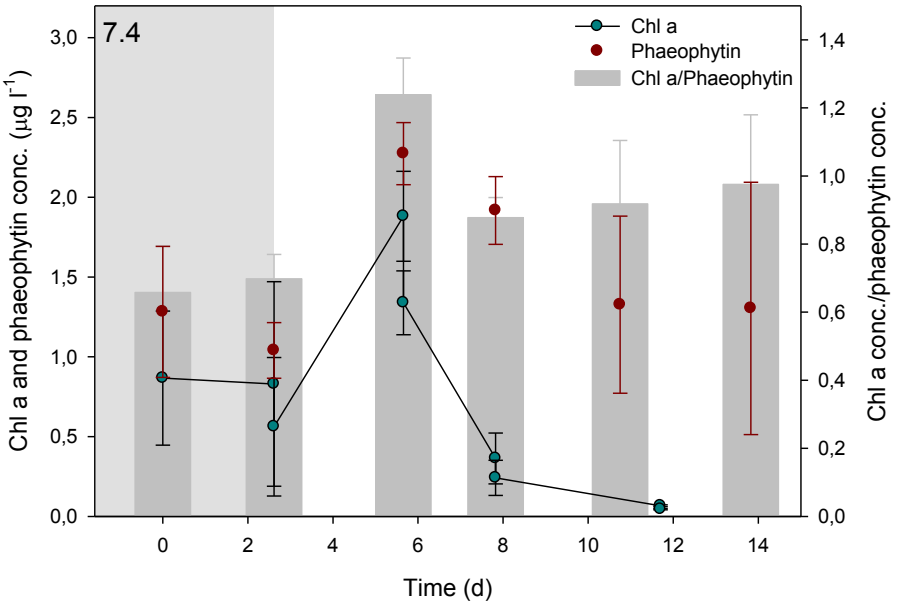
7.4
Chl a
Phaeophytin
Chl a/Phaeophytin
Chl a and phaeophytin conc. (µg l-1)
Chl a conc./phaeophytin conc.
Time (d)
0,0
0,5
1,0
1,5
2,0
2,5
3,0
0,2
0,4
0,6
0,8
1,0
1,2
1,4
0
2
4
6
8
10
12
14

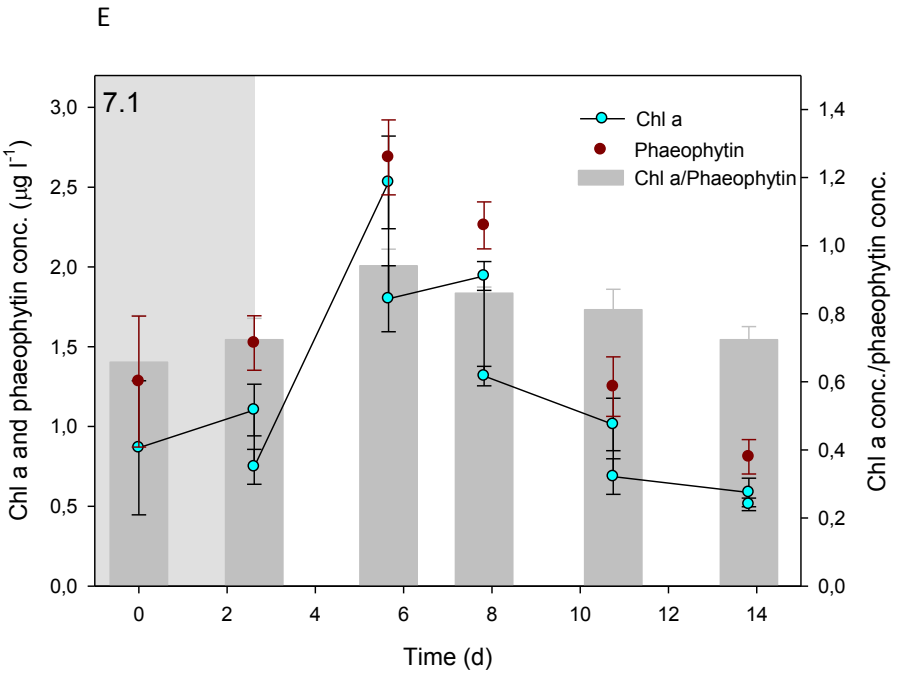

Figure 9 A-E Illustrates the experimental chlorophyll a (Chl. a) and phaeophytin concentrations from day 0 to 14 in the four treatments, pH 8.1, 7.7 (7.7A), 7.4 and 7.1. The data marks in blue illustrates the chl. a concentrations (µg l^{-1}). The red data points are phaeophytin concentrations (µg l^{-1}) and grey bars the chl. a:phaeophytin ratio. The first 2.5 days were the acclimation period (shown as the grey shaded area). All data points are means±SD (n=3).

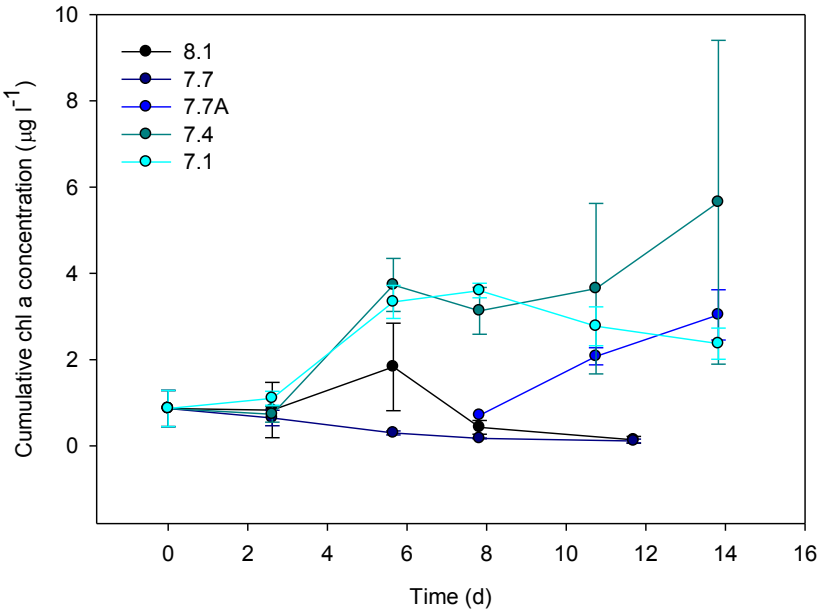

Figure 10 Cumulative chl. a concentrations over time for the different pH treatments

For the cumulative concentrations (see Figure 10) fitted by using OLS, the result showed a significant higher chl. *a* concentration in interaction with time for treatment 7.4 and 7.1 when compared to treatment 8.1 (Table 1). Accounting for temporal autocorrelation and residual variance heterogeneity considerably improved model fit shown by the decrease in AIC. Regardless of the model used, the above mentioned interaction terms remained significant.

Table 1: Results from three linear models where two are fitted using generalized least squares (GLS) all using treatment pH8.1 as intercept. The first GLS accounts for temporal autocorrelation in the samples, the second GLS additionally accounts for residual heteroscedasticity. Both were evaluated against a model fitted with ordinary least squares (OLS), not accounting for any internal structure data, using Akaike information criterion (AIC).

	OLS	
	Coefficients	*P-value*
pH7.7	-0.181	0.392
pH7.4	-0.170	0.409
pH7.1	0.050	0.808
time	-0.047	0.036
pH7.7:time	-0.007	0.824
pH7.4:time	0.148	0.000
pH7.1:time	0.098	0.001
AIC_1	91.440	
ΔAIC_{1-1}	0.000	
	GLS (temporal autocorrelation)	
pH7.7	-0.012	0.969
pH7.4	-0.133	0.628
pH7.1	0.114	0.631
time	-0.052	0.100
pH7.7:time	-0.021	0.595
pH7.4:time	-0.154	0.000
pH7.1:time	0.087	0.016
AIC_2	80.200	
ΔAIC_{1-2}	11.240	
	GLS (temporal autocorrelation + heteroscedasticity)	
pH7.7	-0.060	0.812
pH7.4	-0.199	0.570
pH7.1	0.089	0.703
time	-0.060	0.115
pH7.7:time	-0.009	0.803
pH7.4:time	0.167	0.001
pH7.1:time	0.103	0.005
AIC_3	66.913	
ΔAIC_{1-3}	24.527	

Species enumeration

Overall, and regardless of pH treatment, all four quantified species obtained similar concentrations throughout the experiment with an overall general decrease (Figure 11). Notably, all treatments (except pH 7.7A which only grew 6 days), lacked one or more of the enumerated species at day 16 when the experiment was terminated. *Thalassiosira* spp. were not observed after day 8 in treatment pH 8.1 and after day 14 at pH 7.1. Likewise, *Phaeocystis* spp. were not observed after day 8, 11 and 14 in treatment pH 7.1, 7.7 and 7.4, respectively, *Cryptophyta* spp. were missing after day 14 in treatment pH 7.1 and *Pseudo-nitzschia* spp. was not detected in any treatment group at day 16. The rare *Chaetoceros* spp. observed in the first periods in treatment pH 7.7 and 7.7A remained undetected after day 8 and 14. A minimum detection level of 20 cells per liter was required for *Phaeocystis* spp. in treatment pH 7.7A at day 11 and 14 and day 12 for treatment pH 8.1, for *Cryptophyta* spp. at day 12 and for *Pseudo-nitzschia* spp. at day 8 for pH 7.4, at day 11 for pH 7.7A and 7.1. The concentrations of heterotrophic ciliates were only counted on the last day because they seemed to dominate the community completely at this endpoint. In pH treatment 7.7, 7.4, and 7.1 the concentrations were relatively high in comparison to the concentrations of the photo-autotrophic plankton. Respectively, the treatments were estimated to contain 5600, 720 and 13440 cells per liter. In treatment pH 7.7, this was vastly higher than any other concerned plankton concentration (i.e. *Cryptophyta* spp. with 80 cells per liter and *Thalassiosira* spp. with 80 estimated cells per liter).

Chain length for *Thalassiosira* spp. was generally homogeneously small throughout the experiment with approximately three cells per chain. Especially by the end of the experiment, many chains looked fragmented with individuals having large bodies of stored lipids storage (exemplified in Figure 13B). A few large colonies were observed in treatment pH 7.7 at day 8 explaining both the high mean and standard deviation at this point. Figure 12-14 provides a general overview over the counted species found in our experiments.

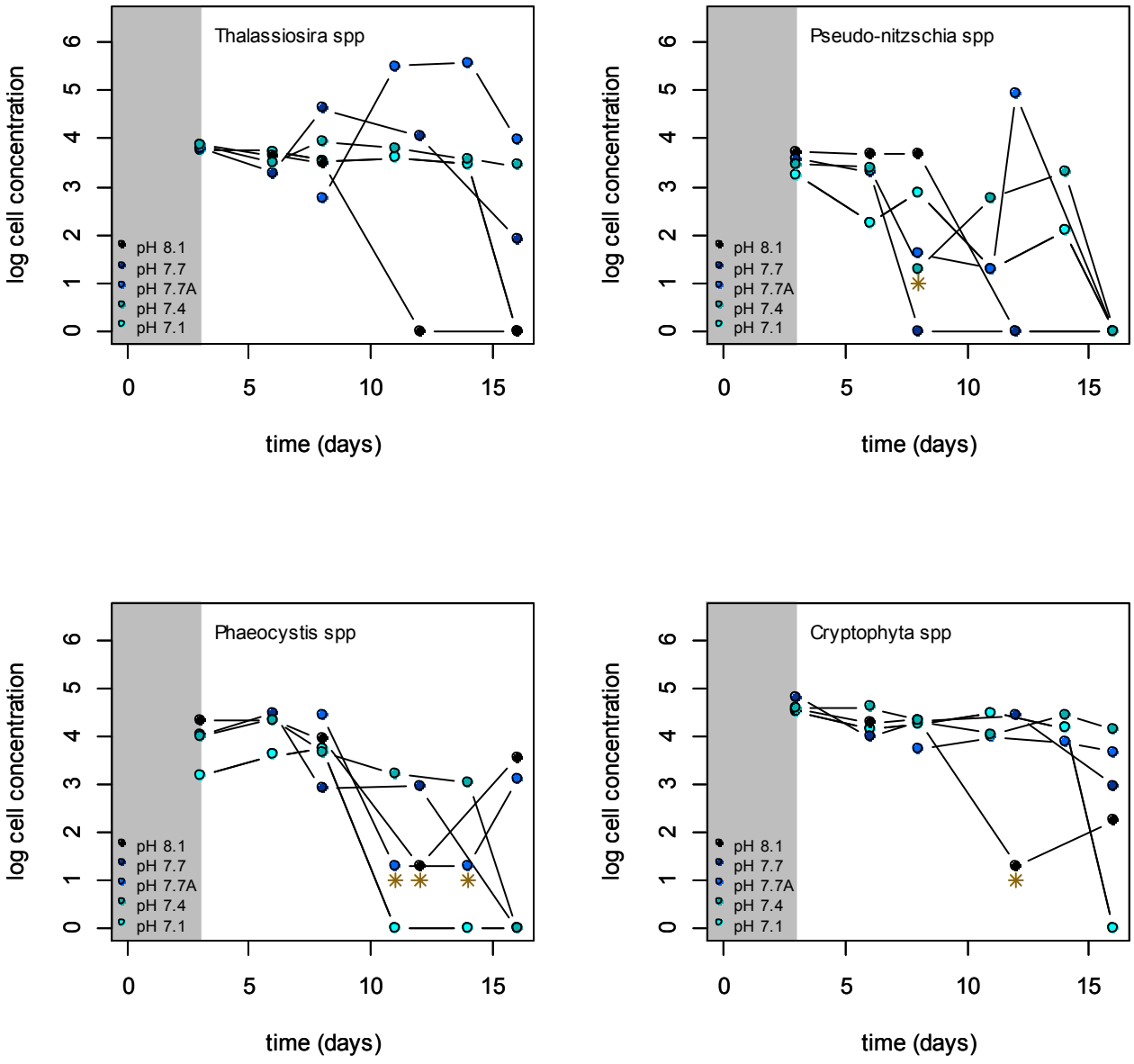

Figure 11: Graphs showing the temporal variation in cell concentration (cells l^{-1}) for four key plankton groups across the five pH treatments. The first samples were enumerated after three days of acclimatization (indicated by the grey shaded areas). Points associated with a yellow star represent samples where a minimum detection level of 20 cells L^{-1} was applied. All concentrations were log transformed to improve visualization where after zero values were inserted for samples from where the given plankton group was no longer detected.

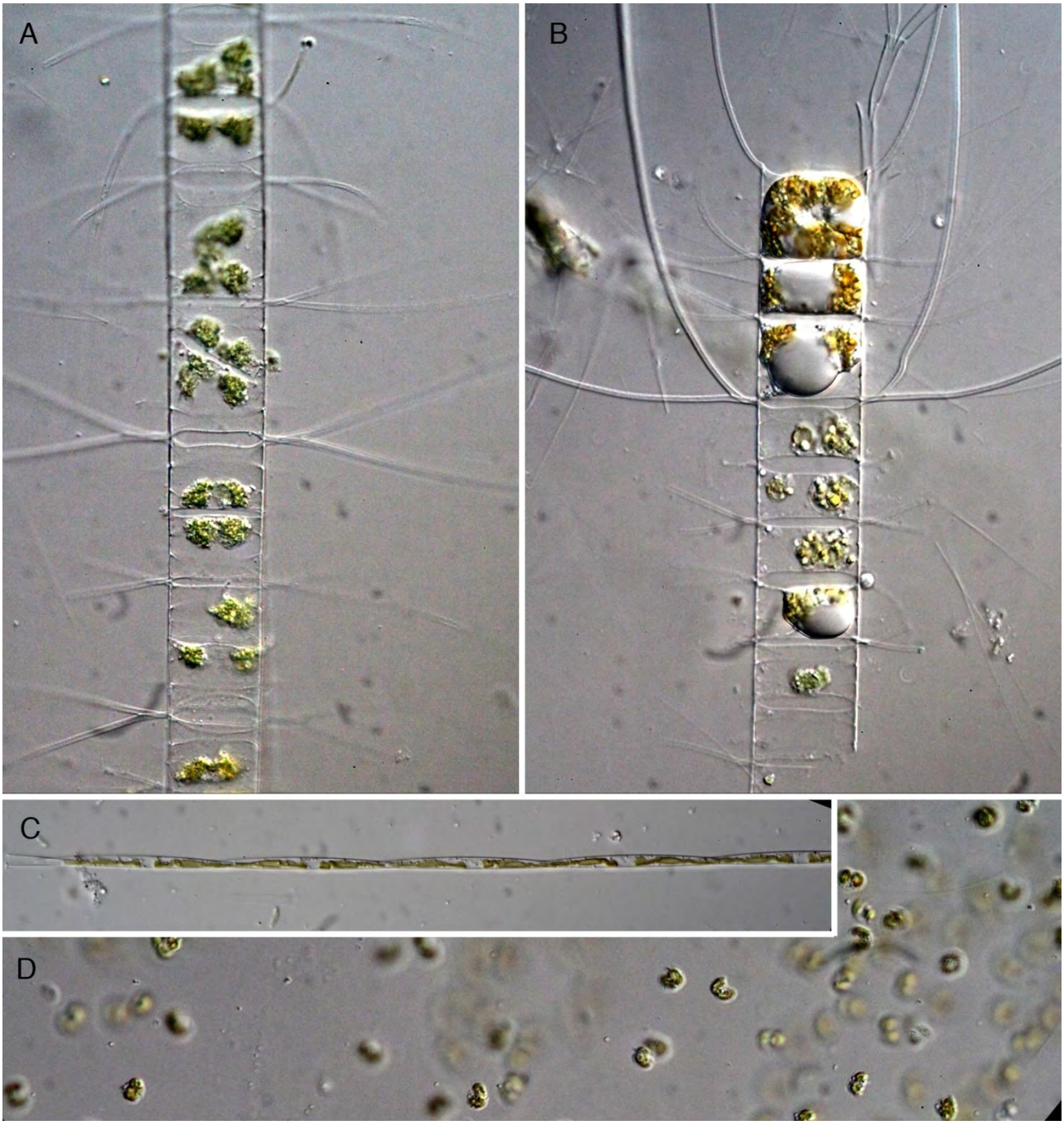

Figure 12 A: Chaetoceros decipiens. Fig. B: Chaetoceros terres. Fig. C: Pseudo-nitzschia seriata. Fig. D: Phaeocystis pouchetii.

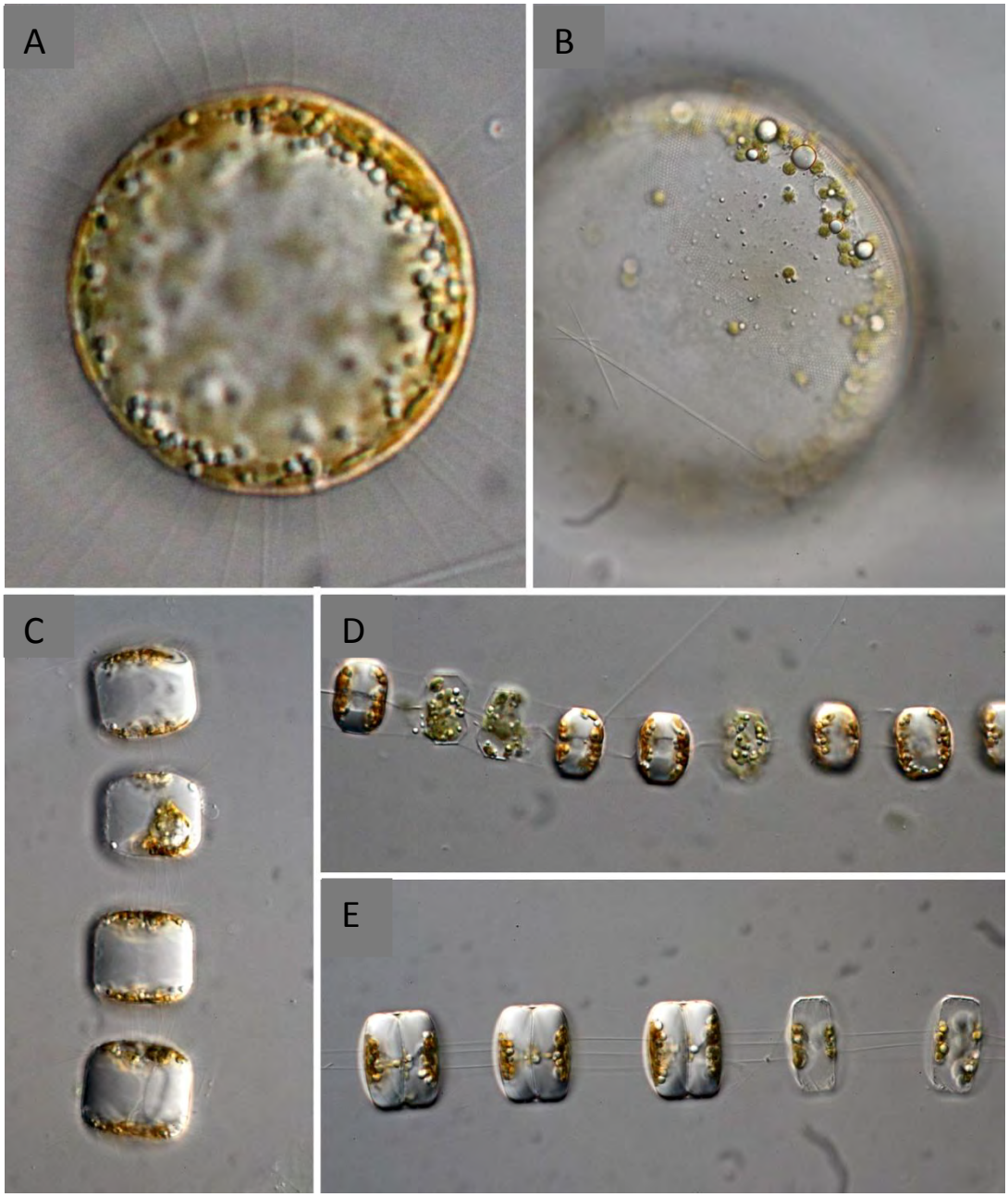

Figure 13 Centric diatoms containing numerous lipid droplets. Figs A-C: Porosira glacialis (A-B in valve view, C in girdle view). Fig. D: Thalassiosira nordenskioeldii (girdle view). Fig. E: Thalassiosira anguste-lineatum (girdle view).

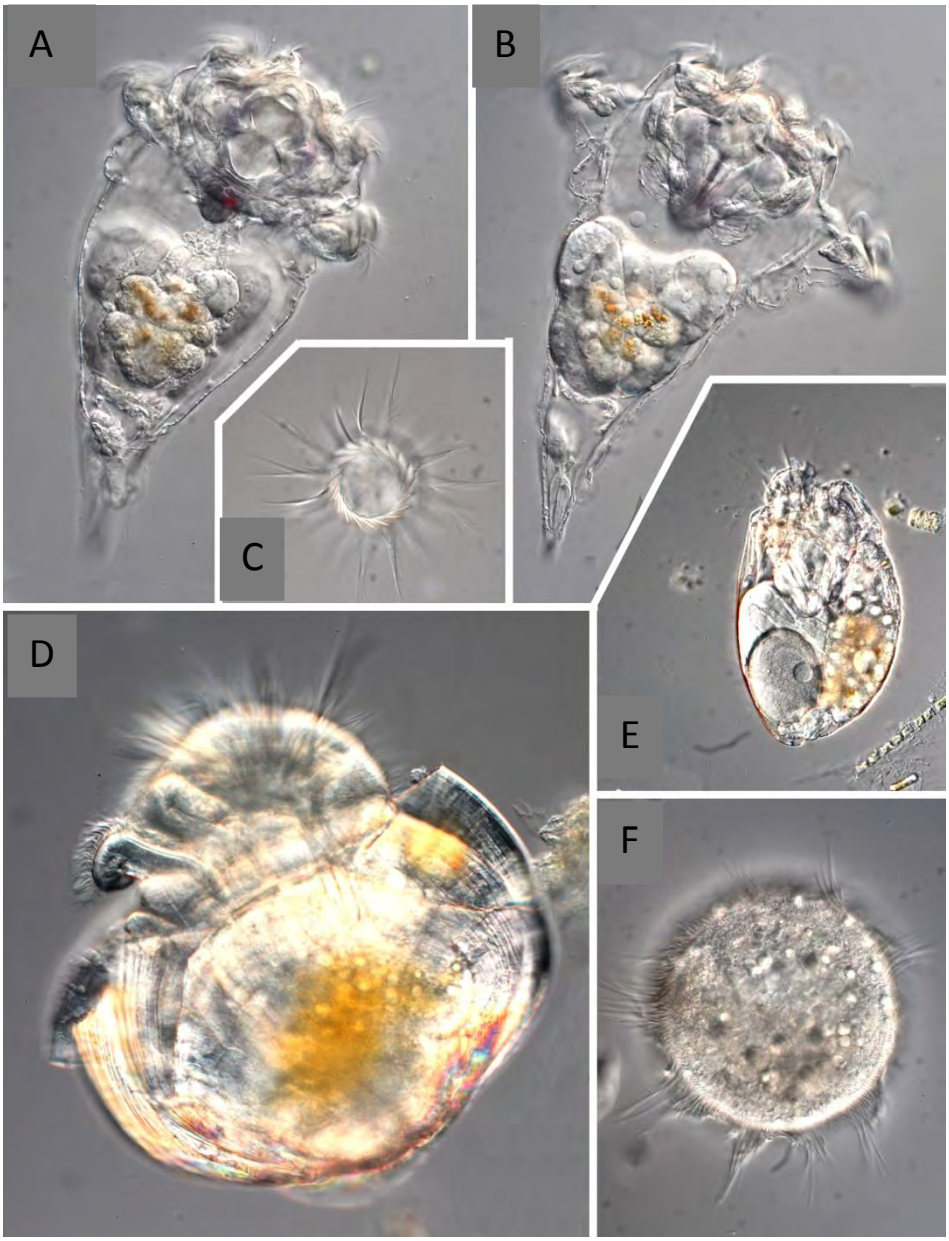

Figure 14 Protozoans. Figs A-B: Rotifer, Synchaeta. Fig. C: probably a rotifer belonging to Colurella. Figs D-E: Ciliates. Fig. F: Veliger larva from, mussel.

Discussion

Summer conditions in Disko bay, during the experimental period, were dominated by relatively low concentrations of nutrients (N and P) and phytoplankton biomass (Backhaus et *al.* 2015). On the day of experimental sampling, we found a chl. *a* concentration of 0.87 ±0.40 µg l^{-1} in the fluorescence maximum water samples, and the corresponding total nitrogen and phosphorous concentrations were quite low; 4.80 ±2.27 µM, and 0.13 ±0.03 µM, respectively. Not only was the upper water-column depleted in nutrients but this also accounted for the deeper layers. This violated our assumption that deeper seawater would be rich in nutrients. We expected the water below the pycnocline to be nutrient rich and therefore able to facilitate growth in our experiment. During spring, Thoisen et *al.* (2014) found nitrate and phosphorous concentrations approx. 2.5 and 5 times higher than ours, respectively.

The water collected from 80 m and therefore below the pycnocline (found between 20-60 m, figure 3A) contained equally low concentrations of total nitrogen and phosphorous as were found in the upper water layers (35 meters). This could be due to, drifting of the boat during sampling which would result in the depth of collection to be less. However, it was relatively calm weather and not much drifting on the day of sampling. The water below the pycnocline could potentially consist of admixed former surface water, which could cause depletion of nutrients as these have been fixed in the photic zone. By examining data collected at several other stations south of Disko Island, equally low values were found below the pycnocline as well as in the whole water column. Total nitrogen and phosphorus concentrations measured in the upper water layers, at chl. *a* maximum and below the pycnocline showed concentrations of about 0.2 µM P and 3-4 µM N at all three depths (Backhaus et *al.* 2015). The measured nutrient concentrations were expressed as both inorganic and organic phosphorus and nitrogen. Thus, parts of it could have been fixed within organisms and therefore not bioavailable. However, the deep seawater (80m) was filtrated through a 0.2-0.4 um filter, sorting out the biomass, and should therefore hardly contain any organic phosphorus or nitrogen. The deep seawater concentrations of total phosphorus and nitrogen were very similar to the values found at chl. *a* maximum. Since the deep seawater was filtrated, most nutrients were probably dissolved below the pycnocline in contrast to the nutrients at chl. *a* maximum, which were more likely fixed as organic compounds within organisms. The Redfield ratio is the ratio between carbon, nitrogen, and phosphorus (C:N:P) needed for algal growth are defined as 106:16:1. Our measured values of total P and N from the experiment do not have this relationship, we find a concentration ratio at 16250:20:1, which means P probably are the limiting nutrient in the present experiment. The DIC values are however considerably higher than the N and P concentrations prescribed by the Redfield ratio, stressing that the organisms in the experiment did not experience any carbon limitation.

Measurements of nitrate from summer 1996 in the same area showed corresponding low concentrations of 0-4 µM within the first 50 meters, lowest values were found near the surface and highest at 50 m. Furthermore, the summer period were found to be the most nitrate limited period throughout the year (Nielsen 2005). The concentrations of inorganic phosphorous, also measured in 1996, measured in the upper 200 m varied between 0-0.9 µM during summer. In July around 80 m, phosphate concentrations were measured to approx. 0.2-0.4 µM. Even though we, in the present study, use measures of the total concentrations of phosphorous and nitrogen, and a direct comparisons with the above presented studies are not possible, they all point to an overall low nutrient concentration in the area during summer, thus supports our findings.

In the measurements from 1996, phosphate and nitrate were present in very low concentrations above the pycnocline where as they below started to increase slowly towards the bottom (Hansen et *al.* 2012). We do not find nutrient rich water right below the pycnocline, however it may have been found in even deeper layers.

The measurements of vertical distribution of pH that were carried out in Laksebugten and Torkels station indicated small spatial and temporal differences during one month at summer. When comparing all pH profiles, there is a tendency of decrease in pH down through the water column from a stable value around chlorophyll maximum at 8.3 to 8.0 below the pycnocline. The higher pH at chlorophyll maximum could indicate activity of photosynthesis even though the overall plankton populations are declining (figure 3-A, C, D and F).
Taken together, pH is relatively stable during the summer period since low concentrations of inorganic nutrients result in little to no primary production of the standing algal biomass. This contradicts the spring situation where decreasing ice cover and increasing solar radiance facilitate the annual plankton bloom with associated larger fluctuation in pH. For instance, a study from 2012 measured fluctuations across two weeks in spring from 7.5 to 8.3 (Thoisen et *al.* 2014).
In general measurements of pH in the Arctic region is very limited. Charalampopoulou et *al.* (2011) measured pH from Norway to Svalbard in August 2008, as a transect in 5 meters depth, and pH ranged from approximately 8.0-8.4. These values correspond with our pH-measurements, which are close to pH 8.3 at the surface.

The experiment has documented an overall decreasing biomass for the grown communities of phytoplankton. In addition, we find no statistical support for the hypothesized negative effect of acidification on phytoplankton growth. In relation to previous studies within the topic, the results presented here are against most expectations (see introduction). Hence, for validating our experimental design, we searched for discrepancies with our basic assumptions regarding unlimited nutrients in deeper seawater, unlimited availability in dissolved inorganic carbon (DIC), appropriate intensity in photosynthetic active radiation, little to no fluctuations in temperature and minor deviations in pH from the set values for each treatment. The three latter points are assessed to be unlikely sources of error as light and temperature were kept constant (see results), and pH at desired levels throughout the experiment (Figure 4).
The DIC concentration in surface ocean waters is usually around 2 mM (Key et *al.* 2004), which corresponds well with our findings at pH 8.1, 2.0-2.4 mM. As pH decreases to 7.1, the speciation of carbon changes towards less CO_3^{2-} and, more CO_2, mimicking the predicted effects of increased atmospheric CO_2 and acidification. Considering that most phytoplankton species can utilize both CO_2 and HCO^-_3, which in our experiment represent more than 90% of the total DIC, we find no reason to think that limitation of inorganic carbon is likely in this case.

In contrast, based on the low concentrations of total phosphorus and nitrogen compounds (presented above), we assess limitation in the basal nutrients to be the single most important cause of the declining algal biomass throughout most of the experiment.

Chlorophyll a and phaeophytin **ratio** is generally assumed to give an indication of the physical state of the phytoplankton community. A chl. *a*:phaeophytin ratio above 1 indicates a developing community while a ratio below 1 suggests degradation (Niels Daugbjerg, pers. comm. 2014). We

observed a ratio less than one for most of the experiment; which indicate of a community in degradation.

Growth and enumeration of phytoplankton species

Following the pattern for chlorophyll a, the low and relatively homogeneous cell concentrations throughout the experiment before eventually dying out contradict our expectations about an exponential growth when using sea water from below the pycnocline for dilution. For all treatments, some species were not even observed at day 16 where the experiment was terminated. Combined with frequent observations of individuals with large bodies of lipids in storage and fragmented from once larger colonies (Figure 13), this clearly supports the previous interpretation of having an ocean plankton community in degradation after having reached maximum summer productivity. Previous studies have documented a limitation of silicate for the growth of ocean diatoms (Sarthou et *al.* 2005). As there seems to be no difference between the growth for diatoms and non-diatom species (Figure 11), it is not possible to distinguish between possible growth-limiting effects of silicate and other inorganic nutrients. The high abundance of heterotrophic ciliates in the final samples could indicate extensive grazing of phytoplankton in the nano-sized fraction throughout the experiment and therefore may contribute to the constant decrease of phytoplankton biomass. The small growth we see during the experiment are probably caused by the low concentration of nutrients there are added when diluting the experimental bottles as well as nutrients remineralized during grazing. In addition, the persistence of low concentrations of chlorophyll a could derive from retained chloroplasts from consumed phytoplankton in the cytoplasm of heterotrophic flagellates (Hausmann et *al.* 2003), which could cause a biased estimation of the biomass of living phytoplankton. Taken together, we observe a decrease in the number of all enumerated photosynthetic plankton species where conversely heterotrophic ciliates and dinoflagellates were increasingly encountered throughout the experiment. Supported by the results from the nutrient analyses, the plankton enumeration suggests that only heterotrophic species are able to sustain life under the given conditions with low availability of inorganic phosphorus and nitrogen compounds.

Conclusion

Under the given experimental conditions, we find no empirical evidence of the hypothesized impact of acidification on growth of phytoplankton in an Arctic summer community. We assess that this unexpected result is most likely caused by limitation of nutrients. This draws a picture of a plankton community which has used up much of the nutrients (N and P) and thus maintains itself on regenerated nutrients. This study has contributed with important knowledge of how the impact of acidification seems to be insignificant for nutrient limited plankton communities and additionally of how pH naturally fluctuates down through the water column across the arctic summer.

Acknowledgements
A warm thanks to the entire staff at the Arctic Research Station at Disko Island for invaluable help during our stay, summer 2014. We would as well give a great thank to our supervisor Niels Daugbjerg and to Per Juel Hansen for valuable help and encouragement during all phases of the work. We want as well to thank Christina Thoisen for help with experimental set-up and Thorkel Gissel Nielsen for loan of equipment. Furthermore we would like to thank Marianne Saietz and Ayoe Lüchau for laboratory assistance.

References

Backhaus L.L.V., Fassel N.A.M., and Jensen D.B. (2015). Identity, abundance and biomass of diatoms in Disco Bay and fjords, Western Greenland. Report from Arctic fieldcourse 2014. Not published.

Beardall J. & Raven J.A. (2004). The potential effects of global climate change on microalgal photosynthesis, growth and ecology. Phycologia, 43, 26-40.

Berge T., Daugbjerg N., Andersen B.B. & Hansen P.J. (2010). Effect of lowered pH on marine phytoplankton growth rates. *Marine Ecology Progress Series*, 416, 79-91.

Caron D.A. & Hutchins D.A. (2012). The effects of changing climate on microzooplankton grazing and community structure: drivers, predictions and knowledge gaps. *Journal of plankton research*, fbs091.

Charalampopoulou A., Poulton A.J., Tyrrell T., Lucas M.I. (2011). Irradiance and pH affect coccolithophore community composition on a transect between the North Sea and the Arctic Ocean. *Marine Ecology Progress Series*, 431, 25-43.

Dickson A. & Millero F. (1987). A comparison of the equilibrium constants for the dissociation of carbonic acid in seawater media. Deep Sea Research Part A. Oceanographic Research Papers, 34, 1733-1743.

Diniz J.A.F., Rangel T. & Bini L.M. (2008). Model selection and information theory in geographical ecology. *Global Ecology and Biogeography*, 17, 479-488.

Duarte C.M., Hendriks I.E., Moore T.S., Olsen Y.S., Steckbauer A., Ramajo L., Carstensen J., Trotter J.A. & McCulloch M. (2013). Is ocean acidification an open-ocean syndrome? Understanding anthropogenic impacts on seawater pH. Estuaries and Coasts, 36, 221-236.

Feely R.A., Sabine C.L., Hernandez-Ayon J.M., Ianson D. & Hales B. (2008). Evidence for Upwelling of Corrosive "Acidified" Water onto the Continental Shelf. Science, 320, 1490-1492.

Hansen M.O., Nielsen T.G., Stedmon C.A. and Munk P. (2012). Oceanographic regime shift during 1997 in Disko Bay, Western Greenland. Limnol. Oceanogr.,57, 634-644.

Hausmann K., Hülsmann N. & Radek R. (2003). *Protistology*. E. Schweizerbart'sche Verlagsbuchhandlung.

Houghton J.T., Ding Y., Griggs D.J., Noguer M., van der LINDEN P.J., Dai X., Maskell K. & Johnson C. (2001). Climate change 2001: the scientific basis. Cambridge University Press Cambridge.

Kim J.-H. (2006). The effect of seawater CO2 concentration on growth of a natural phytoplankton assemblage in a controlled mesocosm experiment. Limnol. Oceanogr., 51 (4) 1636., 1629.

Langer G., Geisen M., Baumann K.H., Kläs J., Riebesell U., Thoms S. & Young J.R. (2006). Species-specific responses of calcifying algae to changing seawater carbonate chemistry. Geochemistry, Geophysics, Geosystems, 7.

Lewis, E. & Wallace, D.W.R. (1998). Program Developed for CO2 System Calculations. From http://cdiac.esd.ornl.gov/oceans/co2rprtnbk.html#aboutco2sys.

Middelboe, A.L. & Hansen P.J. (2007). High pH in shallow-water macroalgal habitats. Marine Ecology-Progress Series, 338, 107-117.

Moore C.M., Mills M.M., Arrigo K.R., Berman-Frank I., Bopp L., Boyd P.W., Galbraith E.D., Geider R.J., Guieu C., Jaccard S.L., Jickells T.D., La Roche J., Lenton T.M., Mahowald N.M., Maranon E., Marinov I., Moore J.K., Nakatsuka T., Oschlies A., Saito M.A., Thingstad T.F., Tsuda A. & Ulloa O. (2013). Processes and patterns of oceanic nutrient limitation. *Nature Geosci*, 6, 701-710.

Nielsen L.T., Jakobsen H.H. & Hansen P.J. (2010). High resilience of two coastal plankton communities to twenty-first century seawater acidification: evidence from microcosm studies. Marine Biology Research, 6, 542-555.

Nielsen, T.G. (2005). Struktur og funktion af fødenettet i havets frie vandmasser. Roskilde: Danmarks Miljøundersøgelser, Miljøministeriet. 71 p

Raven J., Caldeira K., Elderfield H., Hoegh-Guldberg O., Liss P., Riebesell U., Shepherd J., Turley C. & Watson A. (2005). *Ocean acidification due to increasing atmospheric carbon dioxide*. The Royal Society.

Riebesell U. (2004). Effects of CO2 enrichment on marine phytoplankton. Journal of Oceanography, 60, 719-729.

Riebesell U., Schulz K.G., Bellerby R., Botros M., Fritsche P., Meyerhöfer M., Neill C., Nondal G., Oschlies A. & Wohlers J. (2007). Enhanced biological carbon consumption in a high CO2 ocean. Nature, 450, 545-548.

R Core Team (2014). R: A Language and Environment for Statistical Computing. R Foundation for Statistical Computing.

Rose J.M., Feng Y., Gobler C.J., Gutierrez R., Hare C.E., Leblanc K. & Hutchins D.A. (2009). Effects of increased pCO2 and temperature on the North Atlantic spring bloom. II. Microzooplankton abundance and grazing. Marine Ecology, Progress Series, 388, 27-40.

Sabine C.L., Feely R.A., Gruber N., Key R.M., Lee K., Bullister J.L., Wanninkhof R., Wong C., Wallace D.W. & Tilbrook B. (2004). The oceanic sink for anthropogenic CO2. science, 305, 367-371.

Sarthou G., Timmermans K.R., Blain S. & Tréguer P. (2005). Growth physiology and fate of diatoms in the ocean: a review. *Journal of Sea Research*, 53, 25-42.

Stroeve J., Holland M.M., Meier W., Scambos T. & Serreze M. (2007). Arctic sea ice decline: Faster than forecast. Geophysical research letters, 34.

Thoisen C, Riisgaard K, Nielsen TG, Hansen PJ. (2014). Effect of acidification of an Arctic phytoplankton community from Disko Bay, West Greenland. Marine Ecology Progress Series.

Tortell P.D., DiTullio G.R., Sigman D.M. & Morel F. (2002). CO2 effects on taxonomic composition and nutrient utilization in an Equatorial Pacific phytoplankton assemblage. Marine Ecology-Progress Series, 236, 37-43.

Zuur A., Ieno E.N., Walker N., Saveliev A.A. & Smith G.M. (2009). *Mixed effects models and extensions in ecology with R*. Springer

Web 1: http://www.arcgis.com/ 17.12.2014

Appendix 1:

A

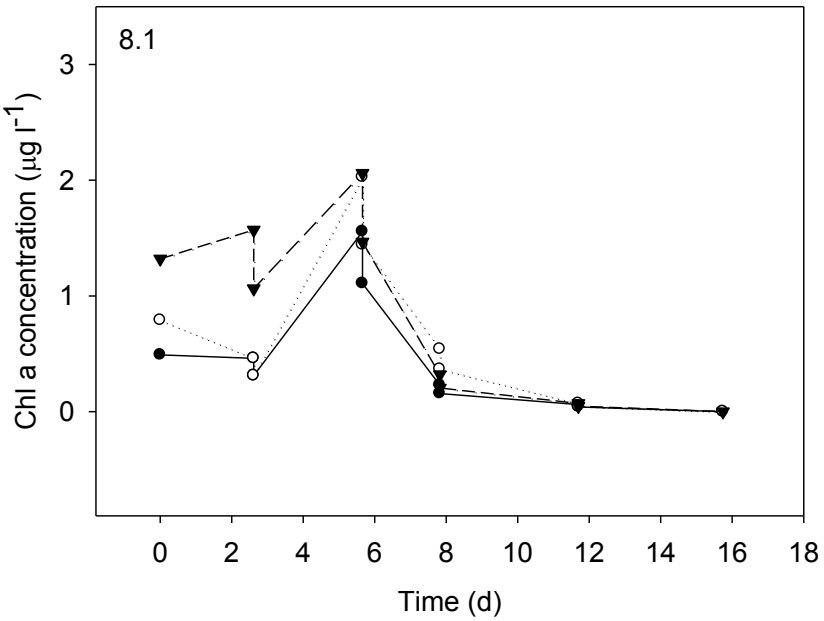

B

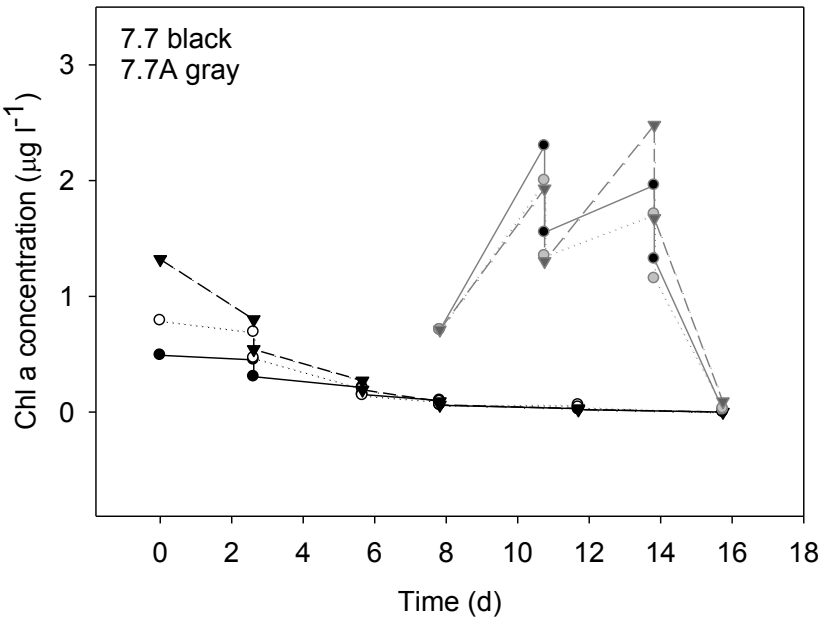

C

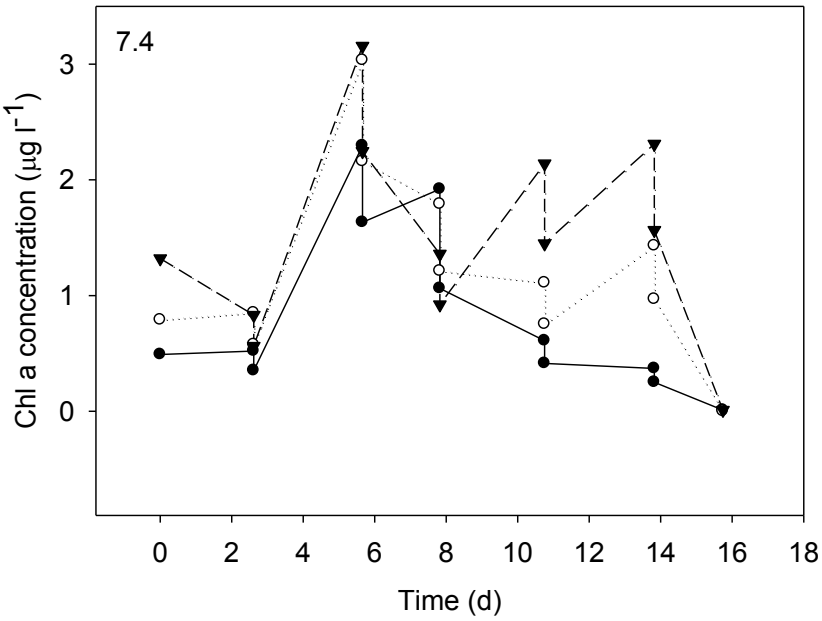

D

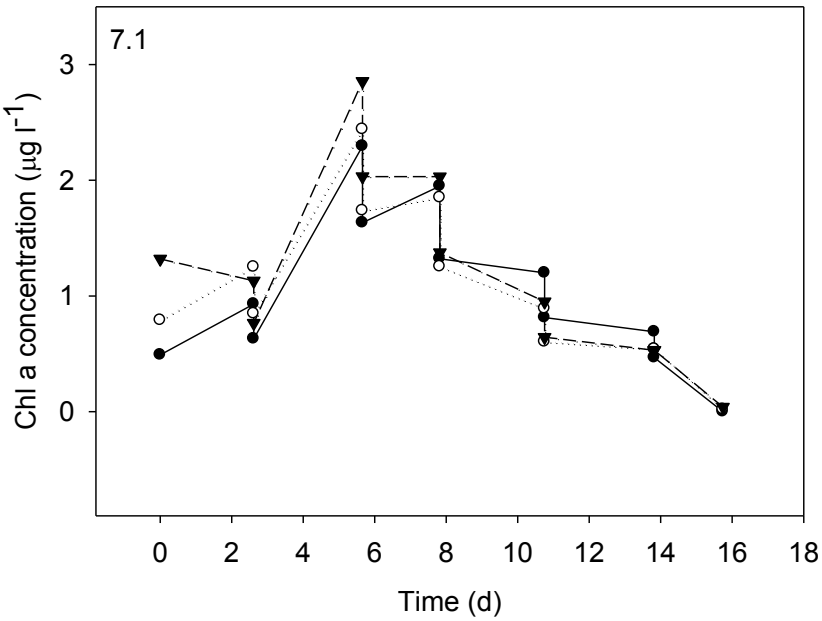

Figure A-D: The chl. a concentrations for the four pH treatments throughout the experiment including day 16 which have been excluded. Two values are found for each sample time, the high value measured and the low value calculated to represent the concentration after dilution.

E

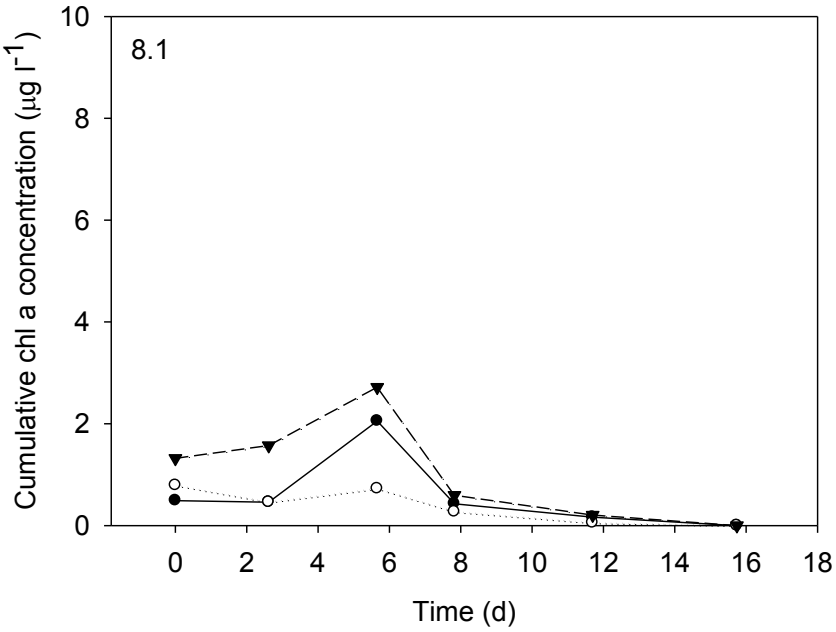
8.1
Cumulative chl a concentration (µg l-1)
Time (d)
0
2
4
6
8
10
12
14
16
18

F

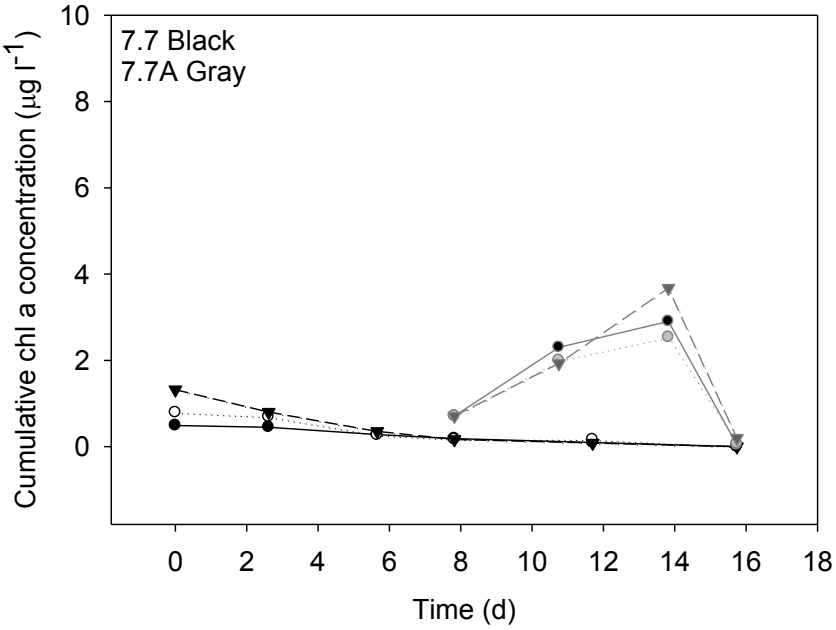
7.7 Black
7.7A Gray
Cumulative chl a concentration (µg l-1)
Time (d)
0
2
4
6
8
10
12
14
16
18

G

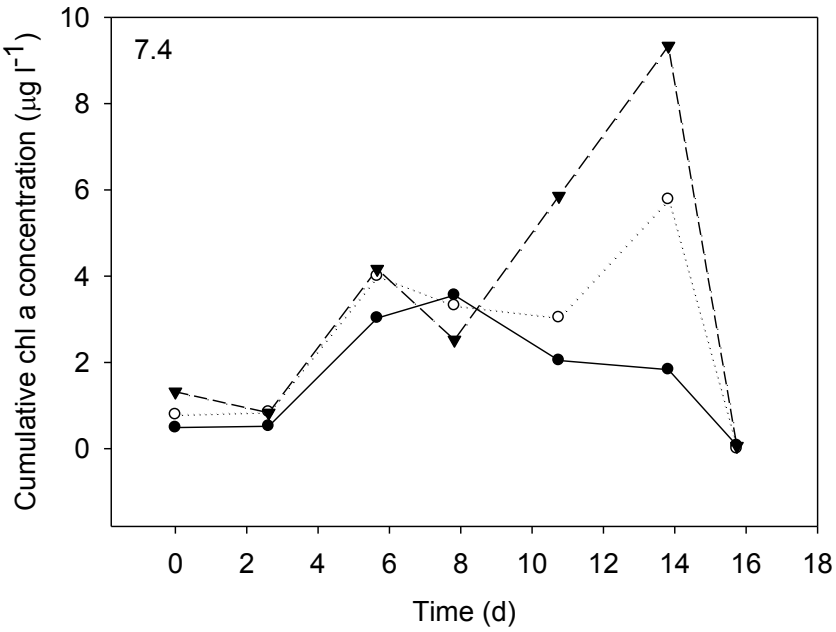

H

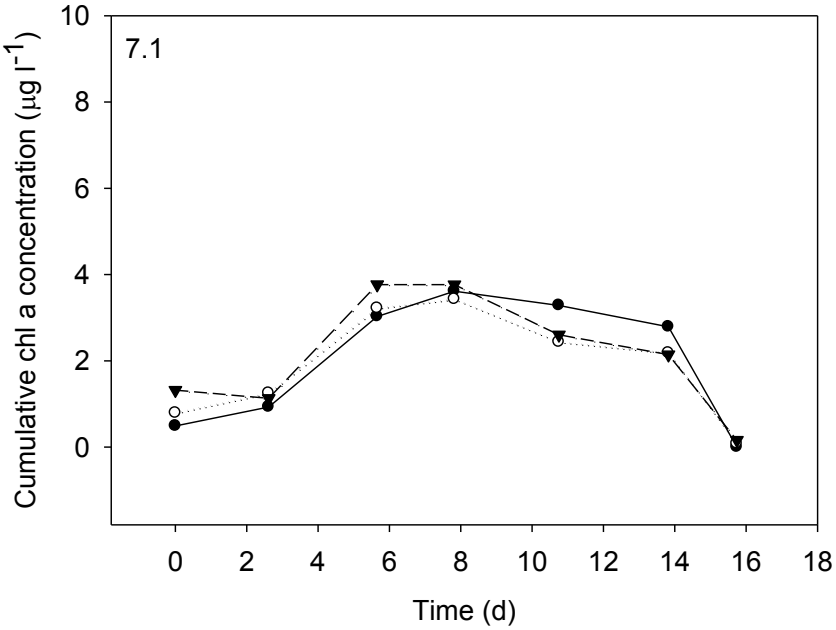

Figure E-H: The cumulative chl. a concentration for the four pH treatments throughout the experiment including day 16 which have been excluded.

DET NATUR- OG BIOVIDENSKABELIGE FAKULTET
KØBENHAVNS UNIVERSITET

Identity, abundance and biomass of diatoms in Disco Bay and fjords, Western Greenland

Liv Backhaus, Nicolai Fassel and Ditte Bjerregaard Jensen

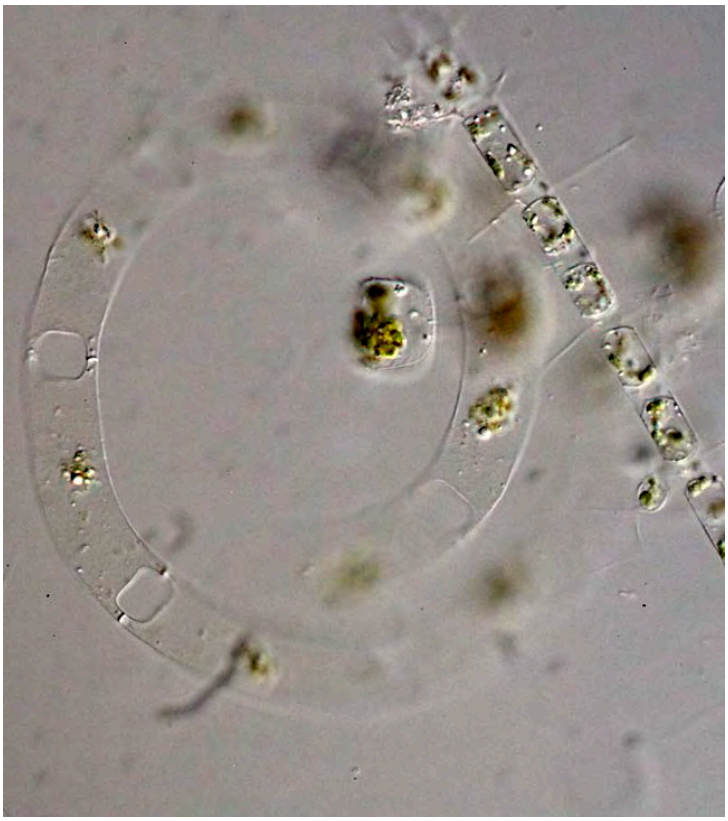

Arctic Field Course, July 2014
Supervisor: Niels Daugbjerg
Submitted: 17. May 2015

Abstract

A study on the Arctic marine diatom assemblage contribute to the understanding of their spatial and temporal distribution. In this study, diatoms were analyzed from water samples collected while onboard the research ship *Porsild* with a Niskin water bottle sampler combined with a CTD along the waters of Disco Island, West Greenland (N and W) during summer 2014. The phytoplankton biomass was measured using Chlorophyll *a* extraction followed by fluorescent measurements and by sedimentation in an Utermöhl chamber followed by estimations of biomass converted from cell biovolumes.

Based on our field campaign, three stories were made: (1) The Fjordsystem: 'A comparison of the biomass present in inner and outer fjord respectively', (2) The waters surrounding Disco Island: 'A comparison of the biomass present in the Fjordsystem and the open ocean respectively' and (3) Temporal succession at Fortune Bay: 'An examination of the changes in phytoplankton biomass over time'.

Overall our results show similar patterns; that we are in the end of the growth season i.e. with low amounts of nutrients and a decaying community of phytoplankton e.g. low ratios of chlorophyll *a*:phaephytin *a*. We found that there was a significant change in the carbon biomass during the investigated time period in Disco Bay. This corresponds to disappearance of nutrients, down to very low levels of phosphorous (0.20±0.01 µg P/l) and nitrate (4.02±0.1µg N/l) and in the depth with the fluorescence maximum at the last date of sampling. We noted high abundances of *Chaetoceros spp* in the end of our sampling period. From the literature this indicates a shift in species composition from a summer to an autumn bloom. We did not find a significant difference in biomass between the outer and in the inner fjord and in the comparison between a fjord system and the open ocean. Adjustment of the sampling method is needed for further investigations.

High diversity of diatoms, with a total of 18 different species, was noted in total from all the 12 stations and very interestingly we found a new record of the genus *"Skeletonema"* not earlier seen (to our knowledge) in these waters.

Introduction

Diatoms

Diatoms are relatively old organisms with the earliest generally accepted record dating back 190 Myr ago from the Early Jurassic (Sims et al., 2006). But they might even have arisen as early as 250 Myr ago in the Triassic period as indicated by molecular-clock-based estimates (Sorhannus, 2007), (Sims et al., 2006). When the larger eukaryotic phytoplankton, namely the diatoms and dinoflagellates emerged, this initiated a period where atmospheric O_2 increased and the CO_2 concentrations declined as a shift in the global organic carbon cycling occurred. Before the appearance of diatoms, cyanobacteria and small green algae had been the main constituents of the phytoplankton (Armbrust, 2009). At the great Cretaceous mass extinction approximately 65 Myr ago where about 85 % of all species went extinct, the diatoms survived the happening and subsequent began colonizing the open ocean (Armbrust, 2009). The marine planktonic diatom diversity peaked later on at the Eocene/Oligocene boundary around 30 Myr ago (Rabosky & Sorhannus, 2009).

Today diatoms play an important role in the world's oceans where they function as food for life in the sea as they produce 25-40 % of the organic matter that serves as a base in marine food webs (Armbrust, 2009). They contribute considerably to the world's overall photosynthesis as their overall generation of organic carbon is as large as that from all the terrestrial rainforests together (Field et al., 1998).

Diatoms are, with an estimation of 100,000 different species, the most diverse group of phytoplankton. They can be found as single cells or as colonies and they range in size generally from 10 to 200 µm (Kooistra et al., 2007). Unlike other phytoplankton groups, the diatoms have cell walls that are made out of two silicified "shells" called the frustules. The upper frustule is called epitheca and the bottom frustules the hypotheca. The two frustules are ornamented in different ways, the ornamentation are species specific and provide a convenient method for identification. The frustules provide the diatoms with mechanical protection that requires specialized tools in order to break them. Both the copepods and the euphausiids, which are two of the major zooplankton groups in the ocean, possess these "tools" as they have silica-edged mandibles and gizzards with sharp "teeth" that have probably co-evolved with diatom prey in an evolutionary arms race (Hamm et al., 2003). The reproduction of diatoms primarily happens by mitotic division, where they are able to bloom rapidly making a vast increase in cell numbers in only a few days - but sexual reproduction occurs as well. At the mitotic division one daughter cell is smaller than the other because of the difference in the size of the frustules. Therefore, one will find a wide variety of cell sizes within a diatom population (Kooistra et al., 2007). As long as sufficient light and nutrients are available diatoms are often the dominating phytoplankton group in the phytoplankton communities (Sarthou et al., 2005) whether in upwelling regions, in well-mixed coastal waters or along the sea-ice edge (Armbrust, 2009).

The Arctic food web

The Arctic region includes the Arctic Ocean, Greenland, and the northern part of Europe, Russia, Alaska and Canada. The southernmost part of the arctic is defined by the Arctic Circle and provides an imaginary line, which is located at 66 °, 30'N latitude. A single word to describe the climate in the arctic is extremity. The freezing temperatures, ice, snow and continuous daylight in the summer replaced with long periods with no light at all in the winter. In spite of this, the basic structure of the pelagic and benthic realms of the Arctic oceans is similar to other oceans. However, unique adaptations and diversity to the Arctic environment is seen e.g. plankton living within brine channels in the sea ice. When light arrives at early spring the sea ice allows the light to penetrate down to the phytoplankton. Gradually the thickness of the ice and snow is reduced and unsets an ice algal

community and a higher microbial activity beneath the sea ice. The contribution of sea ice algae (also known as the photosea ice biota) to the yearly phytoplankton biomass production is variable due to seasonal variability (Nielsen, 2004) and their role in the phytoplankton bloom has been discussed in the literature (Horner and Alexander 1972 and Michel et al 1993). When the sea ice disappears in the arctic areas it is correlated to phytoplankton spring bloom (Thomas et al., 2008). Stratification in the water column, with more freshwater and higher temperature in the surface waters, enables the non-motile algae to thrive at the euphotic zone.

The concentration of phosphorous and nitrogen available in the worlds deep ocean waters are 2.2 µmol kg^{-1} PO_4^{3-} and 30.9 NO_{3-} which reflects the optimal ratio of plankton growth in sea water i.e. Redfield ratio of C:N:P = 106:16:1 (Lenton & Watson 2000).

But nutrients such as nitrate and phosphate are limited due to e.g. seasons, coast or open oceans and geography. The Arctic areas are more nutrient limited compared to e.g. the Baltic Sea, which is influenced by human activities. Nitrate in the Arctic is limited after the sea ice is gone and negatively correlated to phytoplankton biomass (Nielsen, 2004).

When nitrate is limited, diatoms will sink through the water column towards the bottom. The sinking dead diatoms are “hotspots” for microbial activity and may form aggregates together or with other particles composed of various components (Møller 2007). Attached bacteria colonize and process these aggregated particles, where free-living bacteria uptake dissolved organic matter and dissolved organic carbon. Both the attached and free living bacteria process a flux of matter to upper trophic levels i.e. regenerate phytoplankton growth in the microbial loop (Azam *et al* 1983). The nitrate concentration increases steadily after august through autumn to winter with high concentrations of nitrate until the disappearance of the sea ice (Nielsen, 2004).

Hydrography

The water around Disco Island is a mixture of the warm and saline water from the Irminger current and the colder and less saline East Greenland current. Due to the runoff from glaciers and rivers the West Greenland current runs underneath the lesser saline water. A fraction of The West Greenland current runs east of Disco Island while the rest runs west of Disco. The West Greenland current results in an upwelling along the south coast of Disco Island. This upwelling supplies the upper water masses with new nutrients. In the spring and summer, the increase in runoff from glaciers and rivers create a top layer of low saline water. Underneath the top layer there is a colder and more saline layer, this layer originates from the winter convection. The third layer is a warmer layer. (Lett, et al 2010).

Another effect of runoff is the amount of freshwater added to the fjords. This changes the salinity at the inner part and can cause the salinity to drop to 5 PSU. The adding of freshwater to the fjord has an effect on water column stratification. The lighter freshwater and solar irradiation forms an early stratification of the upper 5 m of water (Bendtsen et al., 2014).

Like any other places around the world runoff from rivers and glaciers carry a range of particles to the ocean in the Arctic areas (Thomas et al., 2008 Dittmar and Kattner, 2003). These different particles are inorganic and organic matter along with mud, sand and silt. The input from rivers and glaciers to the ocean acts like a “sword with two edges”. On one hand the runoff causes the light to be absorbed faster. This greater absorption of light has a negative effect on the phytoplankton growth. The greater absorption of light forces the phytoplankton to move higher in the water column. This is only possible for the motile phytoplankton. The immobile phytoplankton cannot move, but the less saline water originating from the rivers and glaciers makes sure that the phytoplankton is located higher in the water. On the other hand the increased nutrient loading can lead to an increase in production. The runoff from glaciers and rivers transport nutrients to the ocean. The increase of available nutrients is used by the phytoplankton, this is seen as a higher

biomass near glaciers and rivers (Arendt et al., 2010). A common way to examine seasonal changes of glaciers and their impact on the surroundings like runoffs, is satellite images (Riyaz Ahmed Mir et al., 2014). The focus of these images to investigate the runoffs, is situated at the mouth of glaciers, where the watercolor changes from blue to white. The technical term for this is turbidity. Turbidity is a measurement of suspended particles in the water, the higher turbidity the more particles present.

The environment in the pelagic water is very different from that of the mouth of rivers and glaciers. Arendt et al. (2010) investigated the plankton community in Godthaabs Fjord, they found that the chemical and physical gradients along the transect of nearly 200 km had an effect on the community and the production in the fjord system. They found a higher amount of chlorophyll *a* nearer to the ice sheet and that the phytoplankton community changed from 60 % diatoms at the beginning of the transect to 100 % diatoms nearest to the ice sheet. The phytoplankton production in the open ocean was located mainly from 10 m down to 50 m, the depth of production moved higher the closer to the ice sheet (Arendt et al., 2010). This is where the pycnocline prevents the algae from sinking; it is also here that the nutrients from the colder and denser water mixes with the water layers above. The different physical forces, which have an effect on algae are current and wave actions. Currents influence the spatial distribution to algae to e.g. areas with warmer waters or less nutrients, which might have a negatively effect on the algae species. Wave actions such as winter storms causes a mixing of the upper water column, which influences the plankton position in the water body to below the photic zone. A mixing of the water body elevates the stable gradient like the pycnocline, and non-motile plankton sink to the bottom.

Global changes

An important reason why scientists have been interested in the arctic is due to the concern of the consequences of the global warming. Global warming might have a bigger impact on the arctic, but the effects on the arctic would potentially have global consequences. Climate models with a rise in global temperatures show that the thickness, quality (seasonal or multiyear ice) and expansion of the Sea Ice in the arctic diminish (Thomas et al 2008). Among others this will influence the water balance and potentially the formation of the deeper waters and hence an impact on the global thermohaline circulation (Shäfer *et al* 2001). Locally consequences on the areas where it used to have Sea Ice cover would be less saline surface waters and a more stratified water body, a longer growth season for phytoplankton which leads to an impact on the marine food web system. Less Sea Ice will also have socio economic consequences on the local natives who live near the coast and are thus depending on the fisheries catch from the Sea. Looking at Greenland the natives are traditionally close to the Sea i.e. the society structure, industrial and cultural. Knowledge on the marine food webs, which is the fundament on e.g. fish production, is important for an ecosystem assessment.

Hypothesis

With this study we hypothesize the following. (1) We expect to see a difference in the phytoplankton biomass with a higher amount of biomass present in the inner fjord compared to the outer fjord and likewise we expect (2) a higher amount in the fjordsystem compared to the open ocean due to runoff from the coast. This was examined by estimations of the biomass by extraction and measurements of chlorophyll a. (3) We also expect to observe a decline in the phytoplankton biomass during a succession event due to the ~3 week sampling period, where a shift from spring/summer to summer/autumn conditions is expected to take place. This is examined by collecting water continuously at the same site during the 3 weeks and then estimating the biomass by extraction and measurement of chlorophyll a.

With these hypotheses we will present three main stories under the following:

(1) The Fjordsystem: 'A comparison of the biomass present in inner and outer fjord respectively'

(2) The waters surrounding Disco Island: 'A comparison of the biomass present in a Fjordsystem and the open ocean respectively'

(3) Temporal succession at Fortune Bay: 'An examination of the changes in phytoplankton biomass over time'

Moreover we will present further investigations as following:

(4) Utermöhl cell count: 'Identification and biomass estimation of Diatoms'

(5) Photo-documentation of Diatom species found in the waters surrounding Disco Island

Methods

Sampling and study area

The samples were collected from the research vessel Porsild at various field sites located in Disco Bay and fjords in July summer 2014 (Fig. 1). When arriving at a field site firstly a CTD profile was generated using a Seabird SBE, model 19 which was lowered from the side of the boat to a depth of 20 m above sea floor (in most cases). CTD profiles of temperature, conductivity for the determination of salinity, pressure, turbidity, dissolved oxygen and chlorophyll fluorescence in the whole water column was recorded (Appendix: CTD). The CTD data were transferred to a Dell computer where they were imported and analyzed in Seasave version 7 and determination of the depth where the fluorescence maximum occurred as well as the depth just below the pycnocline were established.

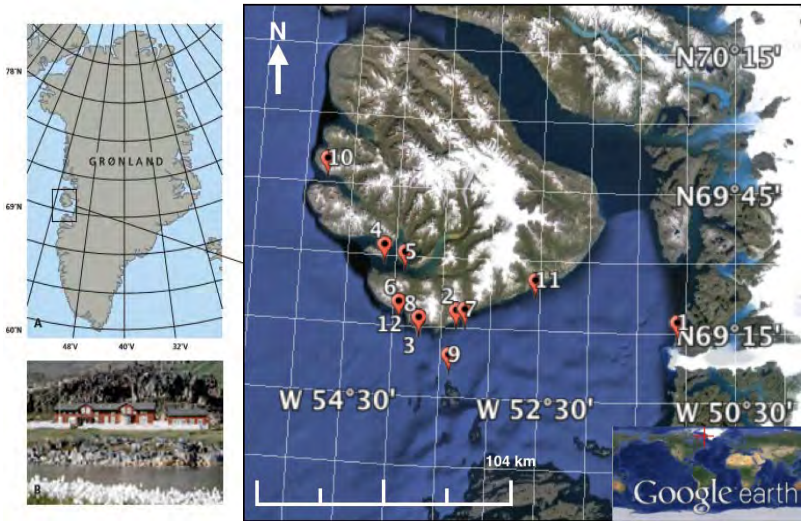

Fig. 1 shows a map of Greenland (upper left) and a focus of Disko island with the 12 stations (right) and the Resarch station "Arktisk station" (left bottom) in "Qeqertarsuaq (Godhavn) (Nielsen Dsc 2004 and Google Earth).

Afterwards, water samples for the purpose of filtration and chlorophyll extraction were obtained from three depths, namely, the surface layer which was fixed at 3 meters, the depth of the fluorescence maximum, ranging from 18 to 30 m depending on the station, and the depth of the pycnocline, located at 30 to 70 m, also depending on the station. The water was collected using a 5 L Niskin water sampler. For each of the three different depths 3 replicate samples (A, B and C) each containing 2 liters were collected. Before the water was transferred into the 2 liters sample bottles these were first rinsed with the water brought up and then completely filled. Whenever the A samples were collected a 50 mL plastic container with lid was completely filled with the same water for later determination of the nutrient content in the water. Likewise, a 125 mL amber-coloured glass bottle containing 1 % (1.2 mL) Lugol was filled with 120 mL of the "A-water" so that the phytoplankton was instantly killed and could be used for species identification and biomass estimation.

Fig 2 (left) Niskin water into a 2 L plastic container with lid for chlorophyll measurements. (right) Niskin water into a 50 mL plastic container for nutrition analysis and 125 mL amber-coloured glass bottle for phytoplankton species identification and biomass estimation.

While collecting the water samples an integrated netplankton sample was simultaneously assembled from the surface to ca. 9 m (depending on the field site) (fig. 3). For this collection a 20 µm plankton net was used having a 500 mL Nalgene bottle attached at the end. The net was brought down several times to get a concentrated sample. All samples were kept on the boat in a cooler containing blue-ice and brought back directly to the Arctic Field Stations laboratory where they were further processed.

Fig. 3 Nicolai pulling the 20 µm plankton net up on a sunny day on Porsild.

Waterfiltration and extraction

Filtration and extraction from the three seawater fractions were done with the least possible delay at the Arctic station in a temperature-controlled metal container of approx. 2 to 4˚ C. The three replicates from each depth were filtered as shown in Fig 4. A volume of 2 L seawater was filtered through Whatman PC membranes with different pore sizes i.e. each replicate filtered through 20 µm filters to collect the netplankton fraction. The collected water was then filtered through 0.3 µm filters to get the fractions of nano - and pico-plankton i.e. the rest of the photosynthetic biomass fraction in a sample from respective depths. At the second half of the experiment the 0.3 µm filters were replaced by 0.4 µm filters which we assumed to be as efficient to collect the nano- and pico-plankton in Greenlandic waters; as the smallest eukaryotic cell known is 0.3 µm and not expected to be present in these cold

waters. Thus, the samples are representative for the biomass in Greenlandic waters of Disco Bay. The volume of filtered water was adjusted to avoid the filter to clog and the final volume was noted. To create a vacuum and speed up the filtration procedure and to handle the phytoplankton carefully, a hand pump was used. The filter was folded and transferred to glass vials with 5 mL 90 % ethanol to extract chlorophyll *a* from the cells; then covered in aluminum foil to prevent degradation of chlorophyll *a* and kept cold at 5˚ C.

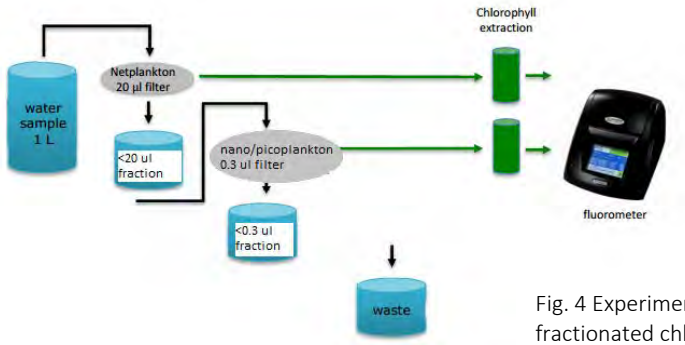

Fig. 4 Experimental setup of size fractionated chlorophyll α measurements.

Fluorescence measurements

After 24 hours the extracted samples were first acclimatized to room temperature and finally the fluorescence of chlorophyll *a* measured using a Triology Laboratory Flurometer from Turner Design equipped with the CHL-a ACID modul. This was done by adding 1.3 mL from the samples to 2 mL glass vial after having centrifuged the samples for 5 minutes at maximum speed. The initial measurements were stored by the flurometer representing chlorophyll *a* of the filtrated volume without HCL (5 %). One drop of acid was added to the 2 mL glass vials followed by measurements of phaephytin *a* i.e. degraded chlorophyll *a*.

Nutrient measurements

The frozen water samples were thawed prior to treatment. 8.4 ml from each sample were transferred to 25 ml vials. 1.6 ml solution of persulfate was added to the vials and then carefully mixed. After mixing the vials were autoclaved for 30 min. at 120 °C. 500 ml borate buffer was made by adding 30.9 g boric acid (H_3BO_3) and 4 g NaOH to MQ water. 2.5 ml borate buffer was mixed with the autoclaved vials. A standard curve of nitrate and phosphorus was prepared. In each curve there are six flasks with different concentrations, 0, 50, 100, 200, 500, and 1000 µg L^{-1} of nitrate or phosphorus. The curves are used to determine the concentration of nutrients in the samples. A reagent was made of 1000 ml MQ water, 50 g potassium peroxodisulfate ($K_3S_2O_8$) and 3 g NaOH. This reagent reacts when added to the samples with nitrate and phosphorus. Dependent on the amount of nutrient in the sample, a coloration of blue will happen within minutes. 2.5 ml of the reagent is added to vials and set aside for a few minutes. The nitrate samples are then analyzed in a spectrophotometer at 700 nm. Based on the absorption and the known concentrations from the standard curve, the concentration of nutrients can be calculated.

Identification and biomass estimation of diatoms

Each sample collected from the three water depths (3 m, FM and P) fixed with 1,2 mL Lugol iodine (1%) at sea, was processed by Utermöhl cell count using an inverted microscope. This included

identification and measurements of cell dimensions of diatoms at genus or species level and biomass estimation. The samples were shaken gently to homogenize the content prior to pouring 50 ml into a sedimentation chamber. These samples were left for 24 hours at room temperature allowing the cells to reach the bottom of the counting chamber. The settled cells were identified and enumerated based on the assumption that cells are *Poisson* distributed in the counting chamber. The process of enumeration of diatoms and other protists were initiated by counting at the lowest magnification in an inverted microscope i.e. objective X10 (final magnification: X100). To increase the accuracy of the cell counts we attempted to count at least 400 cells of each species. This gives a 10 % level of precision. The cell counts were transformed to number of cells per liter and the biovolume of all reported species were calculated using the geometric shapes proposed by Hildebrand et al. (1999). When converting biovolume to carbon; data was multiplied by a conversion factor of 0.11 pg C µm (Mulin et al., 1966). Furthermore in order to compensate for the shrinkage of cell size due to 5 % Lugol iodine fixation data was then multiplied with another conversion factor of 1.33 (Montagnes et al., 1994).

Statistical analysis

All statistical analyses have been done with ANOVA procedure in SAS Enterprise 9.4. For the statistics done in (1) The Fjordsystem: 'A comparison of the biomass present in inner and outer fjord respectively', data from station 4 represents 'outer fjord' (ydre fjord) and data from station 5 represents 'inner fjord' (indre fjord). For (2) The waters surrounding Disco Island: 'A comparison of the biomass present in a Fjordsystem and the open ocean respectively', the data from the stations 2, 3, 6, 7, 8 and 9 represents 'open ocean' (hav) while data from station 4, 5 and 10 represents the 'fjordsystem' (fjord). For (3) Temporal succession at Fortune Bay: 'An examination of the changes in phytoplankton biomass over time', data from the stations 3, 8 and 12 were used. Station 3 represents the 'beginning' station 8 the 'mid' and station 12 the 'end' of the time period.

Results

(1) The Fjordsystem: 'A comparison of the biomass present in inner and outer fjord respectively'

Physical and chemical conditions at study site

Below is the CTD data from station 4, outer fjord and 5, inner fjord. The measured parameters for the CTD were salinity, temperature, fluorescence (RFU) and irradiance. At the outer fjord we see a temperature gradient going from 2° C in the surface waters to 3° C at a depth of 150 m. At the inner fjord the temperature ranged from approximately 13° C at the surface to 2°C at ~ 75 m. We found temperatures in inner fjord at chl. *a* maximum to be approximately 8° C, which differs from outer fjord with lower temperatures at 1.5 °C. In the upper 2 to 4 meters we observed a thermohalocline in the inner fjord while we do not see this in outer fjord. When looking at salinity, the values range from 18 to 34 PSU in inner fjord while we found values from 15 to 21 PSU in outer fjord. The turbidity values in the surface waters differed with a higher amount of particles in the inner fjord (turbidity going up to 6) compared to outer fjord (turbidity going to 1.6). For both stations the fluorescence maximum is found at ~24 m while the penetration of the light is less in inner fjord than outer fjord.

The PAR irradiance values range from 1000 µmol quanta m^{-2} s^{-1} at the surface to ~ 0 µmol quanta m^{-2} s^{-1} at 76 m (inner fjord) and 90 m (outer fjord) respectively.

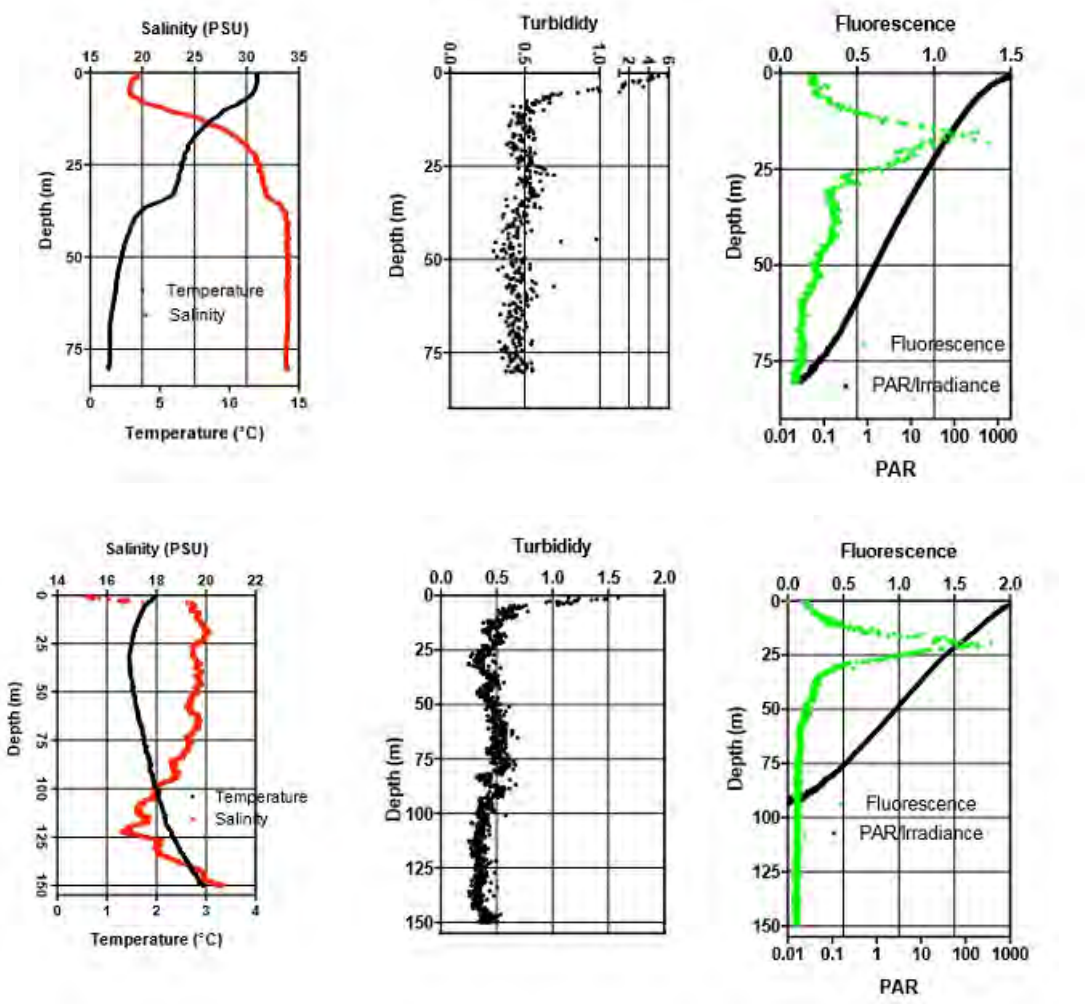

Fig 5 shows the CTD profiles with Temperature and Salinity, Turbidity, Fluorescence and PAR/irradiance for Inner Fjord st. 5 (upper figure) and Outer Fjord st. 4 (bottom figure).

Biomass estimations of Chlorophyll a and Phaeophytin a

We found no significant difference (P = 0.1698) between the amount of carbon present in the inner fjord (5.7 µg C/l) and the outer fjord (3.0 µg C/l), see Fig 6.

Fig. 6 shows the mean amount of carbon in inner fjord (Indre fjord) and outer fjord (Ydre fjord)

We found pico/nano-plankton to be more predominant than net-plankton at both inner and outer fjord (see fig. 7). For the inner fjord P = 0.0012, with the amount of net-plankton being 0.9 µg C/l and the amount of pico/nano-plankton being 10.4 µg C/l. For the outer fjord P = 0.0005, with the amount of net-plankton being 0.3 µgC/l and the amount of pico/nano-plankton being 5.8 µgC/l. Also, to ensure that there had not been any problems concerning our samples we tested whether samples A, B, and C (sampling in triplicates) actually had the same amount of biomass carbon, which we found that they had (P = 0.8836). With the A samples having 4.6 µg C/l, B samples having 4.8 µg C/l and C samples having 3.7 µg C/l.

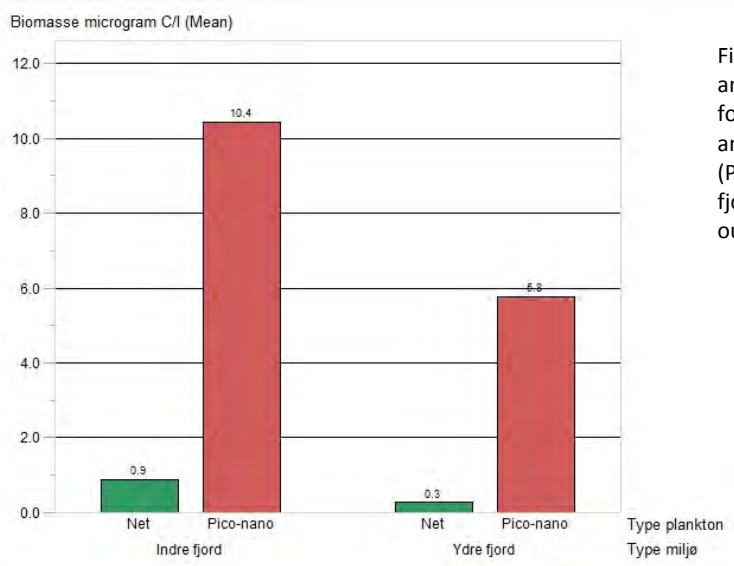

Fig. 7 shows the mean amount of carbon in µgC/l for both net-plankton (Net) and pico/nano-plankton (Pico-nano) in both inner fjord (Indre fjord) as well as outer fjord (Ydre fjord)

We also tested if there were a significant difference in the amount of biomass carbon at different depths in both inner and outer fjord which we found there was not (see Fig 8). For the inner fjord we found that there was no significant difference (P = 0.1312) on the amount of carbon in 3 m (6.9 µg C/l), FM (9.0 µg C/l) and P (1.1 µg C/l). For the outer fjord we likewise found no significant difference (P = 0.2048) with the amount of carbon at 3 m being 4.8 µg C/l, at FM being 3.4 µg C/l and at P being 0.9 µg C/l.

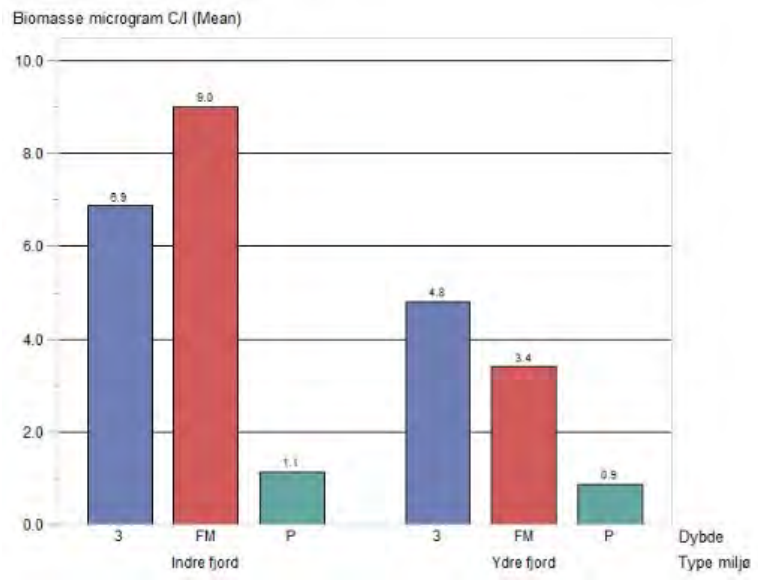

Fig 8 shows the amount of carbon in µgC/l at the different depths 3, FM and P at both inner fjord (Indre fjord) and outer fjord (Ydre fjord)

The development in phytoplankton community

We found the relation between chlorophyll α and phaeophytin to be less than 1 which indicates that the phytoplankton community, for both netplankton and nano-pciplankton, is non-growing (see fig 9).

Fig 9 The relation between µg chl α and Phaeophytin /l for both the netplankton and pico/nanoplankto n at different depths 3 m, FM and P in both inner fjord (indre fjord), right, and outer fjord (ydre fjord), left.

The netplankton community had higher ratios in inner fjord compared to outer fjord across depth. More specificially, the chlorophyll α/ phaeophytin relation for netplankton in inner fjord is found to be in 3 m (0.6 µg Chl/phaeo), FM (0.4 µg Chl/phaeo) and P (0.2 µg Chl/phaeo) and in outer fjord in 3 m (0.3 µg Chl/phaeo), FM (0.2 µg Chl/phaeo) and P (0.08 µg Chl/phaeo). Exept for a higher ratio in netplankton (0.6 µg Chl/phaeo) at 3 m in inner fjord, the ratio of pico/nanoplankton in both fjords were higher compared to the ratios of netplankon. The chlorophyll α/ phaeophytin relation for pico/nanoplankton in inner fjord is in 3 m (0.4 µg Chl/phaeo), FM (0.5 µg Chl/phaeo) and P (0.2 µg Chl/phaeo) and in "outer fjord" in 3 m (0.5 µg Chl/phaeo), FM (0.3 µg Chl/phaeo) and in P (0.2 µg Chl/phaeo).

Nutrition Analysis

We found almost the same rate of low Phosphorous in the whole water column at both inner - and outer fjord (see fig 10). Throughout the water column in inner fjord the phosphorous rates were 0.2±0-0.03 µg P/, and likewise in outer fjord, with a small variation of, 3 m (0.2±0 µg P/l), FM (0.2±0.03 µg P/l) and P (0.3±0 µg P/l). Nitrate rates in outer fjord showed lower values throughout the water column in 3 m (2.1± 0.03 µg N/l), FM (3.6± 0.06 µg N/l) and at P (2.5± 0.02 µg N/l) than in the inner fjord at 3 m (3.0 ± 0.06 µg N/l) compared to FM (4.0± 0.03 µg N/l) and P (5.0± 0.01 µg N/l) (see fig 17).

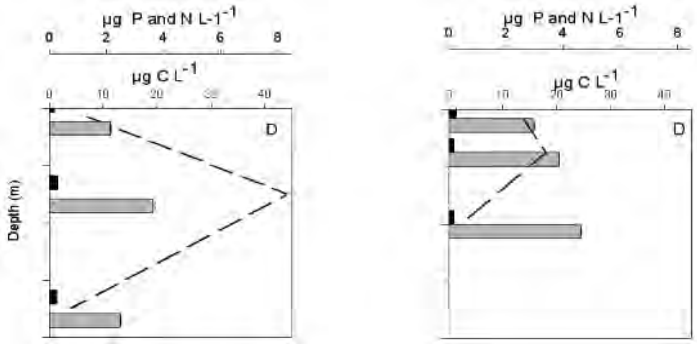

Fig. 10 shows the amount of Phosphorous (µg P/l) (black), Nitrate (µg P/l) (grey) and the amount of Carbon (µg C/l) (--) at different depths, 3 m, FM and P in both inner fjord (right) and outer fjord (left)

(2) The waters surrounding Disco Island: 'A comparison of the biomass present in the Fjordsystem and the open ocean respectively'

For the *Physical and chemical conditions* we have chosen two representative stations (Mellemfjord st. 10 and Kronprinsens Ejland st. 9) for the two type of systems, fjord system and open ocean, to describe these. For the section *development in phytoplankton community* these two examples are again used for comparison.

Physical and chemical conditions at study site

Below is the CTD data from station 10 (fjord) and 9 (open ocean). At both stations the temperature ranges from ~9° C in the surface to ~1-2° C at around 100 m depth. A slow and steady decrease in the temperature is seen in the fjord while the temperature in the open ocean decreases in the upper 40-50 m of the water column and then stays constant. At fluorescence max the temperature in the fjord was approximately 7° C while it was lower in the open ocean with approximately 3° C. When looking at the salinity, for both stations, the values range from 32 PSU in the surface to around 34 PSU at 100 m depth. The turbidity values differ between the two stations with a higher turbidity in the upper 10 m of the water column in the fjord, where the turbidity is 1.5. Hereafter, the turbidity is almost the same, around 0.25, for the fjord and the open ocean. This again changes at approximately 75 m depth in the fjord, where the turbidity starts to rise until it reaches 1.0 at 100 m depth. The fluorescence max is found closer to the surface in the fjord, at around 13 m depth while it is found at around 25 m depth in the open ocean. The PAR irradiance values range from 1000 µmol quanta m^{-2} s^{-1} at the surface to ~ 0 µmol quanta m^{-2} s^{-1} at ~78 m (fjord) and ~106 m (open ocean) respectively.

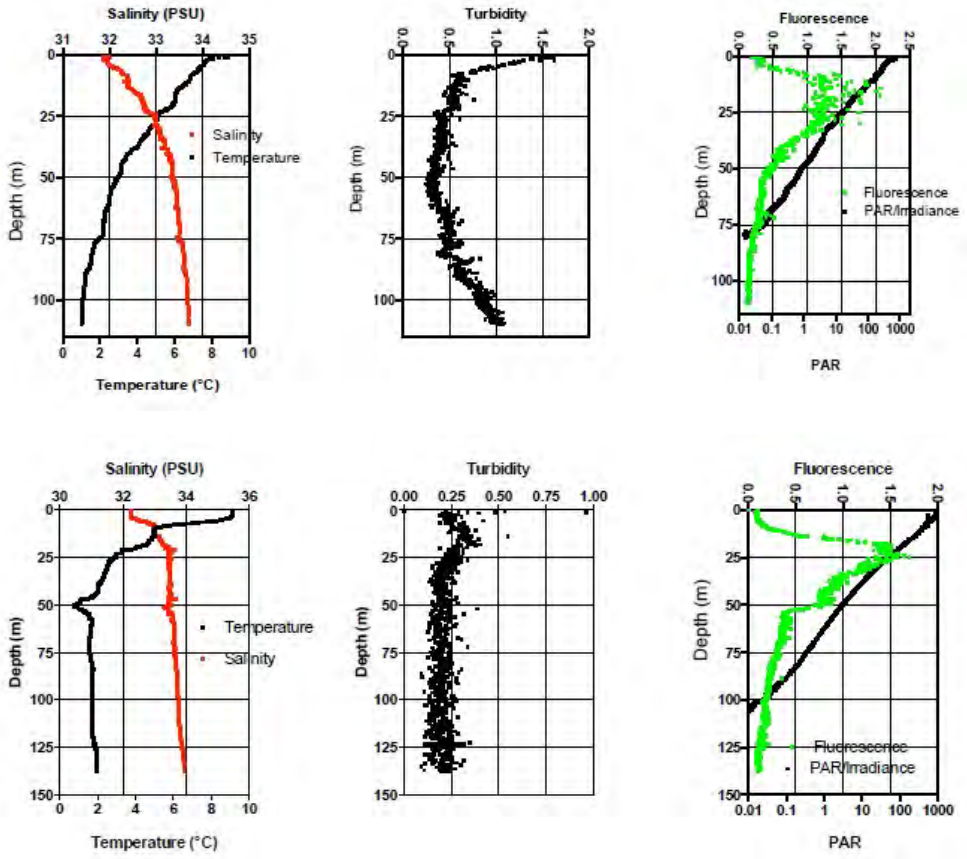

Fig 11 shows the CTD profiles with Temperature and Salinity, Turbidity, Fluorescence and PAR/irradiance for Mellemfjord, station 10 (upper figure) and Kronprinsens Ejland, station 9 (lower figure).

Biomass estimations of Chlorophyll a and Phaeophytin

We found no significant difference (P = 0.1197) on the amount of biomass in fjord systems (6.5 µg C/l) compared to the open ocean (9.0 µg C/l), see fig 12.

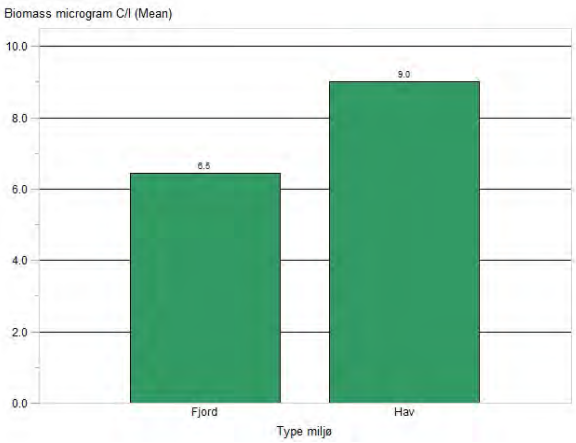

Fig. 12 shows how much biomass in µgC/l were found in the two different environments (Type miljø) the open ocean (Hav) and the fjords (Fjord)

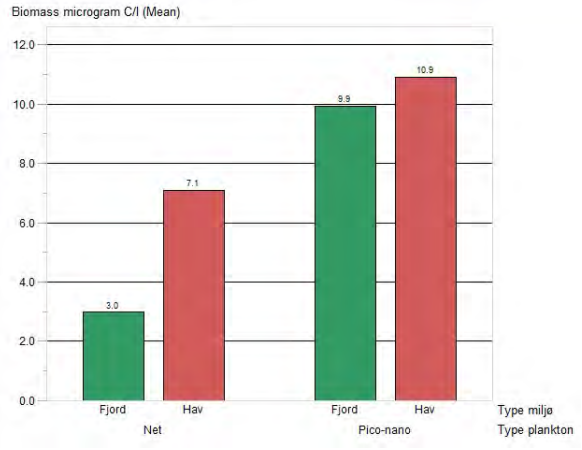

Fig. 13 shows how much in µgC/l net-plankton (Net) and pico/nano-plankton (Pico-nano) was found in the two environments, the open ocean (Hav) and the fjords (Fjord)

We also tested whether there was a significant difference in which plankton size fraction, net-plankton or pico/nano-plankton, that dominated in the open ocean compared to the fjords, see fig 13. We found that there was a tendency (P = 0,0753) for net-plankton to be more abundant in the open ocean (7,1 µgC/l) than in the fjords (3,0 µgC/l). But we found no significant difference (P = 0,6568) in the amount of pico/nano-plankton in the open ocean (10,9 µgC/l) compared to the fjords (9,9 µgC/l). Once again we found no significant difference (P = 0,9381) between our individual samples A (8,0 µgC/l), B (8,5 µgC/l) and C (7,9 µgC/l).

We also found that there was no difference in the amount of plankton at different depths in the fjords (P = 0,0809) with 3 being 6,6 µgC/l, FM being 8,7 µgC/l and P being 4,0 µgC/l, see Fig 14. But in the open ocean there was a significant difference (P < .0001) of how much biomass was found at a given depth with 3 being 2,2 µgC/l, FM being 18,1 µgC/l and P being 6,7 µgC/l, see fig. 21.

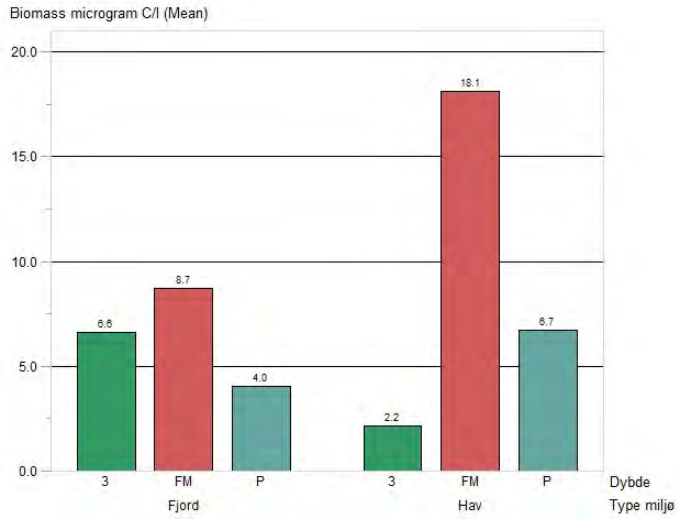

Fig. 14 shows the mean amount of carbon in µgC/l that was found at the different depths (Dybde) 3, FM and P in the two types of environments (Type miljø), the fjords (Fjord) and the open ocean (Hav)

The development in phytoplankton community and nutrition analysis

We found the relation between chlorophyll α and phaeophytin to be less than 1 and the fytoplankton community for both netplankton and nano-pciplankton to be non growing in both the open ocean and "mellemfjord". While the fjord has high ratios throughout the water column, the open ocean primarily has its high ratios at the FM and P depths as they are low in the 3 depth. (Fig 15).

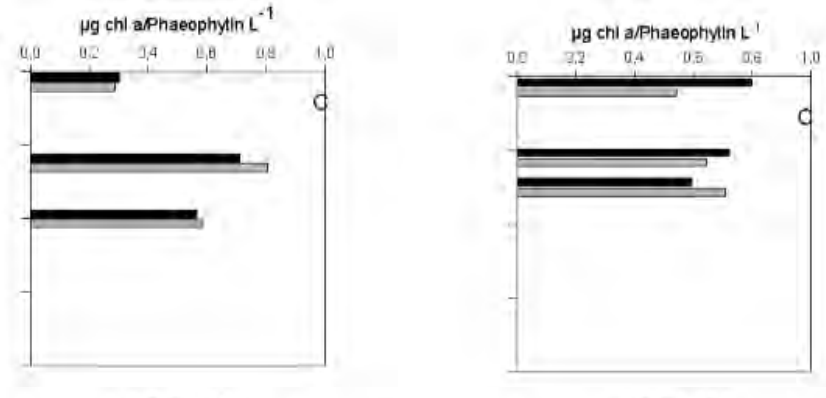

Fig 15 The relation between µg chl α and Phaeophytin /l for both the netplankton and pico/nanoplankton at different depths 3 m, FM and P in both Open Ocean "Kronprinsens Island, station 9, (left) and a fjord system, "Mellemfjord", station 10 (right)

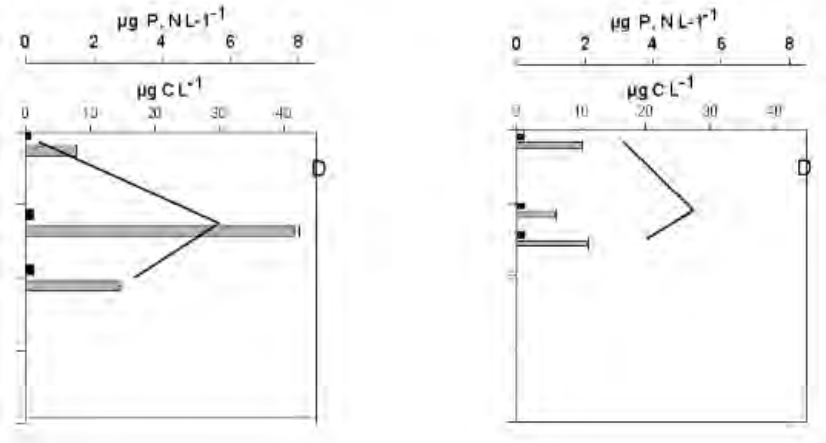

Fig. 16 Shows the amount of Phosphorous (µg P/l) (black), nitrate (µg N/l) (grey) and the amount of Carbon (µg C/l) (--) at different depths 3 m, FM and P both in the open ocean "Kronprinsens Island" st 9 (left) and in the fjord system "Mellemfjord" st 10 (right).

Looking at the total carbon in the open ocean and the fjord system this is similar. But available nitrate is found to be different, where the open ocean has more nitrate especially in FM (8.0±0.2 µg N/l) compared to mellemfjord FM (1.1±0.03 µg N/l), see Fig 16.

(3) Temporal succession at Fortune Bay: 'An examination of the changes in phytoplankton biomass over time'

Physical and chemical conditions at study site

Our CTD data from these two stations, 3 and 8, basically show the same, which makes sense, since they are the same locality at different times (beginning and mid). The salinity values are in the range of 32 PSU in the surface to ~34 PSU at around 80 m depth. The temperature varies from 6-7° C in the surface to ~1° C at approximately 60 m depth. The turbidity at the fluorescence max lies around 0.5 and hereafter decreases to 0.25. For both stations the fluorescence max is found at ~25 m depth. The PAR irradiance values range from 500-1000 µmol quanta m^{-2} s^{-1} at the surface at station 3 and 8 respectively to ~ 0 µmol quanta m^{-2} s^{-1} at ~80 m for both stations.

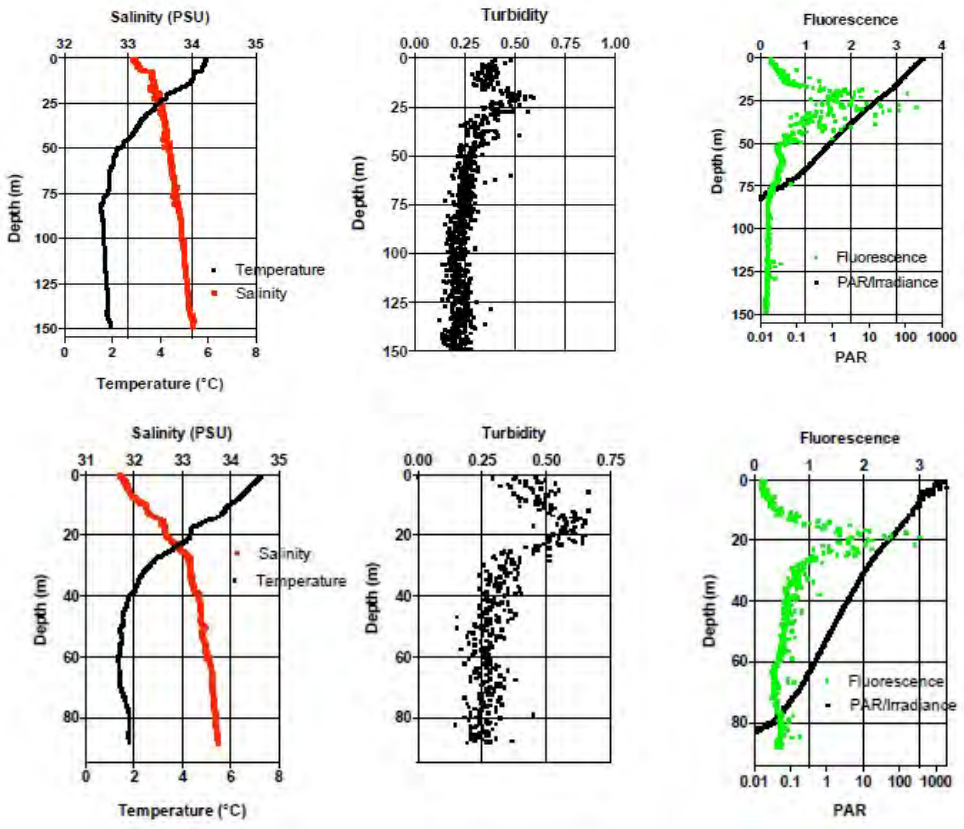

Fig 17 shows the CTD profiles with Temperature and Salinity, Turbidity, Fluorescence and PAR/irradiance for station 3 (upper figure) and station 8 (lower figure).

Biomass estimations of Chlorophyll a and Phaeophytin

We found a significant difference (P = 0.0054) on the amount of biomass carbon at each station. Station 8 had the highest amount (10.9 µg C/l), station 12 the lowest (0.6µg C/l) and station 3 had 9.2 µg C/l (se fig. 18)

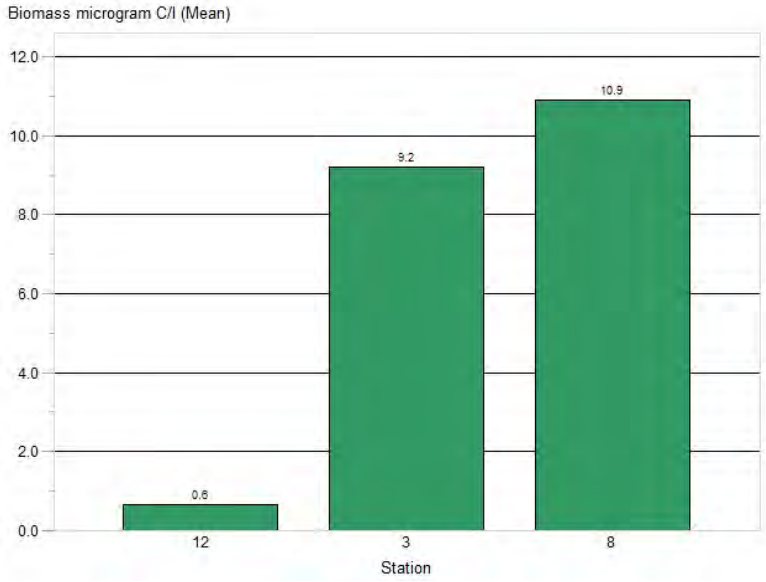

Fig. 18. shows the mean biomass in µg C/l at each of the three stations 3, 8 and 12.

We also examined whether there was a difference in the occurrence of net-plankton and pico/nano-plankton. We found that there was no significant difference of the plankton types at the three stations. For station 3, P = 0.0913 with the amount of net-plankton being 4.4 µg C/l and the amount of pico/nano-plankton being 14 µg C/l (see fig. 19). For station 8, P = 0.2287 with the amount of net-plankton being 14.3 µg C/l and the amount of pico/nano-plankton being 7.5 µg C/l (see fig. 19). For station 12, P = 0.0885 with the amount of net-plankton being 0.1 µg C/l and the amount of pico/nano-plankton being 1.2 µg C/l (see fig. 19). Again we found samples A, B, and C to have the same amount of biomass carbon (P = 0.9980). With the A samples having 7.0 µg C/l, B samples having 6.8 µg C/l and C samples having 6.9 µg C/l.

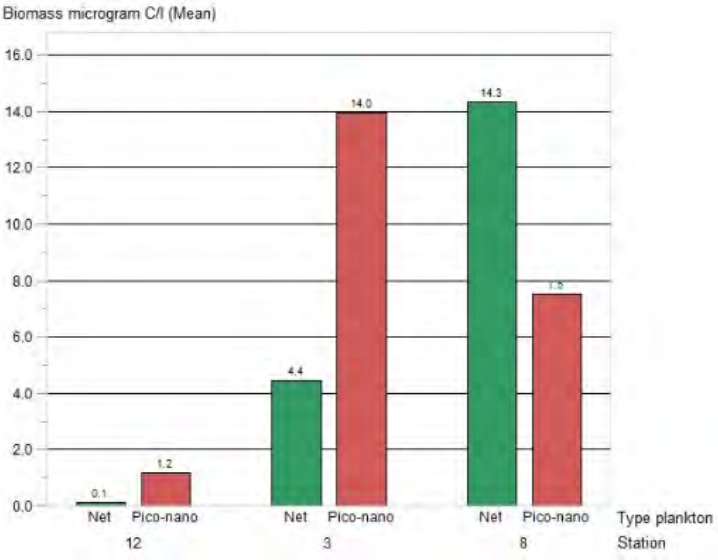

Fig. 19 shows the mean biomass of net-plankton (net) and pico-nano-plankton (pico-nano) in µg C/l at the three different stations 3,8 and 12

We also tested whether there was a difference of the plankton occurrence in total for station 3, 8 and 12 at the different depths which we found it to be (P = 0.0001). With most biomass carbon in the fluorescence maximum, FM (14.9 µg C/l), the smallest amount in 3 m (2.3 µg C/l) and at the pycnocline having 3.6 µg C/l (see fig. 20).

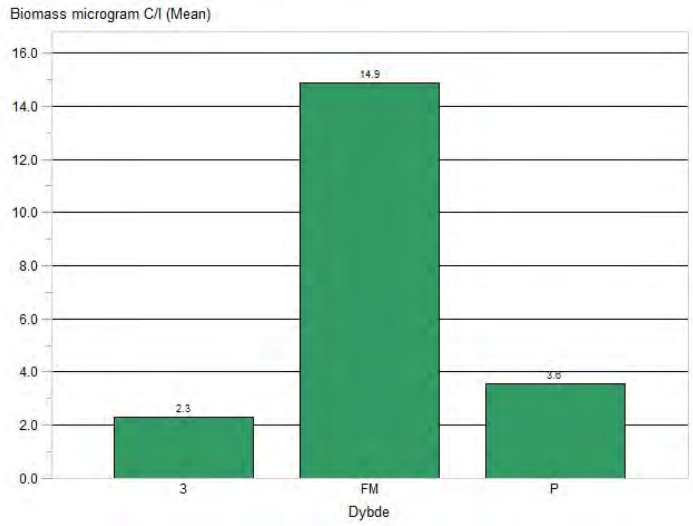

Fig. 20 shows the amount of biomass in µgC/l in total for all three stations at the different depths (Dybde) 3, FM and P

The development in phytoplankton community

We found the relationship between chlorophyll α and phaeophytin to be below 1 which means a non growing fytoplankton community during the investigated time period. Nevertheless the highest ratios was seen in st 8 "mid" at FM for netplankton (0.84 µg chl/phaeo/l) and at 3 m for pico/nanoplankton (0.73 µg chl/phaeo/l). Also we found very low ratios of chlorophyll α/ phaeophytin in the "end" at st 12 for both the netplankton (from 0 to 0.02 µg chl/phaeo/l) and pico/nano plankton (from 0 to 0.036 µg chl/phaeo/l) (fig 21).

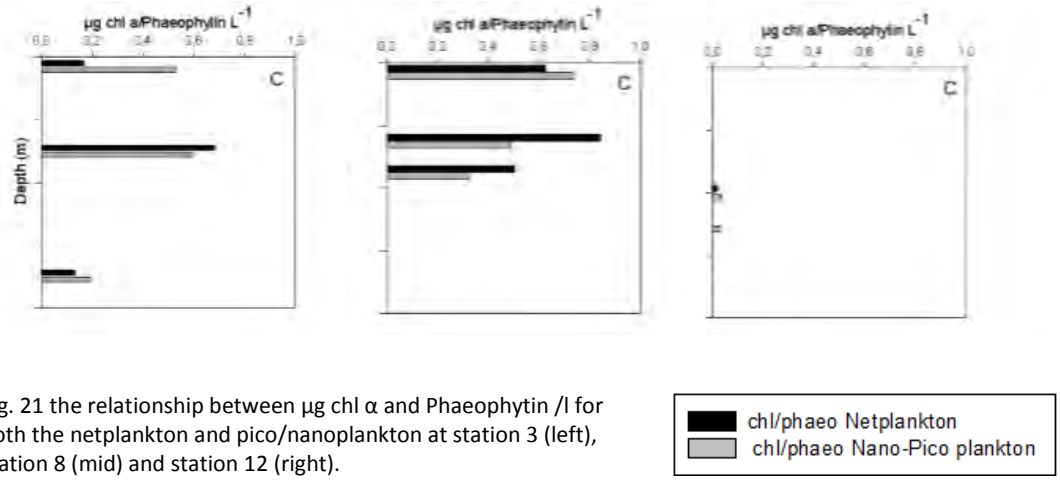

Fig. 21 the relationship between µg chl α and Phaeophytin /l for both the netplankton and pico/nanoplankton at station 3 (left), station 8 (mid) and station 12 (right).

Nutrition analysis

The Nutrition analysis showed very low levels of phosphorous in the whole water column throughout time (beginning, mid and end / station 3, 8 and 12). The phosphorous level in station 3 was found to be lower in the upper 3 m depth (0.17±0 µg P/l) compared to FM (0.23±0 µg P/l) and P (0.23±0 µg P/l) (see fig 22). In station 8, the phosphorous levels in 3 m (0.22±0.07 µg P/l) were similar to FM (0.19±0 µg P/l) and P (0.21±0 µg P/l). Where in station 12 in 3 m we found phosphorous to be a little lower (0.10±0.07 µg P/l) than FM (0.20±0.01 µg P/l) and in P (0.20±0 µg P/l) (see fig 22).

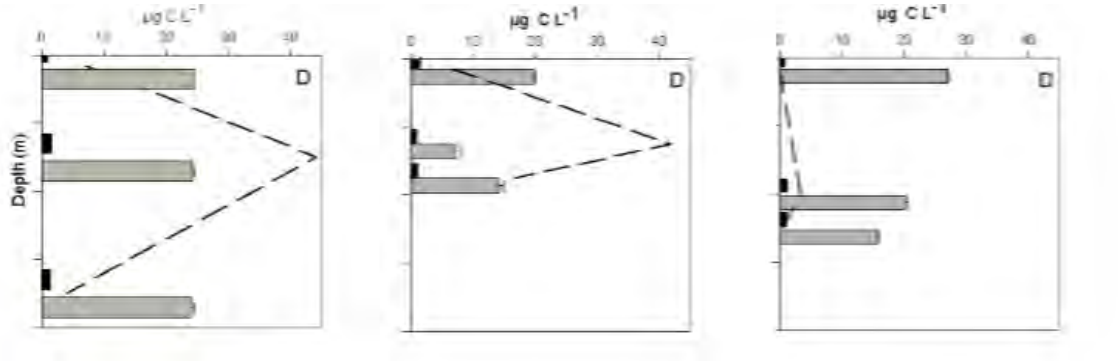

Fig. 22 shows the amount of phosphorous (µg P/l) (black), nitrate (µg N/l) (grey) and the amount of Carbon (--) (µg C/l) at different depths 3 m, FM and P at station 3 (left), station 8 (mid) and station 12 (right).

Where the phosphorous levels were more or less steady through time, the nitrate levels were low in FM (1.41±0.21 µg N/l) and P (3.10±0.21 µg N/l) in station 8, see fig 22. This is compared to higher nitrate levels in station 3 in all depths (i.e. 3 m (5.01±0.01µg N/l), FM (5.00±0.10 µg N/l), P (5.00±0.10

µg N/l)) and with higher nitrate levels in station 12 also in all depths (i.e. 3 m (5.11±0 µg N/l) FM (4.02±0.1µg N/l) P (3.10±0.031µg N/l)) (Fig. 22).

(4) Utermöhl cell count: 'Identification and biomass estimation of Diatoms'

The Utermöhl biomass estimations and counted species

In total we found 11 diatom groups by Utermöhl cell count. In the fjordsystem 7 groups were found in total, i.e. *Pseudo Nitzhia* (4%), *Nitzhia longisima* (1.1%), *Skeletonema* (6.2 %), *Chaetoceros* (85.2 %), *Thalassiosira* (0.77 %), *C. debilis* (2.4 %), *Dactyliosolen fragilissimus* (0.084 %). We found two dominating diatom species in inner and outer fjord with *Nitzhia longisima* spp (20%) and *Chaetoceros spp* (80%) in inner fjord and *Nitzhia longisima spp* (100%) in outer fjord. We also found a shift in the diatom groups (count %) over time. In the beginning Thalassiosira spp (90 %) dominated (station 3), this shifted towards Chaetoceros spp (86.5 %) which was the dominating group at station 8, and then towards a broader variety of groups (9 different groups) at the end (station 12) where Pseudo-nitzhia spp (43.6 %) was now dominating.

Fig 26 shows the distribution (% count) of the enumerated found diatom groups in all the 12 stations. The distribution of diatom groups is different between stations. However, few stations seem to have a similar species composition (i.e. station 7, station 8 and station 11) (see fig 23). The main diatom groups from the 12 stations are *Chaetoseros* (67.4 ug C/l), *Probosia alata* (4,0 ug C/l*), Porosia glacialis* (2.4 ug C/l*), Pseudo Nitzhia* (1.3 ug C/l), *Nitzhia longisima* (0.2 ug C/l), Dactysylem fragillisimus (0.3 ug C/l), Rhizoselena (0.2 ug C/l) Skeletonema (0.02 ug C/l) and Thalasiossira (0.018 ug C/l).

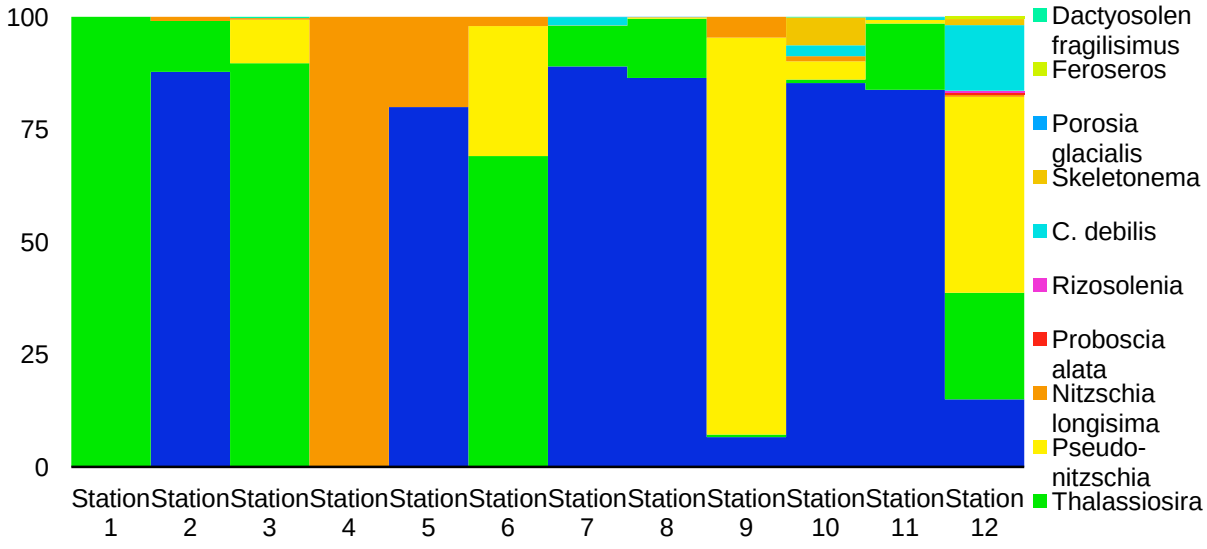

Fig. 23 Shows, the found diatom groups in the 12 stations investigated in % count.

Even though *Chaetocearos* contributes to 87 % of the total biomass, and appear in 9 out of the 12 stations, compared to Thalassiosira which held 0.02 % of the total biomass the later were still represented at 10 out of 12 stations. The Dominating groups (100% within one station) are found in station 1 (*Thalassiosira*) and in station 4 (*Skeletonema*).

(5) Photo-documentation of Diatom species found in the waters surrounding Disco Island

The following is a genus description of diatoms based on the findings from the present study around the waters of Disco Island.

Eucampia groenlandica: The cells are found as chains. Cells are lightly silicified, and are curved or straight, helical chains are rare. Apertures almost square or low elliptical, cells are attached with low horns. *E. groenlandica* is found in the northern cold waters. The cells apical axis are 10-33 μm (Hasle G. R. et al).

Leptocylindrus danicus: Cells are cylindrical 7-10 μm in diameter and two to ten times as long. Cells are connected valve by valve, the end of valves can either be flat, concave or convex. Intercalary bands present but difficult to see. Chromatophores few to numerous oval distributed throughout the cells (Cupp E. E.).

Probiscia alata: Cell diameter, 2.5-13 μm and 200-250 μm long. Bands in two columns with pores scattered between loculate. Short longitudinal slit below end of cell (Hasle G. R. et al).

Rhizosolenia hebetata* f. *semispina: Have pointed otaria extending minimum 3 μm along the basal part of the process.

***Skeletonema* sp.:** Circular, lens-shaped, oblong or cylindrical cells. Valves circular, somewhat arched without distinct structures. A row of fine spines along the cell margin parallel to the apical axis. The spines interlock mid between two neighboring cells and forms a chain of cells (Cupp E. E.).

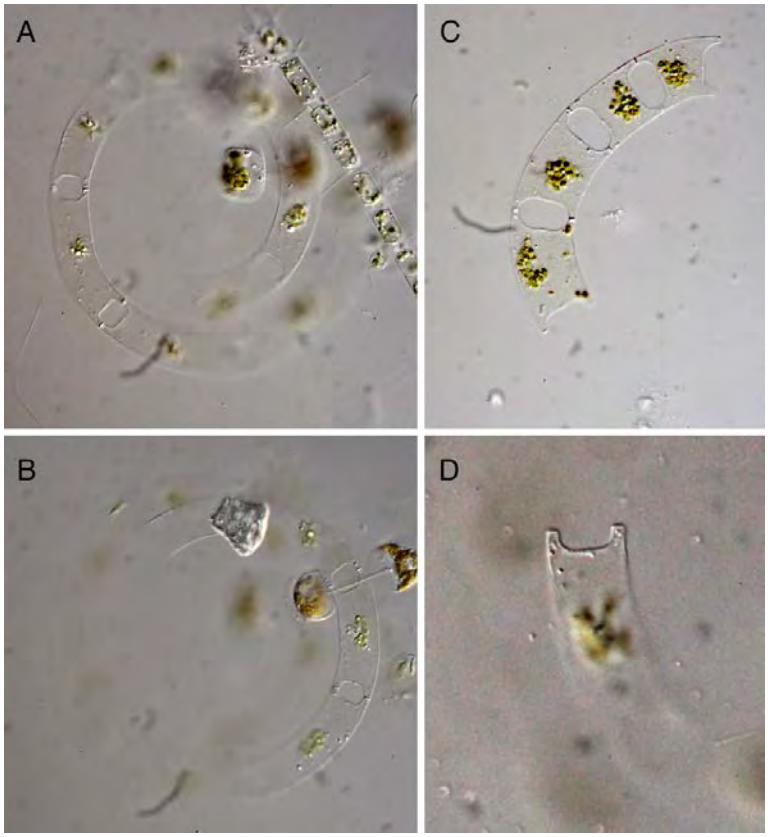

Fig. 24, A-D: *Eucampia groenlandica*

***Nitzschia longisima*:** Cells apical axis ranges from 125 to 450 μm and transapical axis 6-7 μm (Hasle G. R. et al).

Pseudo-nitzschia sp.: The raphe system revealed with EM is like that of *Fragilariopsis,* not elevated above the general level of the valve, and missing connote and lacking poreds in the external canal wall. Many species are fusiform, and in valve view longer and narrower that *Fragilariopsis,* some are rectanglear in girdleview. The species is geographically widely distributed and some species have shown to produce neurotoxin and domain acid. The later has shown to accumulate in mussels and there by produce a threat for passing it further on in the food chain (Hasle G. R. et al).

Pseudo-nitzschia seriata: Apical axis 91-160 μm, transapical axis 5.5-8 μm. Cells found in chains where they overlap each other by one-third to one-fourth of cell length. End of cells narrows to a rounded apices (Hasle G. R. et al).

Detonula confervacea: Cylindric cells 6-20 μm in diameter and 15-30 μm long. Cells are found in chains and is directly connected by a central process and a ring of marginal processes. Many chloroplasts are found inside the cells. They are often found in waters below 0 and is some time seen in blooms after braking of sea ice (Throndsen, Hasle and Tangen). ***Porosia glacialis:*** Cell diameter 36-64 μm, found as single cells or in loose chains. Valves with central annulus, processes, and sector with wavy areolation (Hasle G. R. et al).

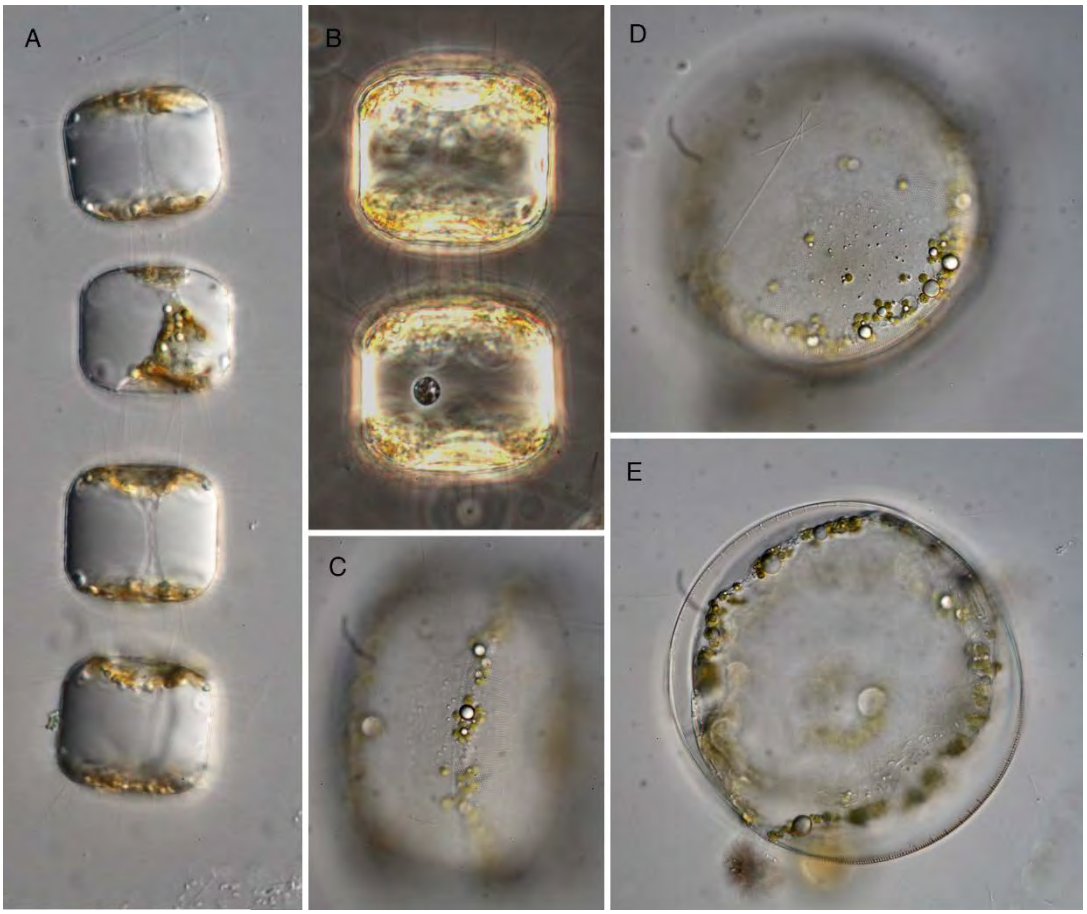

Fig. 25, A-E: *Porosia glacialis*

Thalassiosira anguste-lineata: 14-78 μm in diameter, cells form chains by connections of arrangement of central processes. In valve view the processes are located some distance from valve centrum. Cells rectangular in girdle view, valve face flat or slightly curved (Hasle G. R. et al).

Thalassiosira nordenkioeldii: Round cells with a diameter of 14-35 μm and a depression central where the thread that connects cells extrudes, in girdle view the cells is octangular. Small spines are found at the rim of the cells. Cells are found in chains (Cupp E. E.).

Thalassiosira* cfr. *rotula: Cells are 30-61 μm in diameter, valve is flat with rounded edges. Cells are found in chains that are connected by a central thread, the chains are slightly curved or straight. Chromatophores are small and numerous and located around the edge and along the surface of valves (Cupp E. E.).

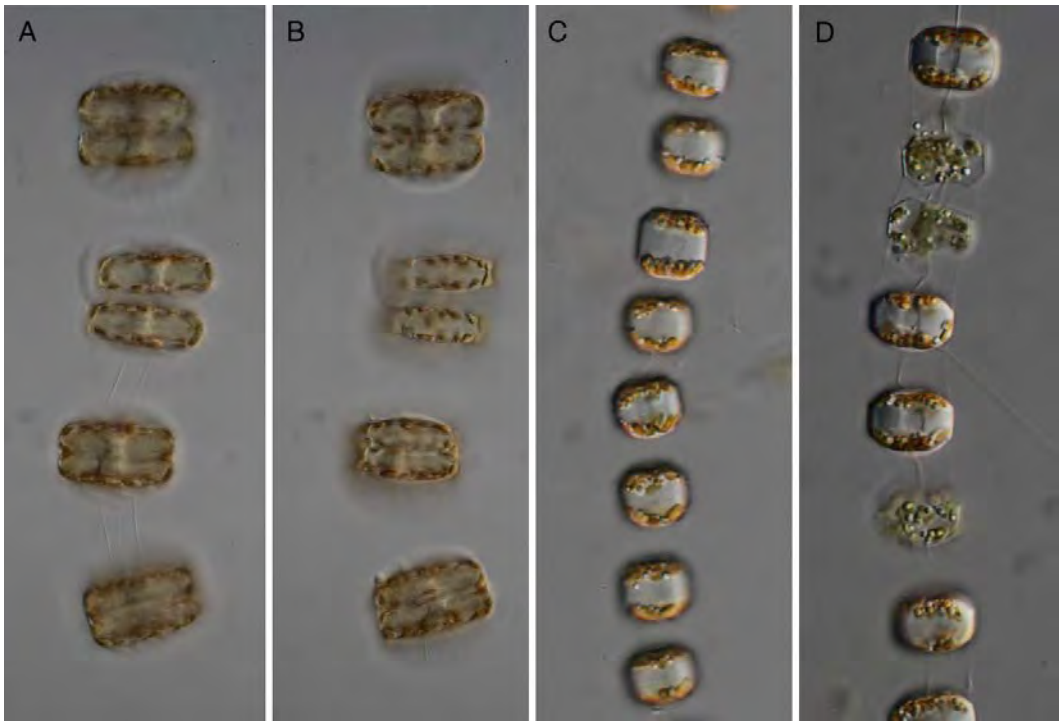

Fig. 26, A-B *Thalassiosira anguste-lineatum,* C-D *Thalassiosira nordenskioeldii*

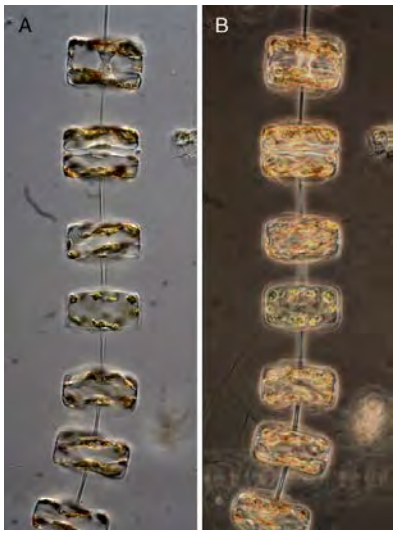

Fig. 27, A-B *Thalassiosira* cfr. *Rotula*

Chaetoceros convolutus: Cells 15-23 μm broad. Valves differs, the upper valve is rounded and the lower valve is flat. At each end of the cell there are two spines. Apertures between cells are more or less covered by setae. Cells are found in chains that are either straight or slightly bend (Cupp E. E.).

Chaetoceros concavicornis: 12-30 μm apical axis. Cells are found in chains, cells are attached***.***

Chaetoceros subtilis* var. *abnormis: This species differs from other chaetoceros by having one seta on the concave valve(Karin G. Jensen and Øjvind Moestrup).

Chaetoceros seriracanthus terres: Cylindrical cells, 18-50 μm apical axis. The aperture between cells is a narrow slit. The inner setae are more or less perpendicular to cell axis, terminal seta differs.

Fig. 28, A-B: *Chaetoceros seriracanthus terres*

Chaetoceros debilis: Apical axis 12-30 μm. Cells are found in spirally twisted chains. Valve face is flat or concave. Corners are usually round and setae relatively short, the terminal setae similar to intercalary ones. The aperture between cells is linear to hexagonal (Karin G. Jensen and Øjvind Moestrup).

Chaetoceros decipiens: Apical axis 27-34 μm. In valve view the cells are elliptical. The cells appear flat to concave in girdle view, sometimes with a small central inflation. Setae originate at the valve edge without basal parts and lie in the apical plane (Karin G. Jensen and Øjvind Moestrup).

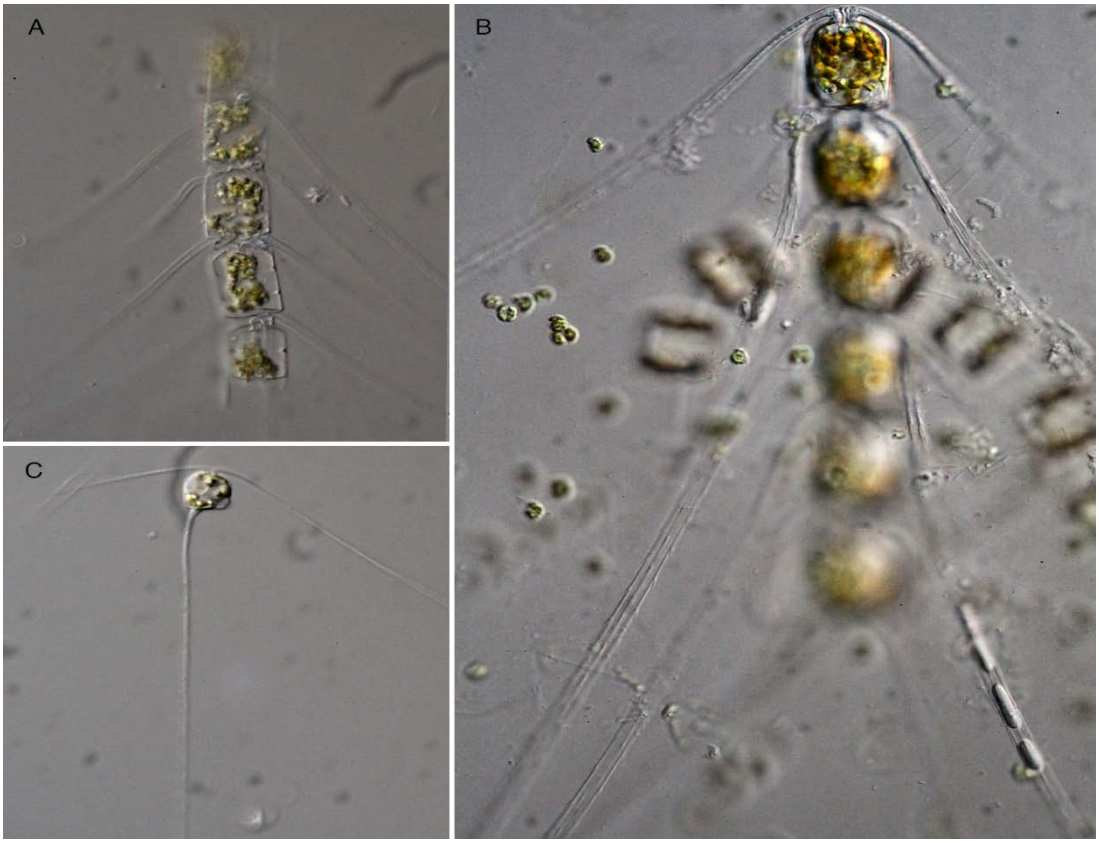

Fig. 29, A: *Chaetoceros convolutus*, B: *Chaetoceros concavicornis*, C: *Chaetoceros subtilis var. Abnormis*

Fig. 30, *Chaetoceros debilis* and *Chaetoceros decipiens*

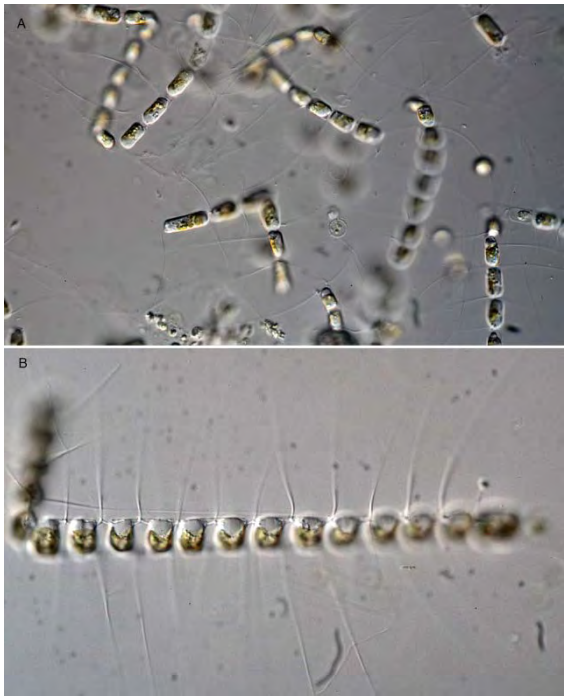

Fig. 31, A-B: *Chaetoceros gelidus diadema*

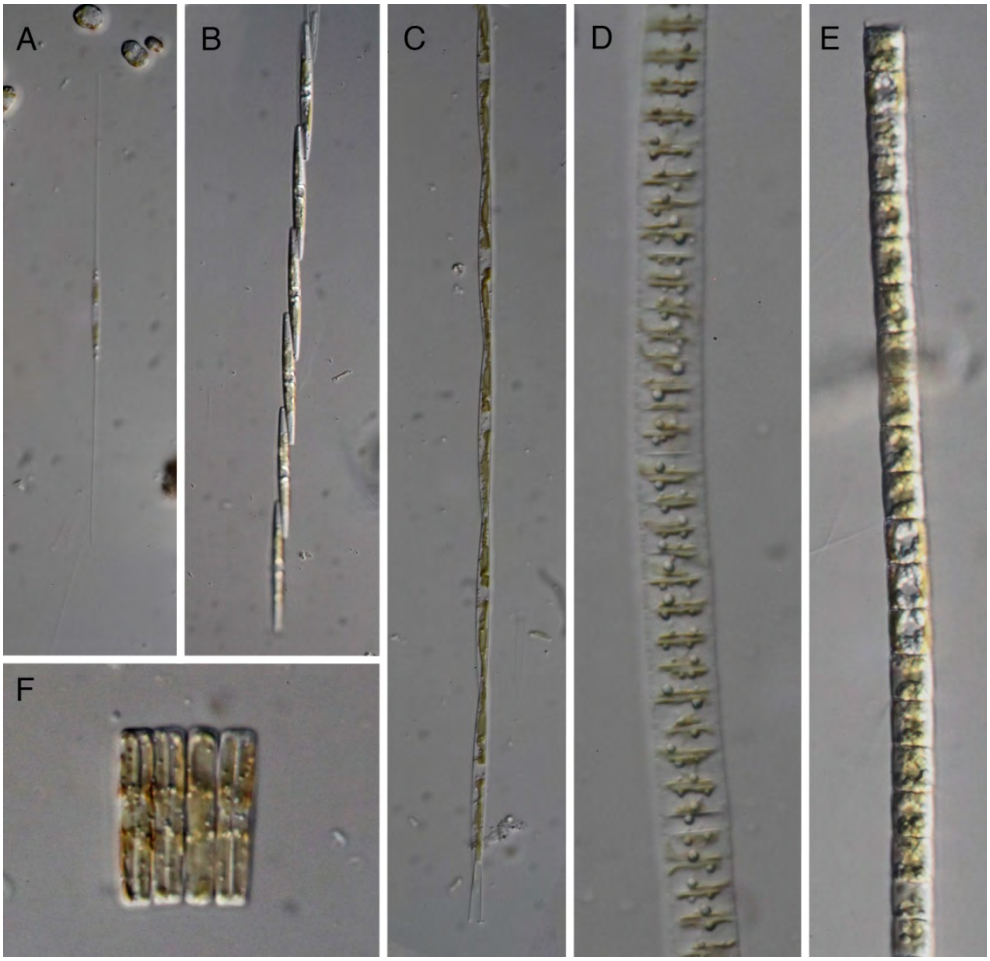

Fig. 32, A: *Nitzschia longissima,* B-C: *Pseudo-nitzschia* sp., D: Pennate diatom 1, E: Diatom 1 [perhaps Detonula confervacea which is in fact a centric diatom], F: Pennate diatom 2

Discussion

(1) The Fjordsystem: 'A comparison of the biomass present in inner and outer fjord respectively'

Differences between inner and outer fjord

When looking at the biomass we did not find a significant difference in the amount found in the inner fjord, which was 5.7 µg C/l and outer fjord where it was 3.0 µg C/l (fig. 6). We expected to find a higher amount of carbon in inner fjord than outer fjord due to the washout of silt and hence higher amounts of nutrients. The reason we did not see this might be because we have not taken the 'inner fjord' sample far enough "in the fjord" at the edge of the gletcher. When choosing where to do the sampling we looked at the water to see a change in the appearance, which shifted from clear water to more murky water because of the presence of silt, and we then took the sample. This might not have been a satisfying way to determine where to take the sample and one should simply have moved in deeper.

We found that the complete fjordsystem was more pico/nano dominated with the biomass for pico/nano being about 10-20 times as high (10.4 and 5.8 µg C/l) as that for the netplankton (0.9 and 0.3 µg C/l) (fig. 7). We did not have any expectations for how the relationship between the appearance of pico/nano and netplankton would be in the inner and outer fjord and thinking about it we would not expect their presence to be much different from each other so it is interesting why it is this way. It might be that the netplankton in the somewhat more quiet water compared to the more violent open ocean sinks out faster in these fjord environments leaving pico/nano to dominate. Since the pico/nano plankton also have a bigger surface/volume area they have an advantage when nutrients are scarce. When looking at our CTD data (fig. 5) we might find the reason for why there is more netplankton in the innerfjord than in the outerfjord since there is a clearcut pycnocline in the innerfjord compared to no pycnocline in the outerfjord and it might be that this pycnocline keeps the netplankton in the watercolumn preventing them from sinking out.

(2) The waters surrounding Disco Island: 'A comparison of the biomass present in a Fjordsystem and the open ocean respectively'

Comparison of a fjordsystem with the open ocean

We would have expected the biomass in the fjord to be higher than that in the open ocean due to the runoff from land and hence a higher amount of nutrients. However, this is not shown in our results where we found no significant difference in the amount of biomass in the fjord (6.5 µg C/l) and the open ocean (9.0 µg C/l), see fig. 12. Also, our nutrition analysis showed that the levels of nitrate was higher for the station representing the open ocean compared to fjord system station (fig. 16). We hypothesize that it is due to the time of the season that we do not find a higher biomass in the fjord compared to the open ocean, and, that if we would have sampled during springtime, with the disappearance of the ice, and where runoff from land is at its highest, and hence a higher amount of nutrients available, that we might have shown this. Also, it would be good with a more detailed study with more sampling sites, especially in the fjord, as we only had 3 stations representing this system. Likewise it would be an idea to move "deeper in to the fjord" before sampling to be sure to get 'true' fjordsamples. This would be our recommendations in future studies of a comparison between such systems.

We found a tendency for a higher netplankton biomass in the open ocean (7.1 µg C/l) compared to the fjord (3.0 µg C/l) which we did not see for the pico/nano plankton with 10.9 µg C/l in the open

ocean and 9.9 µg C/l in the fjord. The fact that it seems like the net plankton biomass might be higher in the open ocean could perhaps be that it experiences a slower sink out rate here due to the more turbulence and hence mixing of the water column. Also, it could be that we simply don't find as high a net plankton biomass in the fjord because of the fjordsystem having low nutrient levels at this time and hence favors pico/nano plankton growth because of its ability to grow at these low levels.

In the fjordsystem we did not find a significant difference in the biomass at different depths making the distribution of the biomass in the fjordsytem's watercolumn more homogeneous that is seen in the open ocean. This could be because of the water being less turbulent in the fjord compared to open ocean thereby having a more evenly distribution of plankton down through the water column (fig. 14).

(3) Temporal succession at Fortune Bay: 'An examination of the changes in phytoplankton biomass over time'

Succession over time for station 3, 8 and 12

We found that there was a change in the carbon biomass during the investigated time period in Disco Bay. The carbon biomass started out with 9.2 µg C/l at station 3 (beginning of sampling) and was somewhat the same at station 8, (mid sampling) with a value of 10.9 µg C/l, thereafter decreasing dramatically to 0.6 µg C/l at station 12 (end of sampling), see fig. 18. It seems that we have sampled at a time, where the diatom society was at the end of its blooming and therefore our last sample at station 12 shows that there is almost no diatoms left.

Even though the results show a very low biomass at station 12, we found a higher diversity of diatoms with 5 groups counted (*Proboscia alata, Rizosolenia, Chaetoceros debilis, Skeletonema, Feroseros*) which were not present in station 3 and 8 (fig. 23).

According to a study from 2007, the species composition in Disko Bay is mainly represented by *Thalassiosira spp* and *Chaetoseros spp* (Krawcyk et al 2014). Overall, this also reflects our findings as the dominating diatom species was *Chaetoceros* (67.4 ug C/l), which appeared at 9 out of 12 stations, whereas Thalassiosira spp did not contribute much biovolume-wise (0.018 ug C/l), but still they appeared at 10 out of 12 stations. The litterature suggests that the high amount of Chaetoceros spp indicates that we sampled in a species composition, which is in its Summer/Autumn blooming period rather than in its Spring/Summer blooming period. This makes sense since our results at all the 12 stations showed a *Chlorophyll a/Phaeophytin* ratio less than 1, which indeed indicates a dying system. Additionally, the low nutrient levels found throughout the stations may indicate that the nutrients have already been depleted.

We expected to find a shift in which size fraction that was the dominating one over time. Shifting from one where net plankton was the dominating type to pico/nano plankton being the dominating type later on. This, since the net plankton are bigger than pico/nanoplankton, which has a lower surface/volume ratio enabling the pico/nano plankton to take up nutrients more efficiently, and we expected low nutrient levels at the end of our sampling. When looking at our data these do not show a significant difference between the two size fractions over time though, see fig. 19. When looking at the nutrient levels we found through our sampling period these were at all times quite low, so this could perhaps be why we do not find a pronounced shift in which size fraction that is the dominating one. If our sampling period had begun earlier, before the depletion of the nutrients, we would maybe have been able to observe such a change

Because we see opposite tendencies of the dominating groups in station 3 and 8, we propose a more detailed study with more sampling, where seasonal variability is also taken into account, since this influences the foodweb and hence the dynamics of the grazers upon our diatoms. Especially, investigating variability in the disappearance of the sea-ice in the spring, because it regulates the

phytoplankton bloom, but also regulates the pelagic foodweb, which then, will influence the phytoplankton growth and composition (Nielsen Dsc 2004). Overall, the upper parts of the oceans have been hotter this year (2014) than ever previously measured (dmi.dk) and some parts of Western Greenland experienced the hottest summer in the period from June to August 2014. On the other hand the sea-ice in the Arctic was thicker than the last 4 years (Polar Portalen Sæsonrapport 2014).

Diatom species found in the waters surrounding Disco Island

Overall, when looking at former reports and in the literature, we have found the expected Diatom groups in the area of Disco Island. Interestingly, we found a new group, not earlier seen (to our knowledge) at these latitudes. This diatom belongs to the group *"Skeletonema"* which has its optimal growth at warmer waters. Looking at the recorded water temperature from Arctic station this year it is indeed higher than previous years which could be the reason for this finding.

Acknowledgements

We would like to thank the people, who have helped making this investigation possible. Thank you, to the captain and crew of the research vessel Porsild, and their families, for their help and cooperation with sampling and the practical work when collecting samples. Also, thank you, to the station manager, at the Arctic Field Station, Aqqaq and his wife, for all their help at the Arctic Station which made daily life possible, and things run smoothly. Finally, thanks to Øjvind Moestrup for the big help during the identification of the diatoms.

References

Armbrust, E. V. (2009, May). The life of diatoms in the world's oceans. *Nature, Vol 459* , pp. 185-192.

Azam, F., Long, R. A., (2001) Oceanography – Sea snow microcosms. Nature 414: 495-496

Bendtsen, J., J. Mortensen, and S. Rysgaard (2014), Seasonal surface layer dynamics and sensitivity to runoff in a high Arctic fjord (Young Sound/ Tyrolerfjord, 74□N), J. Geophys. Res. Oceans, 119, 6461–6478

Field, C. B., Behrenfeld, M. J., Randerson, J. T., & Falkowski, P. (1998, Jul). Primary Production of the Biosphere: Integrating Terrestrial and Oceanic Components. *Science, vol 281* , pp. 237-240.

Hamm, C. E., Merkel, R., Springer, O., Jurkojc, P., Maier, C., Prechtel, K., et al. (2003, Feb). Architecture and material properties of diatom shells provide effective mechanical protection. *Nature, vol 421* , pp. 841-843.

Hillebrand, H., Dürseten, C.,-D., Kirschtel, D. and Pollingher, U., and Zohary, T. (1999) Biovolume calculation for pelagic and Benthic microalgae. J. Phycol. 35: 403-424 (1999) J. Phycol 35:402-424

Horner, R.A. and V. Alexander (1972). Algal populations in Arctic Sea ice: an investigation of heterotrophy. – Limnology and Oceanography 17:454-458.

Kooistra, W. H., Gersonde, R., Medlin, L. K., & Mann, D. G. (2007). The Origin and Evolution of the Diatoms: Their Adaptation to a Planktonic Existence. In P. Falkowski, & A. H. Knoll, *Evolution of Primary Producers in the Sea* (pp. 207-249). Elsevier Academic Press.

Krawcyk, D. W., Witkowski, A., Waniek, J. J., Wroniecki, M, Harff, J., (2014) Description of diatoms from the Southwest to west Greenland coastel and open marine waters. Polar biol 37 : 1589-1606

Lenton, T., M. and Watson, A., J. (2000). What regulates the oxygen content of the atmosphere?, Global Biochemical cycles 14: 249-268

Michel, C., L. Legendre, J.-C Therriault, S. Demers and T. Vandevelde (1993). Springtime coupling between ice algal and phytoplankton assemblages in southeastern Hundson Bay, Canadian Arctic. – Polar Biology 13: 441-449.

Møller, E. F., Riemann, L., Søndergaard, M., (2007) Bacteria associated with copepods: abundance, activity and community composition. Aquatic Microbial Ecology 47: 99-106

Nielsen, T. G., (2005) Struktur og function af fødenettet I havets frie vandmasser. Doktodisputats. Danmarks Miljøundersøgelser. 71 s.

Nelson, D. M., Tréguer, P., Brzezinski, M. A., Leynaert, A., & Quéguiner, B. (1995, Sep). Production and dissolution of biogenic silica in the ocean: Revised global estimates, comparison with regional data and relationship to biogenic sedimentation. *Global biogeochemical cycle, vol. 9 (3)* , pp. 359-372.

Rabosky, D. L., & Sorhannus, U. (2009, Jan). Diversity dynamics of marine planktonic diatoms across the Cenozoic. *Nature, vol 457* , pp. 183-187.

Sarthou, G., Timmermans, K. R., Blain, S., & Tréguer, P. (2005). Growth physiology and fate of diatoms in the ocean: a review. *Journal of Sea Research 53* , pp. 25-42.

Schäfer, P., J. Thiede, S. Gerlach, G. Graf E. Suess and B. Zeitzchel (2001). The Environment of the northern North-Atlantic Ocean: Modern depositional processes and their historical documentation. Pp. 1-18.

Sigen Lett, Maria L. Paulsen and Signe S. Larsen (2010), Marien eukaryote phytoplankton in the waters around Disko Island (West Greenland): a first attempt to evaluate thier relative contribution to total biomass and productivity. Arctic Biology Field Course July 2010.

Sims, P. A., Mann, D. G., & Medlin, L. K. (2006). Evolution of the diatoms: insights from fossil, biological and molecular data. *Phycologia, vol 45 (4)* , pp. 361-402.

Sorhannus, U. (2007). A nuclear-encoded small-subunit ribosomal RNA timescale for diatom evolution. *Marine Micropaleontology 65* , pp. 1-12.

Thomas, D. N., Fogg, G. E., Convey, P., Fritsen, C. H., Gili, J. –M., Gradinger, R., Laybourn-Parry, J., Reid, K., and Walton, D. W. H (2008) The Biology of Polar Regions, Oxford University Press

KØBENHAVNS UNIVERSITET

The muscle twitch, maximal swimming speed and optimal temperature of four species of fish living in the Arctic

Af: Emilie Falk Kallenbach, Jeppe Nedergaard Pedersen, Nivi Kleist Johansen
Dato: 30.12.2014

Abstract

The swimming speed of fish has an ecological significance in, among other things, relation to avoiding predation and catching prey. The swimming speed is related to a several physical and physiological factors for, say, temperature, since it alters the enzymatic processes in the muscles, or alters the expression of genes. The relation between swimming speed and temperature has only been covered to a limited degree with the method used in this study, although it is highly relevant when considering potential consequences of the rising of the ocean temperatures and an easy method. This is the background for these experiments.

The purpose was to evaluate the relation between swimming speed and acute temperature changes for 4 different species caught in the sea around Disko Island in western Greenland during July 2014. Furthermore, two different methods to estimate maximal swimming speed, which we refer to as "filming" and "muscle twitch", were used with the objective of evaluate and compare these. Furthermore, we compare maximal swimming speed by using two different estimation methods, which we refer to as "filming" and "muscle twitch".

A decrease in contraction time and thereby an increase in swimming speed was observed as the temperature increased. This is in accordance with the results of previous studies. However, at certain degrees corresponding to the temperature of the ambient water in which the fishes were caught, the slope of the speed increase curve decreased. This supports the hypothesis that the fish has the highest performance at temperatures to which they are acclimatized.

The results from two methods support each other, which validate these methods as appropriate for estimating the maximum swimming speed of fishes.

1. Index

2. Introduction

Fishes in the Artic include eurythermal as well as more stenothermal species. Stenothermal species of the polar areas are theoretically the most susceptive species to adverse effects of global warming as there will be an increasingly narrower geographical range with colder waters for them to live in. However eurythermal species that live in the Arctic can also express physiological acclimatisation to colder waters and the global warming may affect the species in complex ways. The Atlantic cod is an example of an eurythermal species with a relatively large geographical range (83°N - 35°N, 95°W - 86°E) (http:/www.fishbase.org)
Relative to the surrounding temperatures prevailing in that specific geographical area the cod tend to express different haemoglobin types (Petersen & Steffensen 2003). Haemoglobin properties are one among more physiological factors that can affect limits for oxygen diffusion into, and therefore also properties of the muscle fibers (Johnston *et al*. 2006). Therefore, an optimal temperature for Atlantic cod muscle acclimated to a certain temperature could hypothetically be possible to trace. Other eurythermal fishes in the present experiment were; sculpins; widely distributed from southern latitudes to far above the Arctic circle (80°N -40°N, 95 °W – 60°E), the wolffishes (Anarhichas lupus) (79°N - 37°N, 75°W - 56°E) and the Arctic char (Salvelinus alpinus) (85°N - 42°N, 180°W - 180°E) (http:/www.fishbase.org).

Adaptation to low temperatures affects a wide scope of physiological functions (Tattersall *et al*. 2012) and the effectiveness of molecular functions. Enzymatic compensations strategies to low temperature can vary not only between species, but among individuals of same species with different ancestry related to environmental temperature (Seebacher *et al*. 2014; Stitt *et al*. 2014). Colder temperatures decrease oxygen diffusion rates as the molecular movements are slower. In skeletal muscles of fish the colder temperatures compensation strategies involve altering composition of membrane lipids to preserve fluidity and increasing mitochondrial volume to decrease diffusion distance.

Also the catalytic effect of enzymes in skeletal muscle (among other tissues) is lowered when fish are acutely exposed to low temperatures (McClelland & Scott 2013). To compensate fishes can express different isozymes of the same enzyme (with different temperature optima) in different proportions depending on the surrounding temperature (Willmer *et al*. 2005). It has been shown that acclimatization to lower temperatures in eurythermal species of fish has a marked locomotory performance trade-off in higher temperatures (Johnston & Temple 2002). All in all, acutely or long term, the many tissue adaptations to low temperature may make the fishes more or less vulnerable to adverse physiological effects of rising ocean temperatures (Woodward *et al*. 2014).

The muscle fibers of fish can roughly be divided into two groups based on their colour and function (Hudson 1973). The red oxidative muscles are usually only located as a thin layer just underneath the skin along the lateral line. The red colour is due to a relatively higher vascularization and a high content of myoglobin compared to white muscles. Red muscles are slow oxidative muscles that are used for aerobic and sustained swimming (Bone & Moore 2008). Red musculature may also partly be used for prolonged (faster) swimming together with the white musculature (Bone & Moore 2008; Lauder 2006). The maximum cruising speed for migrating fishes usually increase proportionally with the amount of red musculature. However, red musculature very rarely exceeds

25% of the total myotomal mass as non-specialized fish gills are limited in supplying the oxygen to this highly demanding tissue (Bone & Moore 2008).

The major part of the myotomal mass of the fishes are the fast glycolytic white muscles and these are in use at higher, anaerobic swimming speeds like burst swimming (Hudson 1973; Lauder 2006). As the white musculature is predominant in the fish and are the ones involved when maximal swimming speed is performed this is the focus of present study and is likewise used for other muscle twitch experiments (Brill & Dizon 1979).

The focus of the present study was to estimate if the skeletal muscle activity of 4 chosen species showed the tendencies to have a preferred temperature (a temperature in which they performed best). All of this would reflect how specifically the muscles of the fish were adapted to the temperature in which the fish are living. We would presume that the more adaptations each species have to lower temperatures, the more globally rising ocean temperatures would affect it. The lower range in which the fishes muscle could function, the more specialized the species is to arctic temperatures, and more vulnerable is it to global changes.

As mentioned many modifications of protein and membrane lipid expression are present in skeletal muscles of fish acclimated to low temperatures in the Arctic. One way of investigating the consequences of these modification in whole animals experiments is to look at it from the perspective of muscle functionality, and by that; their swimming capabilities.

The swimming capabilities and swimming speed of fish affects a wide range of their activities, such as successful prey captures and/or escape response from predators or fish trawls (Yanase *et al*. 2007). It can furthermore affect their geographical distribution range by means of affecting the cruising speed of migrating fishes and/or more indirectly affect them by inducing a behavioural response for the fish to locate to a new geographical setting in which the temperature is optimizing their physiology for instance their muscle activity (Stitt *et al*. 2014).

Fishes engage in different swim modes related to the specific activity. These modes have traditionally been divided into 3 categories; sustained, prolonged and burst swimming (Plaut 2001) Sustained and prolonged swimming are used for migration and other aerobic activities and are usually difficult to investigate (Plaut 2001). Burst swimming is an anaerobic metabolic process, which is important for escaping predators/fish trawls and for catching prey (Yanase *et al*. 2007). Burst swimming can more easily compared with than sustained and prolonged be investigated by different methods. Among these are swimming flumes and muscle twitch contraction experiments on tail muscle blocks. Each method has its benefits and drawbacks.

Swimming flume experiments has the benefit of using living fish. As the fish stays alive one can either examine the physiological response to an acute temperature change or let the fish acclimate to a new temperature over a longer time period, allowing it to up regulate different new proteins and enzymes that might optimize its physiological functions in a changing environment. However swim flume experiments has been criticized for representing an unnatural environment to the fish due to the size-restriction of the flume (wall effect) and the artificial flow characteristics of the water in the flume (uniformly micro turbulent flow as opposed to calm or turbulent waters in natural habitats) (Plaut 2001).

Muscle twitch experiments that examine either velocity or force are performed on excised muscles and have the benefit of a comparable simpler and faster experimental set-up. However as the fish are dead, only acute temperature response can be measured and as the muscle is excised it can fail to account for morphological restrictions opposed on the muscles in whole fish like spine resistance and other morphological restrictions.

The contraction time of the lateral tail muscles is limiting for the stride of a fish with subcarangiform swimming mode. A stride consists of oppositely located lateral tail muscles completing a full oscillation i.e. two times the contraction time. The distance of which the fish moves forward in the water following a full oscillation is variable and dependent on the morphology of the fish (Wardle *et al*. 1995) and is usually measured in relation to body length of the fish (Yanase *et al*. 2007).

3. Hypotheses

1. Fish is acclimated to the ambient temperature and therefore have their optimum temperature for swimming at that temperature.

4. Materials and methods

4.1 Twitch Experiment

During July 2014, 4 different species of fish were caught around Arctic felt station on Disko Island, Greenland (69 15' 8'' N, 53 31' 16''). *Gadus morhua*, *Myoxocephalus scorpius and Anarhichas lupus* were caught with fishing rod at Qeqertasuaq harbour (69 24'73'' N, 53 54' 79'') at 3-15 meters. *Salvelinus alpinus* were caught with fishing nets 0-20 meters from shore.

All fish were kept in tanks with aerated water and circulation at 4 °C. The fishes were euthanized prior to the trials with a stroke to the head.

The dead fish was kept in open bucket (30·25·5 cm) with sea water (3,7 L). The water temperature was manipulated in a range of 2-21°C. by use of a digital thermo-controller (PR5714D), an electronic aquarium heater (ViaAqua), a cooler (Hetofrig (heto Birkerød Denmark) and freezing elements. We monitored continuously the temperature both inside the fish, and in the surrounding water with a testo 925 (testo AG Germany 0560.9250 33786211/007).

Our experiment is based on measuring muscle twitch contraction times, but instead of using excised muscles we performed it on whole fish, thereby taking into account (to some extend) the morphological restrictions. It is a relatively unused method, which have the huge benefit of having a simple experimental set-up which can be used practically in-situ. Inspired from the experiment done on bluefin tuna by Wardle *et al*. (1989). Using this method we chose to investigate thermal response in muscles of four different species occurring in the Arctic.

The fish were placed outside the bucket in open air before the electric stimulations. The electrodes were placed in the lateral line at 50 % (±2%) of the length. We did some initial experiments testing if we could find variation in contraction time along the body of the fish, since other studies have found that contraction time increases from the head of the fish towards the tail, on a variety of different fish (Altringham & Ellerby 1999; Wardle 1985), but no differences in contraction time was found along the body. Electrodes were fitted each time to give the clearest signal of contraction and relaxation of the muscle. The fish were stimulated through electrodes connected to a SD9 Stimulator (Astro.Med, Inc. Grass, Product group. Ser 03J0151G) a serial of 7-9 sequential electric shocks of 5 volts (min 1 sec between stimuli) (for illustration of experimental setup see appendix 1) The time from start of stimuli to the maximum force of the contraction, activation time (T_a), and the time from onset to 90 % relaxation T_{90} was recorded with the program Logger Pro (example is shown in figure 1). This time corresponds to half a tail beat (Videler & Wardle 1991) as it takes two opposite located lateral muscles to complete a full oscillation (one 'stride'). The lateral muscles on one side of the fish need to come back to relaxation state before the muscles of the other side can contract. Therefore we did not, as done by (Wardle 1975), measure the time from onset of contraction to peak but instead from stimuli to t_{90} which also has been done in other studies, who found it to be a useful method and comparable with the method described by Archer *et al*. (1990). We repeated the stimulation to archive 5 replicates and a mean was calculated. This is in contrast with Yanase *et al*. (2007) who used only the shortest contraction time to estimate the maximum swimming speed.

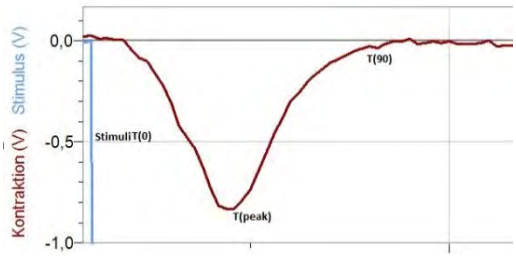

Figure 1 measurement of contraction time for lateral muscle (xx cm apart), indicating a half tail beat.

The maximum swimming speed in body length pr. second was calculated by using the following equation (Wardle 1975; Wardle *et al*. 1989)

$$U_{BL\cdot s^{-1},max} = \frac{L_s}{2 \cdot t_{90}(s)} \rightarrow U_{BL\cdot s^{-1},max} = \frac{0{,}7}{2 \cdot t_{90}(s)}$$

Were L_s is the stride length, that can vary highly (Wardle *et al*. 1995) for instance between 0,4-0,9 (Videler & Wardle 1991) but we used 0,7 as a standard since it is recommended by(Wardle 1975)

The tail beat frequency (F_t) was calculated by following equation

$$F_t = \frac{1}{2 \cdot t_{90}(s)}$$

When calculating the swimming speed from the contraction time we make some assumptions summarized by Brill & Dizon (1979). Among these is that we assume that maximum swimming speed is performed by the white muscles, that the tail beat amplitude won't change when the swimming speed is changing (Bainbridge 1958), that the maximal tail beat frequency limits the speed of swimming as Wardle stated (1975) and last, also stated by Wardle, that the tail beat frequency is limited by contraction of two muscles places laterally on each side of the fish Brill & Dizon (1979).

A summary of the fishes used in the experiment is showed in table 1 in appendix 2

4.2 Films

The video recordings of the cod were performed *in situ* near Qerqertasuaq. A go pro camera attached to a tackle recorded the fish as they hunted the tackle. The films was analysed in the program Windows Movie Maker that allowed the tail beats to be counted. From the videos fish performing burst swimming when hunting the tackle were selected. Furthermore 4 tail beats was decided to be the minimum for being usable for the analysis. The frequency was then calculated by the formula $frequency_{tailbeat} = 1/(\frac{tailbeats}{time})$. From the video it was not possible to obtain exact length of the fish, but the fish length could from a comparison with the length of the tackle be

estimated to have lengths around 30cm ±10cm. This is supported by the lengths of the fish caught, which were all approximately 30cm.

4.3 Data analysis

All graphs and statistical tests were performed with GraphPad Prism 6.0.

5. Results

5.1 Fish size and tail beat frequency.

To test if a relation between length of the fish and tail beat frequency existed, all fish were sorted by their length and all temperatures where tested for significant relation by a simple linear regression test, three representing (high, middle, low) temperature is shown figure 2 to 5. The results shows that there does not exist any relation between length and tail beat frequency for cod (figure 3) and wolfish (figure 5), since the tendency is not significant different from zero (p values 0,20 (2°C) and 0,70 (14°C) for cod (n=10) and 0,82 (2°C) and 0,80 (14°C) for wolfish (n=7)). In contrast a significant relation between frequency and length, was found at some test temperature for trout and sculpin, which have lower frequency as the length increases (figure 4) (p values for sculpin (n=10) 0,03 (5°C)- 0,02 (8°C) and 0,00 (3°C) - 0,03(°C) - 0,00 (15°C) for trout (n=6)).

From this experiment it is difficult to make any clear conclusion for artic char and sculpin, as the relation is found at some temperatures but not at others. It is opposite for wolfish and cod, that have no relation at all. To compensate for this, all results is transformed into body length per second, This unit is independent of fish length, and is well used in other fish studies.

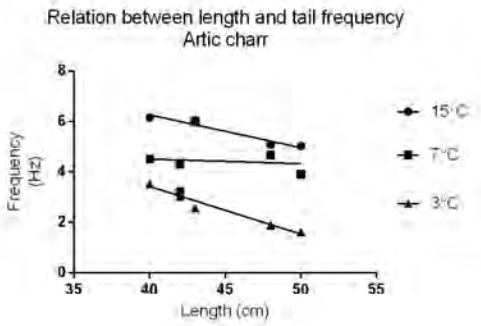

Figure 2 the relation between tail beat frequency and fish length for artic char (n=6). There is a significant tendency (different from zero) that length has an influence on tail beat frequency at 3°C(P=0,0006), 9°C (p0,0249)(not shown) and 0,0006 (15°C) but not for all the other temperatures

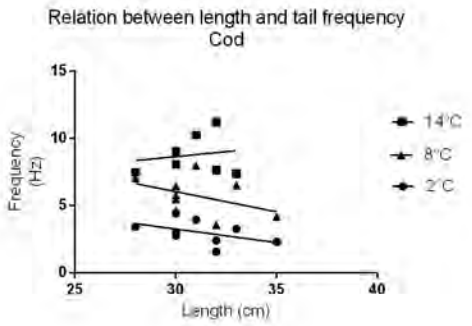

Figure 3 the relation between tail beat frequency and fish length, for cod (n=10), the static test shows no significant relation (tendency line not different from zero) at all temperatures.

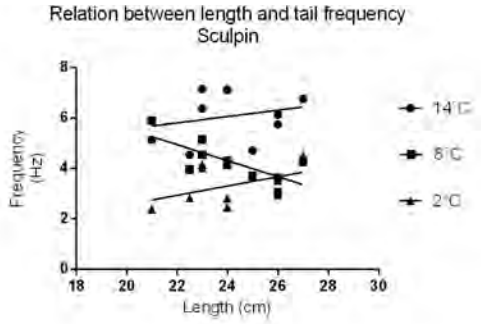

Figure 4 the relation between tail beat frequency and fish length for sculpin (n=10). There is a significant relation between tail beat and length at 5°C (P=0,0339) and 8°C (p=0,0156). But not for all other temperatures tested.

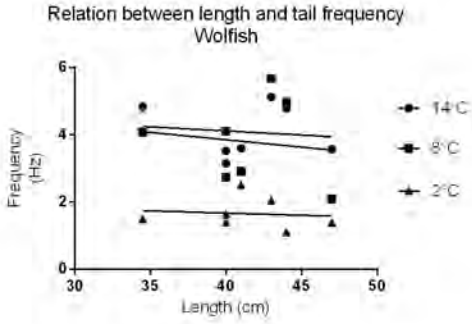

Figure 5 the relation between tail beat frequency and fish length for wolfish (n=7). The statistic test shows no significant relation at any temperature.

5.2 Video experiment

During fish collection (19/7/14) video observations (n=7) of fast swimming cod (*Gadus morhua)* hunting prey (fishing jig) from the depth of 1,7 m. From the recordings, the bust tail beat frequency was manually calculated showing an average of 8,43 Hz ±2,67 Hz in 8°C water. There was no significant (P=0,87, unpaired t-test) difference between the video data and the frequency from the muscle twitch experiment obtained at 8 °C (n=9). The data are showed graphically in figure 6.

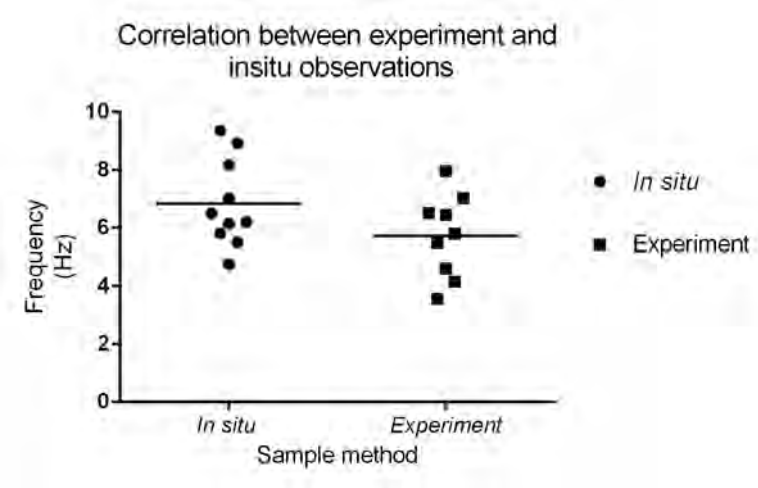

Figure 6, Tail beat frequency from the video recordings (*in situ*) and from the muscle twitch experiment, both from 8 °C water, shows no significant (p=0,87) difference.

5.3 Temperatures influence on swimming speed.

To compare the different species, at different size, the muscle twitch contraction time was converted into speed in body length (BL) per second. For this calculation a stride length at 0,7 were used (as mentioned in chapter 4.1). Figure 7 shows an overview of the correlation between speed and temperature for all tested species.

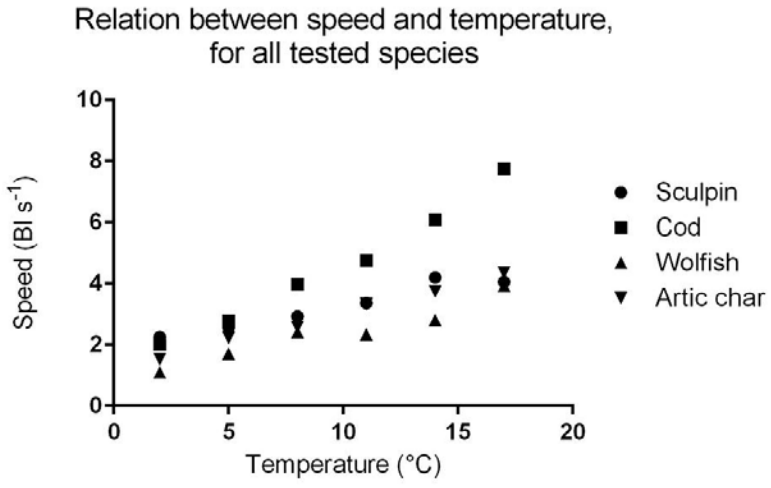

Figure 7, maximun swimming speed for all tested species. Each species is shown indivudially in figure 8. Test size n(sculpin)=10, n(cod)=10, n(wolfish)=7 and n(char)=6.

The general tendency (for temperatures below 11°C) is an exponentially increasing swimming speed with increasing temperatures. In cod the increase is stable throughout the temperature spectrum as seen in figure 8. For the other species the increase in swimming speed slows down when temperatures get above 11°C as illustrated in figure 8.

5.6 The optimised temperature for swimming speed

The swimming speed results were put into an Arrhenius plot, to find the optimal temperature for the different species.

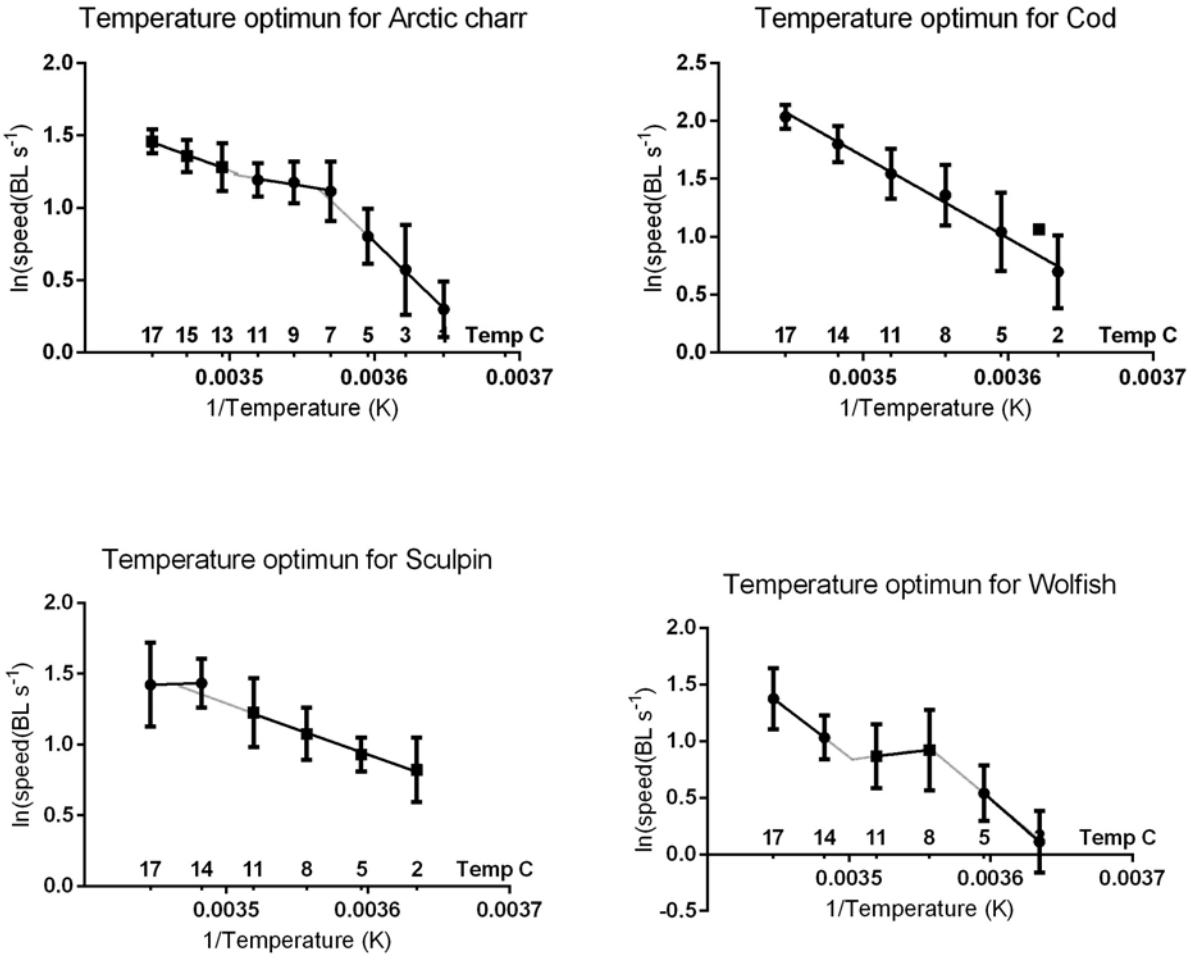

Figure 8, the relation between swimming speed and temperature in a Arrhenius plot, the slopes of the curves indicate the swimming speed of the fish, and kink in the curves gives the optimised temperature for the fish. n(char)=7, n(cod)=10, n(sculpin)=10 and n(wolfish)=7.

The relation between temperature and speed gives an idea on the fish adaption, in theory swimming speed will increase as temperature rise, due to higher speed in cell processes, but as fish is adapted to a certain temperature there fitness will decrease when it is exceed. The kink in the curve shows at which temperature the fitness will start decreasing. For trout (n=6) the fitness increase highest at low temperatures until 7 °C (0,0036 on 1/T scale), thereafter it levels out until 14°C (0,0035 on 1/T

scale) where the slope increasing again. For cod (n=10) the maximum temperature was not found during this experiment. Sculpin (n=10) had an increasing slope until 14°C (0,0035 on 1/T scale), where the slope starts decreasing. The wolfish (n=7) slope levels out at 8°C (0,0036 on 1/T scale) before its starts rising again, giving an optimised temperature for wolfish between 8°C and 14°C.

6. Discussion

6.1 Evaluation of the used method

As mentioned in the introduction a variety of different methods measuring the swimming speed of fish can be used. Among these is to take out muscle fibres and measure their force-velocity relationships while keeping them in a ringer solution. This method requires a relatively smaller set-up, but the data demands quite extensive calculations, as one has to adjust for a lot of the natural factors that affects the muscles in an intact fish. These factors include position of the excised muscle in relation to the length and morphology of the fish. Also, there are other factors influencing the swimming speed of a fish that are difficult to take account for in calculations; like for instance the resistance of the spinal cord and the different arrangements of the myomeres.

In contrast one can make video-analysis of swimming fish, The films, have the advantage that the measurements are done *in situ* and in theory contain all of the factors that affects the muscles (as we are looking at intact and living fish in their natural environments) and give more reliable data of the swimming speed of the fish. However, videos of fish's maximum swimming speed can be quite hard to obtain, taking their different habitats (they could live in a light limited area or very deep) and uncontrollable behaviours (they can be nocturnal, too elusive etc.) into consideration.

In our experiment we measured muscle twitch to calculate maximal tail beat frequency of the fishes. This method is practical since it can be done almost everywhere, and because it is a small and quite mobile setup. However it has the disadvantage that the fish is no longer alive and we have to presume that the muscle twitch obtained from the dead fish (to an acceptable degree) represents the muscle-twitch of a living fish. By using the entire fish, and not just a muscle block, our experiment has the advantage that the resistance performed by the spinal cord and the rest of the fish is included.

6.1.2 Variation of swimming modes of different species

A problem that could be addressed is that we calculate swimming speed based on muscle twitches of the lateral caudal muscles of the fish while some species of fishes may use other muscles in addition to these depending on their preferred swimming mode. Even though the sculpin may have quite prominent pectoral fins a study show that they are held steady and laterally extended during swimming, while oscillation of median fins, the tail and the caudal fin are used for swimming (Taft *et al*. 2008). Artic Char most likely use the lateral caudal muscles together with some yaw of the head for swimming as it is a salmonid like a rainbow trout, which is known to swim with a subcarangiform for swimming (Webb *et al*. 1984). The cod certainly use subcarangiform swimming

(Martinez *et al*. 2003) and we have supplementary video recordings to analyse the speed the cods swim when capturing prey (a fishing lure) i.e. a form for burst swimming. The wolffish is a less investigated fish in the literature, but we assume, even though it is a bit elongated in shape compared to salmonids and gadiforms that it is using a subcarangiform for locomotion.
However, we are measuring muscle-twitches in white anaerobic muscles which are the ones that are used partly in prolonged swimming and are fully engaged in burst swimming (Lauder 2006). For this mode of locomotion they most probably all engage in a c-form or subcarangiform/carangiform where the caudal lateral white muscles are the predominant utilised ones. A problem associated with the experiment rises if it is not exclusively white muscles that are stimulated. However, significant amount of red musculature was only found in the Arctic char, which is a migrating species that travels long distances. We did not notice any significant degree of red musculature in the comparatively less athletic Atlantic cod and neither in the less active sculpin or in the wolf fish.

6.2 Comparing results with studies using other methods

The existence of multiple methods to investigate swimming speed of fishes makes comparison between study results difficult. For instance; when comparing results obtained from a swimming flume and from a muscle twitch experiments one has to take into consideration that the fishes in the flume are being exposed to prolonged swimming which affects the muscles differently than a few electric pulses in a muscle twitch setting. The U_{crit}-value found in a swimming flume experiment is the fish's maximum swimming speed, which should roughly correspond to what we call 'maximum swimming speed' in our muscle twitch experiment. In the flumes though, the fishes usually has to perform prolonged swimming in steps with increasing water flow and, depending on the temporal duration of each step, they may use a lot of ATP and build up lactate in the tissues; all of which in the end influence time to fatigue. As we induce relatively fewer muscle contractions in the dead fish, we do not expose the muscles to same level of depletion of ATP and lactate accumulation. However, dead fishes are obviously not able to renew ATP stores in the muscles during the experiment. We therefore had to assume that we avoided complete depletion of the ATP stores by giving relatively few electrical pulses to induce contractions of the muscles.

Furthermore a problem was observed since a full relaxation of some fish after contraction did not take place. It was tried handled by measuring t_{90}. However this could have been due to some molecular changes. For instance do Ball & Johnston (1996) observe a similar lack of relaxation. They are able to see a pattern that it only occurs for the cold-acclimated fish at high temperatures, which they explains with the Ca^{2+} independent residual force (Ball & Johnston 1996).

To support the validity of our results it has been observed that theoretical maximal swimming speed for a salmonid obtained by a muscle twitch experiment was very close to that which was observed for burst swimming in a swimming flume (Clough & Turnpenny 2001)

The problem with ATP depletion and lactate accumulation can however arise when using our method on newly caught fish, as that there is no way of knowing if they already are in some state of

fatigue. We encountered this problem in an occasion where we were catching Arctic Char in net and the fishes had exhausted themselves previous to the experiment.

6.3 Using Arrhenius breaking point plot to estimate optimal temperature (T_{opt})

If we were using the temperature to estimate the fitness, we would have to assume that a relationship exists between swimming speed and fitness that could allow us to use swimming speed as a proxy for fitness. However there are few only clear experiments showing such a relationship (Johnston & Temple 2002) so we do not in study claim any connection between swimming speed and fitness of the species.

We do however try to estimate the optimal temperature (T_{opt}) for the muscles functioning. For this we use the Arrhenius breaking-point plot. This idea stems from a study by Casselman *et al*. (2012) where they use a two-segment linear regression to estimate optimal temperature for heart rate in *Oncorhynchus kisutch* exposing the fish for acute temperature changes, like we do. Most physiological functions in ectotherms follow a constant Q_{10} response when temperatures increase or decrease (Willmer *et al*. 2005). We therefore assume that the enzymatic processes in the fishes' used in this experiment skeletal muscles responsible for contraction activity follow a typical Q10 response. A typical Q_{10} response is a linear response that shows 2-3 fold increasing activity per 10°C (Schmidt-Nielsen 1997) and this gives one of the linear curves in the Arrhenius plot. When the temperature increases (or decreases) to a point where physiological functions starts to collapse, the linearity with the Q_{10} will cease to exist. That said, the muscle contraction times of the fishes will respond divertingly from that predicted by the Q_{10}. This can be due to denaturing of the proteins responsible for the enzymatic processes for contraction or any number of processes beyond the scope for this report. What we look for is a change in the slope that indicates this physiological collapse. At the temperature where these two differing slopes meet, we assume the muscle has its optimum for performance (T_{opt}).

6.4 Contraction time and length

In our studies we did not find any relation between tail beat frequency speed and body length for cod and wolf fish. This is in agreement with Yanase *et al*. (2007) who tested sand flatheads (*Platycephalus bassensis*) but contrast most other studies that finds that body length affects the contraction time of the muscles thereby allowing a higher tail beat frequency (Wardle 1975, 1980). We did, however find a relation in Arctic char and sculpin at some temperatures, which showed a decrease in maximum tail beat frequency with increasing size. Videler & Wardle (1991) found the Q_{10cm}, which is the ratio of the maximum tail beat frequency per 10 increase in length, for cod (*Gadus morhua*) is 0,89 and 0,88 for salmon (*Salmo salar*). Furthermore has a study done on cods showed that the contraction time is related to length in following way $t = 12 \cdot 9L^{0,29}$ (Archer *et al*. 1990). That only some of our results, show this trend can be because we have a small variation in size (cod 7 cm, arctic char 10 cm, wolfish 12,5 cm, sculpin 6 cm) compared with Archer *et al*. (1990) which have a size span on 50 cm for salmon and 64,5 cm for cod.

6.5. Stride lengths between species

When we compare the swimming speed we obtained in this experiment, it can be seen that there is not any clear difference in the swimming speed between the four species. This however can be due to the method used since we have used the same stride length for each of the four species, which probably will vary due to different morphology and swimming style (Videler & Wardle 1991). If the physics of the fish is taken into consideration, a salmon and cod, have larger area of tail compared to sculpin, thereby moving larger amount of water each beat, which leads us to expect that the two first mentioned species have a higher stride length than sculpin. This is supported by literature were *Gadus morhua* is found to have a stride length around 0,6 (for a fish at 30 cm at 12°C, film) and the stride length of rainbow trout (*Oncorhynchus mykiss*) is measured to be 0,52 BLs^{-1} (15°C fish tunnel, 60 cm) or 0,62 BLs^{-1} (wheel, 40 cm) (Videler & Wardle 1991). In contrast the stride length of sculpin is estimated to be 0,26 BLs^{-1} at (5°C) which is lower than the other two (Johnston *et al*. 1993). Furthermore is has been shown that pelagic species have a longer stride length than species found in the benthic environment such as the sculpin and wolffish (Videler & Wardle 1991). But not only morphology and position in the water column is affecting the stride length, also the swimming speed of the fish has been found to affect the stride length. For bluefin tuna the longest stride length was observed at relatively low swimming speed, but the relation between swimming speed and stride length is not unambiguous since other studies have found that no such relation exist within a normal range of swimming speeds (Videler & Wardle 1991; Wardle *et al*. 1989). However since literature describing the swimming speed of fish uses a general stride length of 0,7 it must be assumed that it is applicable (Arimoto *et al*. 1991; Wardle 1975).

6.6. Discussion of results

All species show a logarithmically increased swimming speed ($\ln(BLs^{-1})$) with increasing temperature. The Arctic char and the wolffish have a decrease in the slope around 8-10°C, which is a T_{opt} corresponding to the ambient water temperature in which the fishes were caught. In contrast the sculpin seems to increase its swimming speed steadily all the way up to 14°C and the Atlantic cod seems to be able to cope with even higher temperatures and there is no decrease in the slope for its swimming speed ($\ln(BLs^{-1})$). In studies done with carps a different expression of the myosin light and heavy chain genes was found (Crockford & Johnston 1990; Hwang *et al*. 1991). Furthermore has the activity of Ca^{2+}-ATPase been found to have an increased activity in cold-acclimated carps compared with warm-acclimated carps which will result in an increased rate of relaxation of the muscles (Fleming *et al*. 1990). In addition myofibrillar ATPase has an increased activity in cold-acclimated fish to maintain a high swimming speed at low temperatures (Davison *et al*. 1975; Hwang *et al*. 1991). Using an ANOVA-test it is seen that the curves for the four different species is not significantly different from each other. This is in accordance with our hypothesis, that suggests that no difference in swimming speed will occur between the fish species since the acclamatory processes is thought to take place. However it is seen that the Atlantic cod and the Arctic char are having a tendency towards a higher swimming speeds than the sculpin and the wolf fish even though we did not take the possible differences in stride length between the species into account. The fact that the Atlantic cod does not show to be negatively affected by increasing temperature can be due to the fact that it, as an Atlantic species, is better adapted to warmer waters with

temperatures raging between -1-20°C (Drinkwater 2005) than for instance the Arctic char which is has a preferred temperature around 9,2 °C (Peterson *et al*. 1979)

An exponential decrease in contraction time and thereby an increase in swimming speed in relation to temperature is also found in other studies (Ozbilgin *et al*. 2011; Yanase *et al*. 2007). This is to be expected since the enzymatic processes works at an optimal temperature and starts denaturation at temperatures higher than this and works at a lower rate at temperatures lower than the optimal. When we compare the swimming speed we obtained in this study with what is found in other studies we see a slight difference.
Videler and Wardle (1991), found that rainbow trout (*Oncorhynchus mykiss)*, which is the closest representative they have to our Arctic char, had maximum speeds (burst swimming) between 9,6 - 10,2 BLs^{-1} for a respectively, 28cm and a 10cm long individual at 15°C. These values are relatively higher than our results which show maximum speeds for Arctic char at 15°C between 4-5 BLs^{-1}. We do not expect that the results obtained by Videler and Wardle's results are an overestimation, since they are produces via a swimming wheel, which is not considered to overestimate the swimming speed of the fish, since the fish experience fatigue after having been tested for a long time, and in most cases are prevented to do burst swimming due to spatial constraints (wall effect). However, there is a noticeable size difference between their and our fishes; 10-28cm vs. 40-50cm in our experiment.
As we are using body length per stride to estimate swimming speed it is not possible to compare fish with size-differences of this magnitude. As the fish grow, the stride length compared to its body size will most often decrease while it's absolute swimming speed increases.

As in the case for our Arctic char our results for sculpin are also lower than values found in the literature. Johnston et al. (1993) found, by analysing videos, that sculpins of approximately same size fish as ours (20-26cm vs. 21-27) moved between 2-4 BL^{-1} during power strokes at 5C.

Our values are in the low end of this. We did find it difficult to place the electrodes correctly on the narrow peduncle of the sculpins, due to their relatively small size and relatively smaller myotomal mass of this species. For this species in particular the video recordings or other experimental approaches may be much better suited than ours. If our method should be applied on sculpins at least a modification of the size and distance between the electrodes should be modified.

6.7 Tail beat frequencies of cod obtained by muscle twitch vs. by video

When we compared our measurements of the cod from the video observation we found that there was no significant difference between tail beat frequency in the video observation and in our muscle twitch experiments. Using films as a method of estimating the swimming speed of fish, has the disadvantage that it is not possible to ensure that the fish swims with it's maximal speed to optimise the data, a fishing lure (without hooks) were used as bait. The observation of frequency was four tail beats during the attack of the lure. However, the potential sources of error listed above has a somewhat of an importance as comparison with the other studies e.g. which finds a TBF for cod is

6,7 Hz (30cm) and 5,1 Hz (42cm) (Videler & Wardle 1991) by video recordings, qiute lower than the average TBF at 8,43± 1,01Hz N=7 (approximately 30 cm ±10cm), we found in our video sample even though the video recording are made at the same temperatures.

In our studies we find accordance between swimming speeds obtained by the videos and twitch experiment and thereby validate the twitch as a useful method to predict the maximum swimming speed.

The data from the video observations agreed well with data from our muscle twitch experiment

Through the times there has been made substantial criticism of Wardle (1975) method, and Johnsrude & Webb (1985) point out that, as there in live, swimming fish are a wide range of mechanical components that will act together in a complex way, it is complicated to predict the swimming speed purely from the properties of the muscles. Johnsrude & Webb (1985) argue that the real contraction times of the lateral muscles at high swimming speeds in a live fish are longer compared to the contraction time of a experimentally induced muscle twitch.

The force i.e the amplitude of our measured contraction (see fig. 1) is affecting the time of contraction. And one of the ways amplitude (force) of a muscle twitch can be affected is if negative work is applied to the muscle right before the contraction; this means that if the muscle is stretched right before it is contracting (as they would be by the lateral muscles of the opposite side of a real life swimming fish) the contraction force will be stronger (Johnsrude & Webb 1985) and this will, as mentioned, affect twitch time. We only measured contractions of one side of the fish that was lying flat on a table; thereby we did not expose the muscles for any negative work prior to the electric pulse. This probably has given us a relatively smaller amplitude and thereby also shorter contraction time, which may in the end have made us overestimate the swimming speed.

Moreover, Johnsrude & Webb (1985) performed experiments to detect fast-start movements in which it was found that the different fish at no time reached a speed as the one suggested by Wardle (1975) and Webb (1978). This, however, was not the case in our experiments, were a perfect compliance existed between the two methods used.

7. Conclusion

As we had limited time and several technical issues we are not confident to say that this study validates the method of choice. We did see a very good correlation between obtained swimming speed for cod by muscle twitch and video recordings, however the sample size was not impressive.

Cod

We did not find an optimal temperature for Atlantic cod by using the Arrhenius plot on our data. We explain this by referring to the geographical range and lifestyle of the Atlantic cod that causes them to be exposed to a wide range of temperatures and thereby they have a less narrow detectable optimum temperature range. The cod (n=10) were between 28-35 cm and the length showed to not significantly influence the muscle twitch contraction time among each other.

Sculpin

Optimal temperature for the sculpin seems to be high (approximately 14-15°C). Sculpins are shallow water- and a relatively less active species and thereby may not necessarily need especially cold adapted muscles during the summer. We had difficulties with our method on the sculpin as their caudal muscles are shallow and it was more difficult to place the electrodes on this particular species.

Arctic char

The optimal temperature for the Arctic char seem to correlate good with the mean environmental temperature (8°C) with a curve breaking point around 7°C. Arctic char is an athletic species with high activity level so a detective cold acclimated muscle tissue makes good sense. This species has a large muscle mass and may be suitable for the method. However unfortunate, we had six samples of this species and many were exhausted prior to use in the nets we caught them in; they went into rigor mortis pretty fast, probably due to depleted ATP stores and lactate accumulation from fighting the nets.

Wolffish

The Arrhenius curve looks peculiar for the wolffish with two breaking points. As for the example of the cod the wolffish has a large geographical range and is found in shallow as well as deep water and is less active so it may be less specialized related to temperature adaptations.

Method

All species show increasing muscle twitch contraction times and this partly validates the method as this indicates a realistic measure of faster enzyme rates in the tissues. More video recordings of the different species would be needed for better comparison and validation of method. The studies of Wardle *et al*. (1989) and Wardle & He (1988) and our results for the cod that show remarkable compliance between muscle twitch activity and video recordings still give optimistic results for the application of this method. For the sculpins other methods may be more appropriate due to their shallow muscle tissue. More studies are needed to validate the method. Application to estimate the fishes response to global rising temperatures may be limited as the data obtained are for acute temperature change in muscles and we saw very little evidence of specialized acclimatization to the surrounding temperatures of the fishes involved.

8. Literature

Altringham, J.D. and Ellerby, D.J. (1999) Fish swimming: Patterns in muscle function. *Journal of Experimental Biology* 202, 3397-3403.

Archer, S.D., Altringham, J.D. and Johnston, I.A. (1990) Scaling effects on the neuromuscular system, twitch kinetics and morphometrics of the cod, gadus-morhua. *Marine Behaviour and Physiology* 17, 137-146.

Arimoto, T., Gang, X. and Matsushita, Y. (1991) Muscle contraction time of captured walleye pollock Theragra chalcogramma. *Bulletin of the Japanese Society of Scientific Fisheries* 57, 1225-1228.

Bainbridge, R. (1958) The speed of swimming of fish as related to size and to the frequency and amplitude of the tail beat. *Journal of Experimental Biology* 35, 109-133.

Ball, D. and Johnston, I.A. (1996) Molecular mechanisms underlying the plasticity of muscle contractile properties with temperature acclimation in the marine fish Myoxocephalus scorpius. *Journal of Experimental Biology* 199, 1363-1373.

Bone, Q. and Moore, R.H. (2008) Biology of fishes, Taylor and Francis.

Brill, R.W. and Dizon, A.E. (1979) Effect of temperature on isotonic twitch of white muscle and predicted maximum swimming speeds of skipjack tuna, katsuwonus-pelamis. *Environmental Biology of Fishes* 4, 199-205.

Casselman, M.T., Anttila, K. and Farrell, A.P. (2012) Using maximum heart rate as a rapid screening tool to determine optimum temperature for aerobic scope in Pacific salmon Oncorhynchus spp. *Journal of Fish Biology* 80, 358-377.

Clough, S.C. and Turnpenny, A.W.H. (2001) Swimming speeds in fish: Phase 1. *Environment Agency Research and Development Technical Report* W2-026/TR1, i-xii, 1-94.

Crockford, T. and Johnston, I.A. (1990) Temperature-acclimation and the expression of contractile protein isoforms in the skeletal-muscles of the common carp (*Cyprinus carpio* L.). *Journal of Comparative Physiology B-Biochemical Systemic and Environmental Physiology* 160, 23-30.

Davison, W., Goldspink, G. and Johnston, I.A. (1975) Adaptations in Mg-2+-activated myofibrillar ATPase activity induced by temperature acclimation. *FEBS letters* 50, 293-295.

Drinkwater, K.F. (2005) The response of Atlantic cod (Gadus morhua) to future climate change. *Ices Journal of Marine Science* 62, 1327-1337.

Fleming, J.R., Crockford, T., Altringham, J.D. and Johnston, I.A. (1990) Effects of temperature-acclimation on muscle-relaxation in the carp - a mechanical, biochemical, and ultrastructural-study. *Journal of Experimental Zoology* 255, 286-295.

Hudson, R.C.L. (1973) Function of white muscles in teleosts at intermediate swimming speeds. *Journal of Experimental Biology* 58, 509-522.

Hwang, G.C., Ochiai, Y., Watabe, S. and Hashimoto, K. (1991) Changes of carp myosin subfragment-1 induced by temperature-acclimation. *Journal of Comparative Physiology B-Biochemical Systemic and Environmental Physiology* 161, 141-146.

Johnsrude, C.L. and Webb, P.W. (1985) Mechanical-properties of the myotomal musculoskeletal system of rainbow-trout, salmo-gairdneri. *Journal of Experimental Biology* 119, 71-83.

Johnston, I.A., Abercromby, M. and Andersen, O. (2006) Muscle fibre number varies with haemoglobin phenotype in Atlantic cod as predicted by the optimal fibre number hypothesis. *Biology Letters* 2, 590-592.

Johnston, I.A., Franklin, C.E. and Johnson, T.P. (1993) Recruitment patterns and contractile properties of fast muscle-fibers isolated from rostral and caudal myotomes of the short-horned sculpin. *Journal of Experimental Biology* 185, 251-265.

Johnston, I.A. and Temple, G.K. (2002) Thermal plasticity of skeletal muscle phenotype in ectothermic vertebrates and its significance for locomotory behaviour. *Journal of Experimental Biology* 205, 2305-2322.

Lauder, G.V. (2006) Physiology of fishes. , Taylor and Francis.Third edition

Martinez, M., Guderley, H., Dutil, J.D., Winger, P.D., He, P. and Walsh, S.J. (2003) Condition, prolonged swimming performance and muscle metabolic capacities of cod Gadus morhua. *Journal of Experimental Biology* 206, 503-511.

McClelland, G.B. and Scott, G.R. (2013) The physiology of fishes., CRC press, Taylor and Francis group.

Ozbilgin, H., Pehlivan, M. and Basaran, F. (2011) Maximum swimming speed predictions for Mullus barbatus (Linnaeus, 1758) and Diplodus annularis (Linnaeus, 1758). *Turkish Journal of Zoology* 35, 79-85.

Petersen, M.F. and Steffensen, J.F. (2003) Preferred temperature of juvenile Atlantic cod Gadus morhua with different haemoglobin genotypes at normoxia and moderate hypoxia. *Journal of Experimental Biology* 206, 359-364.

Peterson, R.H., Sutterlin, A.M. and Metcalfe, J.L. (1979) Temperature preference of several species of salmo and salvelinus and some of their hybrids. *Journal of the Fisheries Research Board of Canada* 36, 1137-1140.

Plaut, I. (2001) Critical swimming speed: its ecological relevance. *Comparative Biochemistry and Physiology a-Molecular and Integrative Physiology* 131, 41-50.

Schmidt-Nielsen, K. (1997) Animal Physiology, Adaptation and Environment, Cambridge.Fifth Edition

Seebacher, F., Beaman, J. and Little, A.G. (2014) Regulation of thermal acclimation varies between generations of the short-lived mosquitofish that developed in different environmental conditions. *Functional Ecology* 28, 137-148.

Stitt, B.C., Burness, G., Burgomaster, K.A., Currie, S., McDermid, J.L. and Wilson, C.C. (2014) Intraspecific Variation in Thermal Tolerance and Acclimation Capacity in Brook Trout (Salvelinus fontinalis): Physiological Implications for Climate Change. *Physiological and Biochemical Zoology* 87, 15-29.

Taft, N.K., Lauder, G.V. and Madden, P.G.A. (2008) Functional regionalization of the pectoral fin of the benthic longhorn sculpin during station holding and swimming. *Journal of Zoology* 276, 159-167.

Tattersall, G.J., Sinclair, B.J., Withers, P.C., Fields, P.A., Seebacher, F., Cooper, C.E. and Maloney, S.K. (2012) Coping with Thermal Challenges: Physiological Adaptations to Environmental Temperatures. *Comprehensive Physiology* 2, 2151-2202.

Videler, J.J. and Wardle, C.S. (1991) Fish swimming stride by stride: speed limits and endurance. *Reviews in Fish Biology and Fisheries* 1, 23-40.

Wardle, C.S. (1975) Limit of fish swimming speed. *Nature* 255, 725-727.

Wardle, C.S. (1980) Effects of temperature on the maximum swimming speed of fishes. *NATO ASI (Advanced Science Institutes) Series Series A Life Sciences* 35, 519-531.

Wardle, C.S. (1985) Swimming activity in marine fish. *Symposia of the Society for Experimental Biology* 39, 521-540.

Wardle, C.S. and He, P. (1988) Burst swimming speeds of mackerel, Scomber-scombrus L. *Journal of Fish Biology* 32, 471-478.

Wardle, C.S., Videler, J.J. and Altringham, J.D. (1995) Tuning in to fish swimming waves - body form, swimming mode and muscle function. *Journal of Experimental Biology* 198, 1629-1636.

Wardle, C.S., Videler, J.J., Arimoto, T., Franco, J.M. and He, P. (1989) The muscle twitch and the maximum swimming speed of giant bluefin tuna, Thunnus-thynnus L. *Journal of Fish Biology* 35, 129-137.

Webb, P.W. (1978) Fast-start performance and body form in 7 species of teleost fish. *Journal of Experimental Biology* 74, 211-226.

Webb, P.W., Kostecki, P.T. and Stevens, E.D. (1984) The effect of size and swimming speed on locomotor kinematics of rainbow-trout. *Journal of Experimental Biology* 109, 77-95.

Willmer, P., Graham, S. and Johnston, I. (2005) Environmental Physiology of Animals, Blackwell Publishing.Third edition

Woodward, A., Smith, K.R., Campbell-Lendrum, D., Chadee, D.D., Honda, Y., Liu, Q., Olwoch, J., Revich, B., Sauerborn, R., Chafe, Z., Confalonieri, U. and Haines, A. (2014) Climate change and health: on the latest IPCC report. *Lancet* 383, 1185-1189.

Yanase, K., Eayrs, S. and Arimoto, T. (2007) Influence of water temperature and fish length on the maximum swimming speed of sand flathead, Platycephalus bassensis: Implications for trawl selectivity. *Fisheries Research* 84, 180-188.

9. Appendix 1.

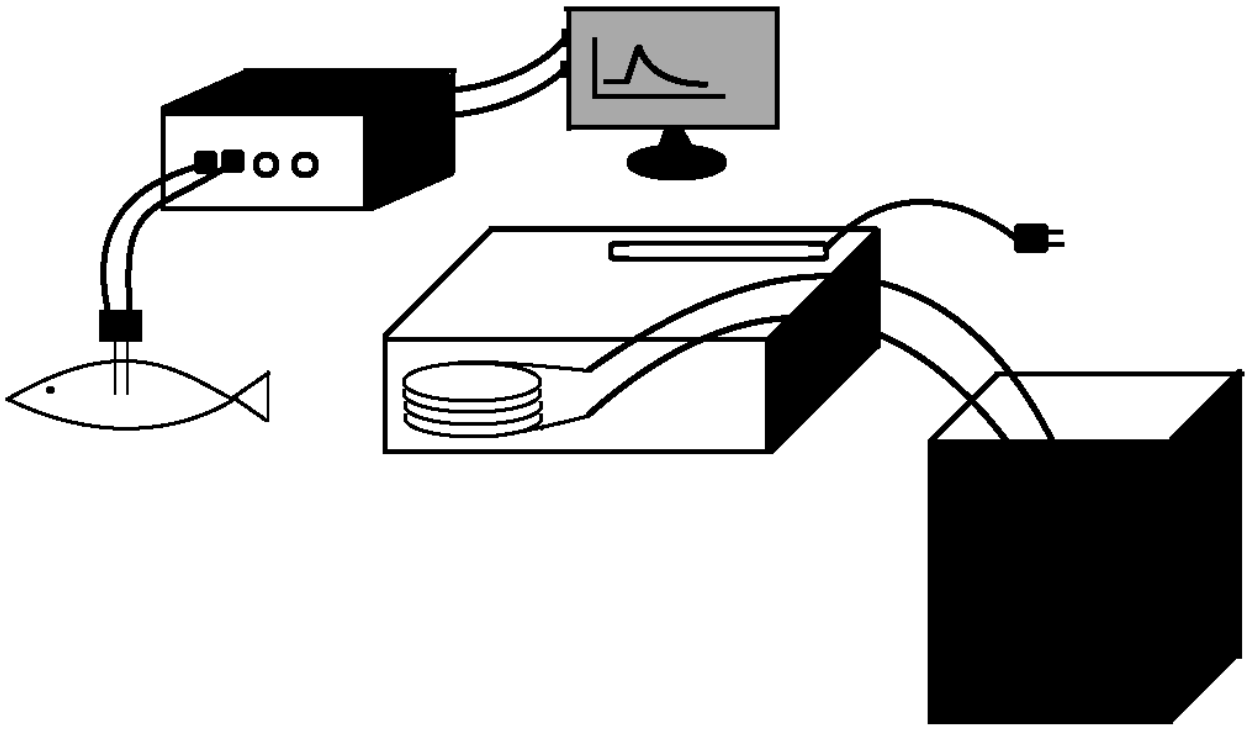

10. Appendix 2

Cod nr.	*Length (cm)*
2	30
4	32
5	31
6	35
7	28
8	30
9	30
10	32
11	30
12	33

Sculpin nr.	*Length (cm)*
2	26
4	26
5	27
6	23
7	23
8	21
9	22,5
10	24
11	25
12	24

Wolffish nr.	*Length (cm)*
1	34,5
2	41
3	44
4	40
5	40
6	43
7	47

Arctic char nr.	*Length (cm)*
3	43
4	42
6	40
7	48
8	50
9	42

Determining the optimum temperature for aerobic scope of a northern population of Arctic charr (*Salvelinus alpinus*) using maximum heart rate.

by Aslak Kappel Hansen, Mads Reinholdt Jensen, David Bille Byriel

Abstract

Assessment of optimum aerobic scope in ectoderms can help predict species' distributional responses to warming. The waters of the Arctic regions represent one of the most vulnerable ecosystems to climatic change. At these latitudes Arctic charr represents the only anadromous species, playing a critical role in both fresh- and seawater. In this study we use the maximum heart rate (f_{Hmax}) to determine the optimum aerobic scope of 9 adult Arctic charr (*Salvelinus alpinus*) around Qeqertarsuaq, Greenland. The Arrhenius breakpoint occurred between 5.9 °C and 8.3 °C (average = 7.1 °C ± 0.8) when determined using maximum heart rate. The Q_{10} breakpoint happened between an average of 6.1 °C ± 0.9 and 7.1 °C ± 0.9. There was no significant difference between the breakpoint temperature found using Q_{10} and Arrhenius [two-sample t-test, d.f. = 16; P > 0.05]. The highest f_{Hmax} was found at 12.8 °C ± 2.9 reaching an average of 61.8 BPM ± 9.2. Arrhythmia occurred at between 11 °C and 18 °C (average = 15.2 °C ± 2.5). We found that this northern population of Arctic charr lives at summer temperatures that are optimal for their oxygen uptake. To fully understand how the Arctic charr is going to respond to warmer temperatures, combining research on several physiological processes including aerobic scope might be applicable.

Keywords: Arctic charr, aerobic scope, metabolic rate, optimum temperature, global warming, Greenland

Introduction

Aquatic ectoderms have evolved into optimizing biochemical and physiological capacities so that aerobic scope is optimal within a given temperature range. The aerobic scope is given by the difference in minimum and maximum M_{O2} on whole body performance (Fry, 1947). This has been widely used in addressing questions relating to the effects of future climate change on fish species (Pörtner et al., 2001). Staying within this given temperature range of aerobic scope helps optimizing fitness related tasks (locomotion, reproduction and growth etc.). This has been coined the oxygen- and capacity-limited thermal tolerance hypothesis (OCLTT) (Pörtner et al., 2001). As Global Circulation Models (GCMs) indicate increasing temperatures with the highest effects on the Arctic and Subarctic regions (Drinkwater, 2005), it would be reasonable to expect an alternation of the fish distributions throughout the waters of the Northern hemisphere. The northward movement of the polar front will inarguably affect the population dynamics of the fish species currently living in the Arctic and Subarctic waters. It is a complex system, but it is very likely that a change in temperature will affect the aerobic scope of various Arctic fish species.

The circumpolar Arctic charr is well-known for being the northernmost freshwater fish. It is widely distributed throughout Scandinavia and reaches as far up north as 82°34´N on Ellesmere Island (Balon, 1980). Population studies have estimated that Arctic charr is represented by 50.000 populations worldwide, with

Greenland and Iceland holding approximately 1.000 populations (Maitland, 1995). It is of special importance in the Arctic regions, as it is here often the only fish species present in the lakes at high latitudes, thereby playing an important role as an apex predator in freshwaters of Arctic ecosystems as well as being an important food source for Arctic inhabitants during the summer months.

The purpose of this study is to assess whether the Arctic charr can cope with increasing temperatures, expected with climate change, given their optimal aerobic scope in wild populations of Arctic charr around Qeqertarsuaq, Greenland.

Conventionally the optimum temperature (T_{opt}) would be found by measuring M_{O2} for fishes at rest and at maximal work for various temperatures, thereby obtaining an aerobic scope curve. This method is both time consuming, as the fish need to fully recover from each measurement, and requires extensive experimental equipment (respirometer, large holding tank etc.). An alternative method for acquiring T_{opt} has been proposed by Casselman et al. (2012). T_{opt}. can be rapidly determined by finding the temperature where the maximum heart rate (f_{Hmax}) stops increasing exponentially. To obviate the problem of the activity state altering heart rate (f_H), fish were anaesthetized during the warming procedure and maximum f_H was achieved through pharmacological means. The method showed that there is no significance difference between the T_{opt} obtained in Pacific salmon, *Onchorynchus* spp. by using heart rate scope (mean ±s.e. = 16·5 ± 0·2 °C) than that of aerobic scope (mean ±s.e. = 17·0 ± 0·7 °C) thus allowing a faster experimental procedure (Gollock et al., 2006).

The study conducted here is, to our knowledge, the first study investigating the aerobic scope of Arctic charr. Other studies have used different approaches to estimate optimal living conditions for Arctic charr. Larsson et al. (2005) adopted a thermoregulatory shuttle-box, initially designed by Neill et al. (1972) to find the optimal growth rate of 11 populations of Arctic charr throughout Sweden, Norway and England to be 16°C ± 0.24 °C, while Peterson et al. (1979) found 9,2 °C as the preferred temperature of Arctic charr across a latitudinal gradient. Using a new method for finding thermal preference, Larsson (2005) found that Arctic charr from two different populations acclimatized to 9 - 11 °C waters showed preference to this temperature (10.8 °C ±1.0 and 11.8 °C ± 1.3), despite it being 4,5 °C lower than their optimal growth rate found in his other study (Larsson et al., 2005) and closer to the temperature preference found by Peterson et al. (1979). It was suggested that this was either due to reduced food availability (Brett, 1971, Mac, 1985) or that optimal temperature for food conversion was lower than the optimal growth temperature (Jobling, 1997).

A recent study on the aerobic scope of the Atlantic salmon (*Salmo salar*), belonging to the same family as Arctic charr, has shown that different populations of Atlantic salmon have different optimum temperature scopes depending on both their geographical population distribution as well as the temperature they have been acclimatized to (Anttila et al., 2014). Because of the wide distribution range and number of populations, it is reasonable to assume that the Arctic charr is locally adapted to a wide range of different temperatures influencing the optimal aerobic scope across different geographical ranges. Therefore, increasing water

temperatures could cause populations of Arctic charr to migrate northwards, acclimating to new temperatures by exploiting its phenotypic plasticity or adapting through natural selection (Hofmann and Todgham, 2010). Failing to do so, the population will ultimately go extinct (Parmesan, 2006). Northern populations of Arctic charr have limited northwards migration possibilities as their existence is dependent on freshwater. Most presumably the competition pressure on the northern populations will continue to grow, as more species will migrate northwards in a changing climate.

Predictive distributional modeling of Arctic charr in Canada estimated a reduction of 40% in their range size from 2005 to 2020 due to climatic changes (Chu et al., 2005). These results were obtained by presence-absence data, which is likely to be influenced by other means than temperature, e.g. human influence, parasites or competition. Such predictive distributional modeling often does not account for underlying physiological processes that govern the actual distribution. This leads to estimate failures that we hope to help uncover. By revealing the optimum temperature for aerobic scope, we might be able to determine how the future distributions of Arctic charr might develop.

Materials and methods

FISH COLLECTION AND STORAGE

Adult Arctic charr were caught daily, using a bottom gillnet set from the shore and 50 meter perpendicular into the ocean. The net was set up with a heavy rock in the water, making sure the net was not dragged back onto shore. It was set just east of Qeqertarsuaq (Godhavn), Greenland (69°14'59.2" N 53°31'10.4" W) in July 2014, with water temperature of approximately 7 °C. We used a pulling system, which allowed us to check the net for newly caught fish every two hours, without going too far into the water.

Figure 1: Site of fish collection (red circle), situated on the Disko Island of the Greenlandic West coast

They were transported in 100 L buckets directly to one of two holding tanks containing seawater obtained from the local harbor. Holding tanks were constructed using two 450 L isolated polyethylene food containers, connected by soft PVC tubes. Water was recycled from the lower one to the upper one using an EHEIM pump (1046 Universal Pump). An overflow between the two tanks through a perforated bucket filled with filter cotton was established in order to keep the water clean. The holding tanks were placed in a cooling container (standard 40 feet) set up prior to our arrival, cooling towards 4 °C and maintaining a steady water temperature of 4.5 °C, range ±0.5 °C.

EXPERIMENTAL SETUP

Fish were transported from the 450 L holding tank one at a time to the lab, where they were anaesthetized (100 mg l^{-1} MS-222) in a 10 L bucket with constant aeration. After the fish were fully anaesthetized, tested by holding the tail upwards until the fish had no reaction, they were put in a 15 L water container (containing 50 mg l^{-1} MS-222) where the experiment was performed during the following 3-6 hours.

The fish were placed with their dorsal fin pointing downwards in the water container, and two coated stainless steel wires (M-N-Systems) were inserted on either side of the heart, which gave us the ECG-output. f_{Hmax} was measured using a preamplifier (ECG 100C) connected to a data acquisition unit (Biopak MP-150) which collected data to our computer through the program AcqKnowledge (version 4.3).

Oxygen saturation of the water container was maintained by an air pump (Rena Air 200). An EHEIM-pump was inserted in the mouth to maintain oxygen flow as well as the anaesthetized state of the fish with gill irrigation. This also helped recirculating the water in the container.

In order to adjust the temperature of the water, and thereby of the fish, we used a PR5714 multi-instrument connected to the PT100 temperature sensor. Temperature was measured to a precision of 0.1 - 0.2 °C using the PT100 temperature sensor. Desired temperature was set on the PR5714, which would either cool, using an EHEIM-pump, which pumped cooling liquid from a cooling bath (Heto-Holten) through a closed stainless steel coil, or heat, using a 250 W titanium aquarium heater.

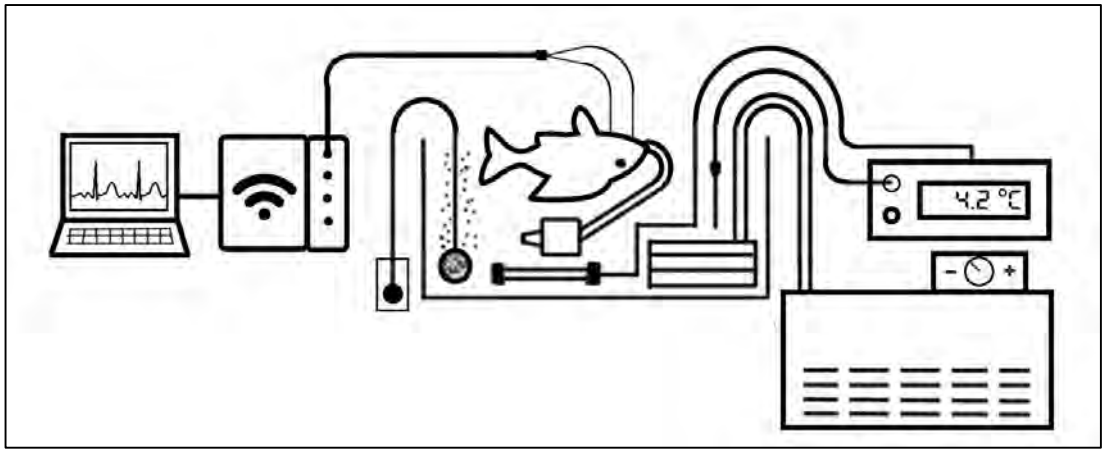

Figure 2: Experimental setup, a) Computer with AcqKnowledge running, b) Biopak MP-150 data acquisition unit, c) ECG 100C preamplifier, d) M-N-Systems coated stainless steel wires, e) Rena Air 200 air pump, f) EHEIM-pump, g) 250 W titanium aquarium heater, h) closed stainless steel coil, i) PT100 temperature sensor, j) PR5714 multi-instrument, k) Heto-Holten cooling bath.

MEASURING MAXIMUM HEART RATE DURING ACUTE WARMING

After resting in the anaesthetizing water for 30 minutes, the fish was injected with first atropine (0.1 ml of 1.2 mg ml^{-1} per 100 g of body mass) and subsequently isoproterenol (0.1 ml of 4 µg ml^{-1} per 100 g of body mass). We usually saw an

increase in heart rate of around 2-3 beats per minute (BPM) during the following 15 minutes, after which we started the experiment.

We raised the temperature of the water in 1 °C increments, pausing between intervals for the fish's heart rate to stabilize. In order to accelerate the process of stabilization and avoid the long waiting time associated with heating the core of the fish, we would always let the surrounding water rise 0.2 - 0.3 °C more than the temperature that we wanted the fish to become, before cooling towards the temperature we wanted. Using K-value described by Stevens and Sutterlin (1976) this would result in much faster desired temperature. The experiments were started at 1 °C and were likewise continuously warmed until arrhythmia occurred. The fish would be warmed around 8 $^{\circ}$C h^{-1}. We kept increasing the temperature at 1 °C increments until arrhythmia (T_{arr}) occurred.

INTERPRETING THE PREAMPLIFIED SIGNAL

Using AcqKnowledge we were able to monitor the heart rate signal and intensity of the fish. When the signal was good, we would use the program's estimation of the fish's heart rate as our BPM, but when the signal ceased or became unclear, we would count heartbeats for 15 seconds, and multiply it with 4 to calculate the BPM of the fish in the experiment.

As we were about to reach the critical point of arrhythmia, the fish would in many cases start to skip heart beats or in other ways show incomprehensible QRS-waves in the ECG. This was determined to be the T_{arr}.

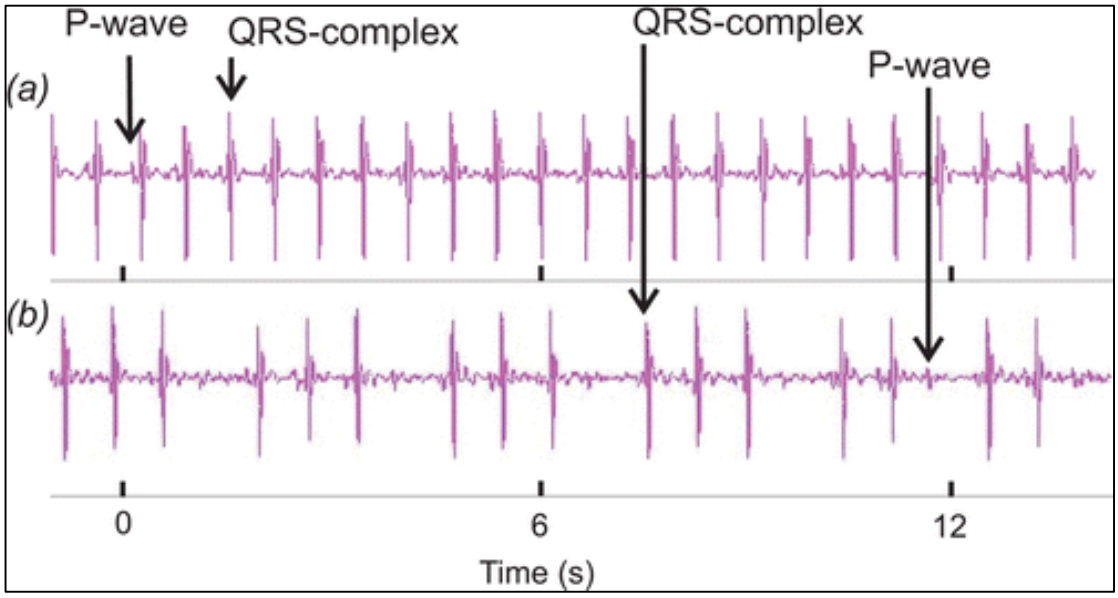

Figure 3: Shows the changes in the electrocardiogram when arrhythmia occurs. The signal is skipping beats and is becoming incomprehensible. From Ferreira et al. (2014)

DATA ANALYSIS

Following method by Yeager and Ultsch (1989) the Arrhenius breakpoint temperature was calculated for all individuals, by plotting the natural log of the heart rate ($\ln(f_{Hmax})$) against the inverse of temperature (1000 K^{-1}). The breakpoint was determined by finding the intersection of two best-fit linear

regressions. This was done for all individuals and an average Arrhenius breakpoint temperature and standard deviation for all samples was found. The Arrhenius breakpoint temperature for individual fish was thought of as an index of the optimal temperature (T_{opt}) for living conditions by Casselman et al. (2012). Q_{10} increments were calculated using the formula,

$$Q_{10} = \left(\frac{f_{H2}}{f_{H1}}\right)^{10/(T_2-T_1)}$$

This was done for all individuals and for each 1 °C increment. When Q_{10} for each individual dropped and stayed below 2.0, the temperature was recorded. The low Q_{10} breakpoint temperature is the last temperature where the Q_{10} is above 2.0, whereas the high Q_{10} breakpoint temperature is recorded as the temperature when Q_{10} is dropped and stays below 2.0. A Q_{10} value of 2.0 is regarded as a normal rate of change of routine metabolism with temperature (Fry and Hochachka, 1970, Miller and Mann, 1973, Holeton, 1974). We are using the high Q_{10} breakpoint, as the T_{opt}, as this is the temperature where Q_{10} stays below our set critical value of 2.0. Arrhythmic breakpoint temperature was recorded when the heart started to fail, causing heart rate to drop dramatically, this was proposed by Casselman et al. (2012) to be an index of the critical temperature (T_{crit}) of the fish. t-tests (fiducial limit $P < 0.05$) were performed to test (1) if the means found by Q_{10} were different to those found by Arrhenius breakpoint temperature, (2) if there was a difference between the means of Q_{10} between 2-6 °C and those between 8-temperature at highest f_{Hmax}. All data are presented as a ± standard deviation unless otherwise stated.

Results

As shown in figure 4, all fish showed a steadily increasing heart rate when exposed to acute warming, until the Arrhenius breakpoint occurred, at which point the increments were decreased until it crashed. Most individuals showed a rapid decrease in f_{Hmax} (associated with heart arrhythmia) soon after reaching the highest f_{Hmax}. At 1 °C, average f_{Hmax} was 28.6 ± 2.7 BPM and mean f_{Hmax} increased steadily until 10 °C, after this point there were large variations between individuals. The Arrhenius breakpoint occurred between 5.9 °C and 8.3 °C (average = 7.1 °C ± 0.8) when determined using the method applied by Casselman et al. (2012) on individuals. The Q_{10} breakpoint happened between an average of 6.1 °C ± 0.9 and 7.1 °C ± 0.9. There was no significant difference between the breakpoint temperature found using Q_{10} and Arrhenius [two-sample t-test, d.f. = 16; $P > 0.05$]. At the Arrhenius breakpoint temperature the average f_{Hmax} was 47.8 ± 4.4. Heart rate increased steadily across the temperature interval 2-6 °C (Q_{10}, average = 2.3 ± 0.4), but slower between 8 °C and the temperature at Arrhenius breakpoint (Q_{10}, average = 1.5 ± 0.4) [two-sample t-test, d.f. = 88; $P > 0{\cdot}05$]. The highest f_{Hmax} was found at 12.8 °C ± 2.9 reaching an average of 61.8 BPM ± 9.2. Arrhythmia occurred at between 11 °C and 18 °C (average = 15.2 °C ± 2.5). The accumulated heart arrhythmia of the fish is shown in figure 4.

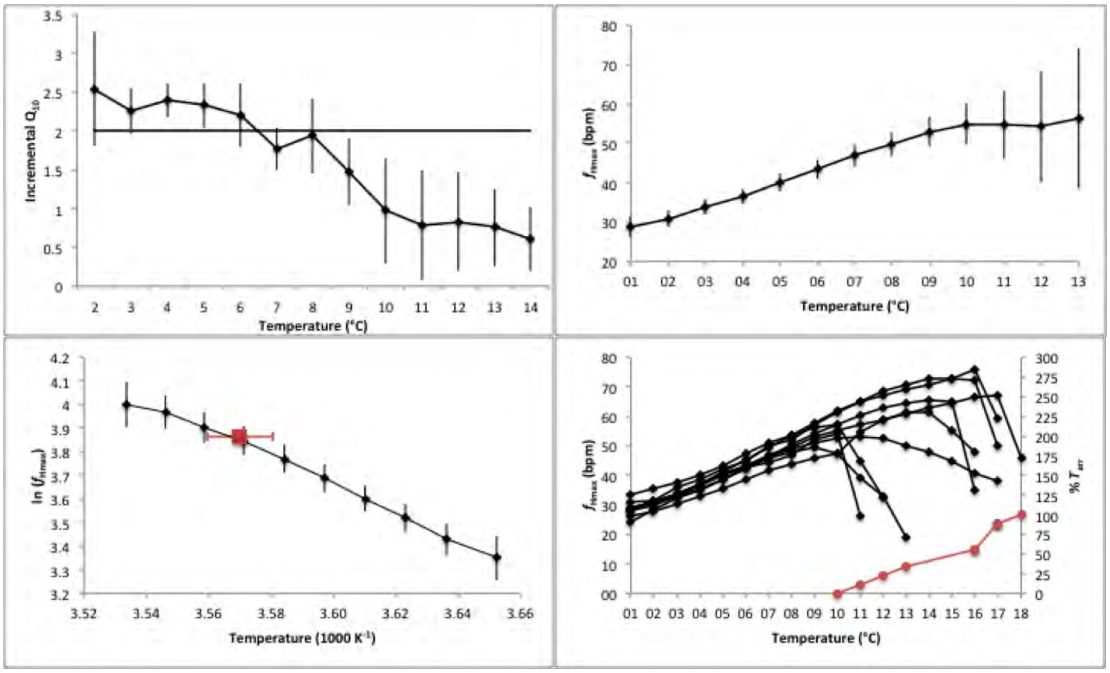

Figure 4: Graphs show the responses of Arctic charr to acute warming. a) Mean maximum heart rate (f_{Hmax}) in response to warming of 1 °C increments, vertical lines show standard deviation. b) Maximum heart rate (f_{Hmax}) of inviduals in response to warming of 1 °C increments. Red line shows the accumulated percentage of fish enduring cardiac arrhythmia and the temperature it occurs. c) Plot of the mean natural log of the heart rate (ln(f_{Hmax})) against the inverse of temperature (1000 K^{-1}) with standard deviation. The red square shows the mean Arrhenius breakpoint temperature with its standard deviation. 4) Mean Q_{10} increments with standard deviation. Horizontal line marks the 2.0 breakpoint, where Q_{10} increments fail to sustain normal metabolism.

Arctic charr, n=9	Average	S.D.
f_{Hmax} at 1°C	28.61	2.70
Q_{10} (2-6 °C)	2.35	0.43
Q_{10} (8 °C - Temp. at Highest f_{Hmax})	1.47	0.41
f_{Hmax} at arrhenius breakpoint	47.76	4.36
Temperature at arrhenius breakpoint	7.12	0.83
Low Q_{10} breakpoint temperature	6.11	0.93
High Q_{10} breakpoint temperature	7.11	0.93
Highest f_{Hmax}	61.83	9.22
Temperature at highest f_{Hmax}	12.78	2.87
Temperature at arrhythmia	15.22	2.54

Table 1: Mean data points of different variables as well as their standard deviation.

Arctic charr, n=9	Average	S. D.
Weight (g)	851,32	144,37
Length (cm)	43,61	2,63

Table 2: Mean weight and length of the Arctic charr used in this study as well as their standard deviations.

Discussion

The method for finding the optimal temperature of fish was originally described by Casselman et al. (2012), and several studies have already been carried out using their method (Anttila et al., 2014, Drost et al., 2014, Ferreira et al., 2014). In the present we show that what before took months to accomplish can be done in a couple of weeks, by correlating the Arrhenius breakpoint temperature and Q_{10} breakpoint temperature to the optimal temperature. Using this 'quick and dirty' method is of special relevance when working in the outskirts of the world, where transportation of fish back to a lab can be difficult. This experiment can be set up quickly on limited space and measurements can be made almost instantaneously, only restricted by the availability of electricity, which is not the case for the older conventional setup. Respirometry required fish to be in tanks for weeks and measurements to be done every couple of days at acclimatized temperatures.

Maximum aerobic scope for Arctic charr was found to be at 7.1 ± 0.9 °C. This is consistent with the water temperatures in which the Arctic charr were caught at (~7 °C), and could imply that the Arctic charr is living under optimal temperature conditions during the anadromous migration to sea in the summer months. In relation to the oxygen- and capacity-limited thermal tolerance (OCLTT) theory, which assumes that aerobic scope is the fundamental physiological process driving overall physiological performance, our results would indicate that optimum for several physiological processes have adapted to this temperature.

A recent study on Atlantic halibuts showed that optimum temperature for growth was not correlated with oxygen uptake, as the aerobic scope failed to explain detrimental effect on growth at increased temperature (Gräns et al., 2014, Jutfelt et al., 2014). This disagrees with the OCLTT theory from 2001, which suggest that these would be linked. This paper was criticized for its methodology, as they fail to maintain similar physiological state between growth and aerobic scope measurements (Pörtner, 2014). It was also argued that the polynomial fit of their aerobic scope curve did not pick up an aerobic scope decline at high temperatures. This new insight questions the OCLTT theory, which makes it further difficult to access the results gained from an optimal aerobic scope experiment alone. More research is needed to determine the implications of these results, as well as how interactions of different physiological processes, including aerobic scope are connected. Whatever the implication of this new study is, one thing is for certain; acclimation and evolutionary adaptation of physiological processes plays an important role.

Peterson et al. (1979) found a preferred temperature of 9.2 °C for the Arctic charr, but our results suggest that our northern population has an optimal temperature of 7.1 °C. The differences found in studies of the aerobic scope of Arctic charr could be largely shaped by quick physiological acclimatization to temperatures. A study

on Atlantic salmon (Anttila et al., 2014) has shown the plasticity and adaptability of a species within the same family. It adapts to the temperature both on an evolutionary scale, as two populations of the same species have different T_{opt} in different areas, but it largely adapts to the temperature on a daily or weekly scale, where adjusting to another temperature is also shown. It is reasonable to suggest that these results could account for the differences found between our population of Arctic charr and the population investigated in Larsson (2005). Future genetic studies may allow us to determine the magnitude of the acclimatization dependency of aerobic scope. A genetic study could also provide knowledge needed on how optimal aerobic scope is affected through evolution or acclimation in wild populations of Arctic charr.

As opposed to the OCLTT theory, the idea of multiple performances - multiple optima (MPMO) assumes that different physiological processes have different optimal temperatures (Clark et al., 2013). Different temperature optima could be present for different processes such as growth, reproduction and locomotion.
The study of physiological optima is particularly interesting in anadromous species, such as Arctic charr, that live in different environments throughout the year and often under different temperatures. Under such conditions it might be optimal for the species to optimize growth for part of the season, while reproduction might be optimized in other parts of the season. More research is needed to determine whether oxygen capacity limits the physiological processes of Arctic charr, or if different optima are governing different activities.

Pörtner and Knust (2007) argued that lab and field studies are needed to shape future distributions models, especially when facing the immediate threat of climate change. To fully understand how the Arctic charr is going to respond to warmer temperatures, combined research on several physiological processes including aerobic scope might be an applicable tool. Our study shows that the northern populations of Arctic charr are currently living at summer temperatures that are optimal for their oxygen uptake. It is uncertain whether the optimal aerobic scope, found in this study also coincides with optima for other physiological processes.

The trade-offs that the fish face when water temperatures increase include pressure from southern fish populations versus moving further north to new spawning sites. Dutil (1986) showed that reproducing individuals of Arctic charr contained as much as 46 % less energy compared to non-reproductive charrs when migrating to sea prior to spawning. Migrating upwards rivers and investing energy into gonads is costly, therefore even small changes in river and lake temperatures could influence the reproduction of the Arctic charr. Another problem of increasing water temperatures is that these northern populations are on the brink of being pushed so far north that freshwater lakes for spawning are no longer present.

It is uncertain whether the optimal aerobic scope found in this study is a result of recent acclimation to warmer temperatures or adaptation through natural selection. More research on this area is needed to elucidate how physiological processes are influenced by these different mechanisms.

References

ANTTILA, K., COUTURIER, C. S., ØVERLI, Ø., JOHNSEN, A., MARTHINSEN, G., NILSSON, G. E. & FARRELL, A. P. 2014. Atlantic salmon show capability for cardiac acclimation to warm temperatures. *Nature communications,* 5.

BALON, E. K. 1980. *Charrs. Salmonid fishes of the genus Salvelinus*, Dr. W. Junk bv Publishers.

BRETT, J. R. 1971. Energetic responses of salmon to temperature. A study of some thermal relations in the physiology and freshwater ecology of sockeye salmon (Oncorhynchus nerkd). *American zoologist,* 11**,** 99-113.

CASSELMAN, M., ANTTILA, K. & FARRELL, A. 2012. Using maximum heart rate as a rapid screening tool to determine optimum temperature for aerobic scope in Pacific salmon *Oncorhynchus* spp. *Journal of fish biology,* 80**,** 358-377.

CHU, C., MANDRAK, N. E. & MINNS, C. K. 2005. Potential impacts of climate change on the distributions of several common and rare freshwater fishes in Canada. *Diversity and Distributions,* 11**,** 299-310.

CLARK, T. D., SANDBLOM, E. & JUTFELT, F. 2013. Aerobic scope measurements of fishes in an era of climate change: respirometry, relevance and recommendations. *The Journal of experimental biology,* 216**,** 2771-2782.

DRINKWATER, K. F. 2005. The response of Atlantic cod (*Gadus morhua*) to future climate change. *ICES Journal of Marine Science: Journal du Conseil,* 62**,** 1327-1337.

DROST, H., CARMACK, E. & FARRELL, A. 2014. Upper thermal limits of cardiac function for Arctic cod *Boreogadus saida*, a key food web fish species in the Arctic Ocean. *Journal of Fish Biology*.

DUTIL, J.-D. 1986. Energetic constraints and spawning interval in the anadromous Arctic charr (*Salvelinus alpinus*). *Copeia***,** 945-955.

FERREIRA, E. O., ANTTILA, K. & FARRELL, A. P. 2014. Thermal Optima and Tolerance in the Eurythermic Goldfish (Carassius auratus): Relationships between Whole-Animal Aerobic Capacity and Maximum Heart Rate. *Physiological and Biochemical Zoology,* 87**,** 599-611.

FRY, F. E. J. 1947. *Effects of the environment on animal activity*, Toronto, University of Toronto Press.

FRY, F. E. J. & HOCHACHKA, P. W. 1970. *Fish,* New York

London, Academic Press.

GOLLOCK, M., CURRIE, S., PETERSEN, L. & GAMPERL, A. 2006. Cardiovascular and haematological responses of Atlantic cod (*Gadus morhua*) to acute temperature increase. *Journal of Experimental Biology,* 209**,** 2961-2970.

GRÄNS, A., JUTFELT, F., SANDBLOM, E., JÖNSSON, E., WIKLANDER, K., SETH, H., OLSSON, C., DUPONT, S., ORTEGA-MARTINEZ, O. & EINARSDOTTIR, I. 2014. Aerobic scope fails to explain the detrimental effects on growth resulting from warming and elevated CO2 in Atlantic halibut. *The Journal of Experimental Biology,* 217**,** 711-717.

HOFMANN, G. E. & TODGHAM, A. E. 2010. Living in the now: physiological mechanisms to tolerate a rapidly changing environment. *Annual Review of Physiology,* 72**,** 127-145.

HOLETON, G. F. 1974. Metabolic cold adaptation of polar fish: fact or artefact? *Physiological Zoology***,** 137-152.

JOBLING, M. Temperature and growth: modulation of growth rate via temperature change. SEMINAR SERIES-SOCIETY FOR EXPERIMENTAL BIOLOGY, 1997. Cambridge University Press, 225-254.

JUTFELT, F., GRÄNS, A., JÖNSSON, E., WIKLANDER, K., SETH, H., OLSSON, C., DUPONT, S., ORTEGA-MARTINEZ, O., SUNDELL, K. & AXELSSON, M. 2014. Response to 'How and how not to investigate the oxygen and capacity limitation of thermal tolerance (OCLTT) and aerobic scope–remarks on the article by Gräns et al.'. *The Journal of Experimental Biology,* 217**,** 4433-4435.

LARSSON, S. 2005. Thermal preference of Arctic charr, Salvelinus alpinus, and brown trout, Salmo trutta–implications for their niche segregation. *Environmental Biology of Fishes,* 73**,** 89-96.

LARSSON, S., FORSETH, T., BERGLUND, I., JENSEN, A., NÄSLUND, I., ELLIOTT, J. & JONSSON, B. 2005. Thermal adaptation of Arctic charr: experimental studies of growth in eleven charr populations from Sweden, Norway and Britain. *Freshwater Biology,* 50**,** 353-368.

MAC, M. J. 1985. Effects of ration size on preferred temperature of lake charr Salvelinus namaycush. *Environmental biology of fishes,* 14**,** 227-231.

MAITLAND, P. 1995. World status and conservation of the Arctic charr *Salvelinus alpinus* (L.). *Nordic journal of freshwater research***,** 113-127.

MILLER, R. & MANN, K. 1973. Ecological energetics of the seaweed zone in a marine bay on the Atlantic coast of Canada. III. Energy transformations by sea urchins. *Marine Biology,* 18**,** 99-114.

NEILL, W. H., MAGNUSON, J. J. & CHIPMAN, G. G. 1972. Behavioral thermoregulation by fishes: a new experimental approach. *Science,* 176**,** 1443-1445.

PARMESAN, C. 2006. Ecological and evolutionary responses to recent climate change. *Annual Review of Ecology, Evolution, and Systematics***,** 637-669.

PETERSON, R., SUTTERLIN, A. & METCALFE, J. 1979. Temperature preference of several species of Salmo and Salvelinus and some of their hybrids. *Journal of the Fisheries Board of Canada,* 36**,** 1137-1140.

PÖRTNER, H.-O. 2014. How and how not to investigate the oxygen and capacity limitation of thermal tolerance (OCLTT) and aerobic scope–remarks on the article by Gräns et al. *The Journal of Experimental Biology,* 217**,** 4432-4433.

PÖRTNER, H.-O., BERDAL, B., BLUST, R., BRIX, O., COLOSIMO, A., DE WACHTER, B., GIULIANI, A., JOHANSEN, T., FISCHER, T. & KNUST, R. 2001. Climate induced temperature effects on growth performance, fecundity and recruitment in marine fish: developing a hypothesis for cause and effect relationships in Atlantic cod (*Gadus morhua*) and common eelpout (*Zoarces viviparus*). *Continental Shelf Research,* 21**,** 1975-1997.

PÖRTNER, H. O. & KNUST, R. 2007. Climate Change Affects Marine Fishes Through the Oxygen Limitation of Thermal Tolerance. *Science,* 315**,** 95-97.

STEVENS, E. D. & SUTTERLIN, A. 1976. HEAT TRANSFER BETWEEN FISH AND AMBIENT WATER. *Journal of Experimental Biology,* 65**,** 131-145.

YEAGER, D. P. & ULTSCH, G. R. 1989. PHYSIOLOGICAL REGULATION AND CONFORMATION - A BASIC PROGRAM FOR THE DETERMINATION OF CRITICAL-POINTS. *Physiological Zoology,* 62**,** 888-907.